LIPOSOME ENCAPSULATED MANGANESE CHLORIDE AS A LIVER SPECIFIC CONTRAST AGENT FOR MAGNETIC RESONANCE IMAGING

BY

MICHAEL ROSS NIESMAN

B.A., Millikin University, 1980
M.S., University of Illinois, 1982

THESIS

Submitted in partial fulfillment of the requirements
for the degree of Doctor of Philosophy in Biology
in the Graduate College of the
University of Illinois at Urbana-Champaign, 1988

Urbana, Illinois

University of Illinois at Urbana-Champaign

DEPARTMENTAL FORMAT APPROVAL

THIS IS TO CERTIFY THAT THE CONTENT, FORMAT, AND QUALITY OF PRESENTATION OF THE THESIS SUBMITTED BY Michael Ross Niesman AS ONE OF THE REQUIREMENTS FOR THE DEGREE OF Doctor of Philosophy IS ACCEPTABLE TO THE Department of Biology

Department/Division/Unit

April 25, 1988

Date of Approval

Christine N. Smith

Departmental Representative

LIPOSOME ENCAPSULATED MANGANESE CHLORIDE AS A LIVER SPECIFIC CONTRAST AGENT FOR MAGNETIC RESONANCE IMAGING

Michael Ross Niesman, Ph.D.
Department of Biology
University of Illinois at Urbana-Champaign 1988
Richard Magin, Advisor

A study was undertaken to examine the possibility of using a liposome encapsulated paramagnetic ion (Mn^{2+}) as a contrast agent for magnetic resonance imaging (MRI) of the liver. Previous work with liposomes had shown that liposomes were concentrated in the liver after intravenous injection. Uptake of the vesicles into tumors was shown to be negligible. This suggested the possibility that the differences in uptake of the Mn^{2+} in liposomes between liver and tumor might provide a means of highlighting tumors using MRI. Electron spin resonance (ESR) and proton nuclear magnetic resonance (NMR) relaxation were used in experiments to study the blood clearance, liver uptake and vesicle break down. The results showed that the Mn^{2+} must be released from the vesicle and transferred to some extent to hepatocytes in order to bring about effective relaxation enhancement in liver tissue. After study of several different liposome preparations, it was found that vesicles composed of phosphatidylcholine, phosphatidylserine and cholesterol brought about the most rapid reduction in liver relaxation times. This vesicle preparation was injected intravenously into Fisher 344 rats with implanted liver tumors. The vesicles caused a marked reduction in the relaxation times of liver tissue, but little change in the relaxation times of the tumor. Magnetic resonance images obtained at 0.5 Tesla

showed a large increase in the signal intensity in the liver and little change in the tumor. The results of this investigation showed the effectiveness of encapsulated Mn^{2+} as an MRI contrast agent for liver metastases.

ACKNOWLEDGEMENTS

I would like to thank the many persons who lent support to the author during the completion of this research project. Professor Richard Magin, my advisor, deserves immeasurable credit not only for scientific guidance, but also for the friendship and the encouragement he provided and for the enthusiasm he imparted to a student who was unsure if a scientific career was the correct choice to be made. I am also deeply indebted to Dr. Goran Bacic who taught me not only NMR, but also imparted a unique philosophy of science which I have attempted to make my own.

My thanks to Wanda Elliott who did a thoroughly professional job in preparing the manuscript and guiding the author through the intricacies of its preparation, and to Bob Cicone and Billy McNeill who were instrumental in providing the materials and instruments needed to complete my experiments.

I am especially grateful to my parents, Barb and Jim, whose dedication to education, encouragement, and continual support were essential to all my educational endeavors.

Finally, I want to express my deepest thanks to my wife Ingrid. It was her hard work, care, and emotional support that helped me to do my best and complete this project. I will always be grateful for her love and friendship.

TABLE OF CONTENTS

CHAPTER 1

INTRODUCTION

Magnetic resonance imaging (MRI) is a rapidly developing, noninvasive diagnostic technology. In current clinical practice, the magnetic resonance properties of the hydrogen protons in the body are exploited to obtain a diagnostic image that is equal, and in many cases superior, to the images obtained using ultrasound or X-ray computed tomography (CT). Images of the head, neck and spine are clearly superior to those obtained using CT, mainly because of the lack of CT-type bone artifacts in MRI. Structures encased in or shielded by bone are thus clearly seen in MRI [Budinger and Lauterbur, 1984; Budinger and Margulis, 1986].

At the time this thesis project was begun in 1985, MRI of the liver and upper abdomen was not as advanced or as successful as imaging in the head, neck and spine. Contrast enhanced CT, ultrasound, and in some cases, radionuclide imaging, were considered better diagnostic modalities for the detection of different focal liver diseases [Sherlock and Dick, 1986; Ohtomo, 1986]. The two factors that limited the usefulness of MRI in the upper abdomen were the lack of a suitable bowel contrast agent and the image artifacts due to various biological motions [Ferrucci, 1986]. The significant use of MRI in hepatological studies in most institutions lagged far behind CT and ultrasound [Sherlock and Dick, 1986]. While the limited availability of MRI equipment may have contributed to the disparity, liver imaging using MRI

needed improvement before it could challenge contrast enhanced CT as the method of choice for liver tumor diagnosis.

A contrast agent that would allow for improved tumor imaging in the liver would enable MRI to be used as a primary method for screening for liver metastases. Furthermore, if the contrast agent could be designed so that images could be acquired with pulse sequences having short TR and TE values, then motion artifacts arising from the heartbeat, respiration, and peristaltic motion would be reduced. This would provide added image clarity. These considerations along with others outlined below, suggested that liposome encapsulated paramagnetic ions might be a possible solution to the problems of liver imaging in MRI.

Liposomes, phospholipid vesicles capable of encapsulating water soluble salts (e.g., paramagnetic salt compounds like $MnCl_2$, $NiCl_2$, etc.), are taken up in large quantities by healthy liver tissue [Abra and Hunt, 1981]. This liver uptake of liposomes is due to the large complement of resident macrophages (Kupffer cells) that are located in the liver. These cells are responsible for the filtering of particulate material from the blood [Wisse and DeLeeuw, 1984] and they efficiently remove liposomes from the circulation. A vast amount of research has been reported examining liposome uptake <u>in vivo</u> [for reviews, see Tom and Six, 1980; Gregoriadis, 1983; Weinstein, 1984]. Much of the early work on liposomes concentrated on attempts to target the vesicles to tumors. Despite concerted efforts in this area, liposomes cannot be designed to leave the circulation and localized in tumor [Poste et al., 1983; Weinstein, 1984, 1987]. Pre-

vious work in our laboratory confirmed that this was the case with temperature sensitive liposomes [Magin et al., 1986a].

Research efforts by many groups have thus shown that liposomes are localized in the liver but do not go to tumors. This suggested that the differences in uptake of liposomes by liver and tumor might potentially be exploited to bring about contrast differences in MR images of metastatic lesions in liver. This project was designed to test this hypothesis. This task is clinically relevant, since many cancer patients (50%) have liver metastases [Ferrucci, 1986].

Manganese was chosen as the contrast agent to be encapsulated for several reasons. First, it is a very effective relaxation enhancing agent [Mildvan and Cohn, 1963]. Second, its ability to increase proton relaxation rates is enhanced upon binding to macromolecules (e.g., proteins, negatively charged membranes) [Mildvan and Cohn, 1970; Koenig, 1985]. Third, there is some data in the literature showing its effectiveness as a potential contrast agent in liposomes <u>in vitro</u> [Caride et al., 1984] and after injection as a free solution <u>in vivo</u> [Mendonca-Dias, 1978, 1983; Koenig, 1985].

Finally, although Mn^{2+} is a divalent cation and is known to be toxic, it is among the least toxic of all trace metals [Underwood, 1977]. Chronic toxicity results from the deposition of the metal in the substantia nigra in the brain, which brings about a Parkinson's like syndrome sometimes referred to as "Manganism" [Venugopal and Luckey, 1978]. Encapsulation of Mn^{2+} in liposomes may prevent high concentrations of the ion from reaching the

brain, since liposomes do not cross the blood brain barrier [Abra and Hunt, 1981]. Liposomes that are stable in the blood should also protect against any acute toxicity due to decreased cardiac function [Wolf and Baum, 1982], since the majority of the Mn^{2+} would remain in the vesicles until they are degraded in the liver. Finally, the liver is the organ that is responsible for the homeostatic balance of Mn^{2+} level of the human. The large concentration of potentially toxic cation would be delivered directly to the liver, the organ responsible for its elimination. This may reduce the toxicity, since the liver can eliminate large quantities of Mn^{2+} in the bile [Papavasiliou, et al., 1966b].

In summary, the objective of this project was to investigate the use of liposome encapsulated $MnCl_2$ as a contrast agent for magnetic resonance imaging. The hypothesis underlying this research was that encapsulation of the contrast agent ($MnCl_2$ in liposomes) would direct a large proportion of it to the liver without toxic side effects. In the liver, the differences between normal and pathological tissues with respect to uptake, accumulation, and breakdown of the encapsulated contrast agent should bring about alterations in the relaxation rates of the respective tissues. These variations in relaxation rates should give rise to different image intensities in the normal and pathological tissue allowing accurate diagnosis of disease states.

CHAPTER 2

BACKGROUND AND SIGNIFICANCE

This chapter outlines the background necessary for understanding the various components of this interdisciplinary research project. The first section (2.1) outlines previous liposome research that led to the choice of liposomes as a carrier for Mn^{2+} and the basic terminology used when referring to these phospholipid vesicles. Sections 2.2 and 2.3 briefly outline somes of the basic principles of nuclear magnetic resonance (NMR) and how this is applied in forming diagnostic images. Section 2.4 introduces the subject of compartmentalization of water and paramagnetic ions in biological systems. Understanding the importance of water exchange is necessary to interpret the data obtained in this project. Finally, Section 2.5 discusses the effects of the binding of the paramagnetic in Mn^{2+} (to protein and lipid vesicles) on the signal measured by electron spin resonance (ESR).

2.1. Liposome Characteristics

Liposomes are phospholipid vesicles consisting of one or more lipid bilayers that enclose an equal number of aqueous compartments. They have been used extensively over the past 20 years as model membranes and have potential as drug delivery systems [for reviews, see Knight, 1981; Gregoriadis, 1983; Ostro, 1987]. The research in this project involves the use of the liposome as a drug carrier.

2.1.1. Liposome formation and structure

Many different methods are available for producing liposomes [Szoka and Papahadjopoulos, 1980; Gregoriadis, Vol. 1, 1984]. The formation procedure employed is important because it determines the final structure of the lipid vesicle. Liposomes are divided structurally into three classes: (1) multilamellar vesicles (MLV); (2) large unilamellar vesicles (LUV); and (3) small unilamellar vesicles (SUV). Each vesicle type has advantages and disadvantages.

Multilamellar vesicles are formed by the hydration of a thin film of dried lipid with an aqueous solution. This formation process was the method used to make the first lipid vesicles described in the literature [Bangham, 1965]. The main advantage of this type of vesicle is that the lipids and the aqueous solution to be encapsulated are not subject to any harsh treatment, such as exposure to organic solvents or high intensity ultrasound. A major disadvantages of this type of vesicle is its heterogeneous size distribution (0.2 - 2.0 μm) [Szoka and Papahadjopoulos, 1980]. Further, the low efficiency of encapsulation (5 - 14%) makes it difficult to encapsulate large amounts of the desired agent (e.g., $MnCl_2$) in MLV.

Small unilamellar vesicles are formed from MLV by subjecting them to high intensity ultrasound for a period of 0.5 to 1 hour. The cavitation produced by this high intensity ultrasound reduces the liposomes in size and greatly narrows the size distribution (to 0.02 -0.05 μm). This relatively uniform size distribution is an advantage for pharmacokinetic studies, since liposomes of dif-

ferent diameters exhibit quite specific tissue deposition patterns [Abra and Hunt, 1981]. The small size allows the SUV to remain in the circulation longer than MLV [Abra and Hunt 1981]. The main disadvantage of SUV is their poor encapsulation efficiency (0.1 - 2% of the original solution phase is encapsulated) and the necessity to expose the prepartion to high intensity ultrasound. Labile molecules (proteins and DNA for example) that one may wish to encapsulate in the vesicles can be easily damaged by this harsh treatment.

Finally, large unilamellar vesicles (LUV) can be formed that have a size range that is intermediate between MLV and SUV (0.1 to 1.0 μm). Several methods may be used to form LUV and the encapsulation efficiently of this vesicle type varies widely. The reverse evaporation method, the method used for vesicle formation in this study, produces liposomes with a size distribution that is more homogeneous than MLV (0.1 - 1.0 μm) and with high encapsulation efficiency (10 - 65%, depending on water soluble molecule entrapped; [Szoka and Papahadjopoulos, 1978]). In addition, the size distribution of the vesicles can be made more homogeneous by filtering the liposome suspension through polycarbonate membrane filters [Szoka, et al., 1980].

A comparison of the characteristics of three types of liposomes (made using the same phospholipid mixture) is listed in Table 2.1 (Tables appear at the end of the text). As can be seen from this data, LUV formed by the REV method encapsulate more of a water soluble compound than do MLV or SUV. Because of the high encapsulation efficiency and because Mn^{2+} was not affected by

sonication or exposure to organic solvents, LUV made using the REV method were used exclusively for this study.

2.1.2. Liposome bilayer composition

The composition of the liposome bilayer is an important consideration when liposomes are to be employed as drug carriers. The membrane is usually composed of different neutral and acidic phospholipids and may also contain cholesterol. This composition is somewhat similar to that of the cell plasma membrane. Unlike the plasma membrane, however, liposomes used for drug delivery usually do not contain proteins [Weinstein, 1984; 1987; see Heath, et al., 1983 for an exception]. The lipid composition of the bilayer has a major influence on the surface charge, size, encapsulation efficiency, and <u>in vivo</u> stability of LUV [Scherphof, et al., 1978; Gregoriadis, Vol. 1, 1984; Magin and Niesman, 1984b]. Also, it has recently been shown that the lipid composition influences the rate of breakdown of the LUV after phagocytosis [Conner, 1986; Spanjer, 1986; Vandenbranden, el al., 1985].

The surface charge of the LUV is a function of the head group of the phospholipids incorporated in the bilayer. At pH 7.4, the headgroup of phospholipids such as phosphatidylcholine (PC) and phosphatidylethanolamine (PE) are electrically neutral (one positive and one negative ionized group) while the headgroup of phosphatdylserine (PS), phosphatidylglycerol (PG), and phosphatidic acid (PA) have a net negative surface charge. Negative surface charge has two effects relevant to this study. First,

the inclusion of negatively charged phospholipids greatly increases the stability of liposome during storage. Whereas most liposome preparations made with neutral lipids were stable for only a day or less, [Papahadjopoulos, 1978; Niesman and Magin, unpublished data), liposomes made with 20 mole% of negatively charged dipalmitoylphosphatidyglycerol (DPPG) were found to be stable in buffer at 4°C for more than a week [Magin and Niesman, 1984a]. It is thought that the negative charge on the liposomal surface prevents liposome fusion and loss of contents.

The second effect of a negatively charged liposome bilayer is that it causes an increased uptake of liposomes by phagocytic Kupffer cells, both in vitro [Dijkstra, et al., 1985] and in vivo [Spanjer, et al., 1986]. These studies have shown that Kupffer cells, the resident macrophages of the liver, have a receptor that is specific for negatively charged phospholipids. For example, negatively charged latex beads were shown to competitively inhibit the uptake of negatively charged liposomes in vitro [Dijkstra, 1985]. Uncharged latex spheres or liposomes made from uncharged phospholipids did not inhibit the uptake of negatively charged liposomes. Hence, liposomes made with a significant proportion of negatively charged phospholipid should be cleared from the blood at a faster rate than uncharged vesicles. This effect has been confirmed by several investigators [Spanjer, et al., 1986; Magin, et al., 1986a].

Changes in the phospholipid composition of the membrane also influence the size and encapsulation efficiency of the liposome suspension. For example, inclusion of cholesterol in liposomes

will cause an increase in mean vesicle size and encapsulation efficiency [Szoka and Papahadjopoulos, 1980]. This increase in encapsulation efficiency is logical since the volume of a sphere (e.g., a liposome) increases as the radius cubed. Thus, an increase in the radius of the liposome from 100 nm to 150 nm results in an increase in the internal volume by a factor of almost 3.8. Further evidence for this was shown when multilamellar vesicles were made without cholesterol. These vesicles had a mean diameter smaller than other multilamellar vesicles containing cholesterol [Magin and Weinstein, 1984].

The phospholipid composition of the bilayer is also very important in determining the <u>in vivo</u> stability of the liposome. A large number of experiments have examined the influence of lipid composition on liposome stability in blood [Knight, 1981; Tom and Six, 1980; Szoka and Papahadjopoulos, 1980]. The main conclusion of this work was that liposomes in blood are subject to attack by high density lipoprotein (HDL). After studying this breakdown process carefully, it was ascertained that a component of HDL, lipoprotein Apo-A-1, was responsible for liposome breakdown in blood and serum [Sherphof, et al., 1978; Jonas, 1984]. Liposomes made with phospholipids containing unsaturated fatty acid side chains were found to be the most unstable. Liposomes made with phospholipids composed entirely of saturated fatty acid side chains were stable in blood or serum at temperatures below the phospholipid gel to liquid crystalline phase transition temperature (T_m). Above T_m, liposomes with saturated fatty acids were found to breakdown as quickly as this with unsaturated fatty

acids [Magin and Niesman, 1984a]. Finally, it was discovered that the addition of 33 - 50 mole percent of cholesterol added to the liposome bilayer was sufficient to make liposomes of almost any composition resistant to attack by Apo-A-1 [Kirby, et al., 1980]. The phospholipid composition, and especially the presence or absence of cholesterol, is a main factor in determining the in vivo stability of lipid vesicles.

The composition of the lipid bilayer is also important in determining the rate of breakdown of the vesicle after it is internalized by Kupffer cells in the liver. One example of this is the pH sensitive liposome. Liposomes made from dioleoyl phosphatidylethanolamine and oleic acids break down very quickly when exposed to a pH less than 6.5 [Huang et al., 1983; Connor and Huang, 1986]. During the process of phagocytosis, the liposome is internalized and the endocytotic vesicle becomes acidified. As the pH drops below 6.5, the liposomes breakdown due to fusion with the endosome membrane, releasing their contents into the cytoplasm. Thus, these liposome can deliver their contents to the cytoplasm and avoid lysosomal degration. In a different set of experiments, another group has shown that the inclusion of phosphatidylserine in the membrane causes an increase in the rate of liposome uptake by Kupffer cells [Spanjer, 1986]. Phosphatidylserine, which contains unsaturated fatty acid side chains, also increase the rate of breakdown of the vesicles [Storm, et al., 1987]. On the other hand, liposomes composed of DPPC and DPPG seem to break down slowly [Magin et al., 1986b]. The research by Storm and collegues [1987] confirms that vesicles

below their phase transition temperature (T_m) at 37^o are degraded more slowly.

In addition to stability, liposomes composed of DPPC and DPPG do have another very important characteristic. Both DPPC and DPPG undergo the gel to liquid crystalline phase transition at 41^{o}C. These liposomes were originally designed to release their contents locally in the capillary bed of the heated tumor [Yatvin, et al., 1978]. This method was marginally successful in increasing the tumor concentration of anticancer drugs [Weinstein, 1980; Magin, et al., 1986a]. More importantly, the temperature-sensitive drug release characteristics of these vesicles made it possible to study the system with the liposome intact and then reexamine the system after heating. Since LUV made with DPPC and DPPG rapidly release their contents when heated above 42^{o}C, it is possible to heat the sample (blood, liver, etc.,) after making a measurement and then to measure the sample again after the liposomes have released their contents.

To briefly summarize, the lipid composition of the liposome determines the characteristics of the vesicle. The size, surface charge, stability, and processing after phagocytosis are all influenced by the bilayer composition. It is important to keep all of these factors in mind when designing and evaluating liposomes as carriers for MRI contrast agents.

2.2. General Principles of Nuclear Magnetic Resonance (NMR)

It is important to understand the general theories underlying the phenomenon of nuclear magnetic resonance (NMR) in order

to understand how liposome encapsulated $MnCl_2$ will interact with water protons and affect the image obtained. This section will deal mainly with proton NMR.

Nuclear magnetic resonance as we think of it today is a phenomena that was discovered independently by Bloch [1946] and Purcell [1946]. The field of NMR spectroscopy developed rapidly after that time. Outlined below is a brief description of NMR and an introduction to the principles that are necessary to understand the pulsed NMR experiments that were undertaken. It also provides information necessary to interpret the mechanisms by which liposome encapsulated paramagnetic ions change the appearance of an NMR image. This section is a summary of information contained in several references [Schlichter, 1980; Dwek, 1973; Budinger and Lauterbur, 1984; Morrison and Boyd, 1973; Abragam, 1961].

2.2.1. Protons in a magnetic field

Angular momentum, or spin, is an intrinsic property of atomic particles such as protons, neutrons and electrons. Hydrogen nuclei, like many other atomic nuclei, posses a nonzero spin (for ^1H, the spin = 1/2). The hydrogen nucleus also has a net positive charge. The rotation of this charged hydrogen nucleus generates a magnetic moment directed along the axis of spin of the nucleus. Thus, the nucleus, when placed in a magnetic field will exhibit two motions. It will spin around an axis through its center, and this spin axis will precess around the directional axis of an applied magnetic field.

This precession of the spin axis is a result of a torque generated by the interaction of the magnetic moment of the spinning nucleus with the applied magnetic field. Accordingly, the angular Larmor frequency (ω) of this precession is given by the equation

$$\omega = \gamma B_o \qquad (2.1)$$

where γ is the magnetogyric ratio of the nucleus under consideration and B_o is the strength of the applied magnetic field. For an applied magnetic field of 0.5 T, this corresponds to a Larmor frequency of 21.1 MHz. From quantum mechanical theory, it can be shown [Abragam, 1961] that the frequency of radiation that is required to induce a transition of the hydrogen nuclei (i.e., between spin 1/2 to spin -1/2) is equal to ω, the Larmor frequency. It is common to express spin +1/2 as being "aligned with" the magnetic field and spin -1/2 as being "aligned against" the field.

Next, one may examine the net magnetization, the sum of the magnetization of all the protons in the sample. In the absence of an applied magnetic field, the magnetic moments of the nuclei will be randomly oriented. When an external magnetic field is applied (in the z direction, by convention), the nuclei must either align along (lower energy level) or opposite the direction of the applied field (the higher energy level). At room temperature, with an applied magnetic field of 1 T, there is an excess of approximately 1 in every 10^5 spin in the lower energy level [Dwek, 1973].

When energy at the appropriate frequency (i.e., the Larmor frequency) is applied to the system, transitions are induced between the two allowed energy states. Since there is a very slight excess of spins in the lower energy state, application of an RF pulse at the Larmor frequency will result in the absorption of energy as the spins are excited to the higher energy state. The absorption of energy, which occurs by applying a quantum of energy equal to the energy separation between the two states, is a resonant process. It is called (nuclear) magnetic resonance. Once the external source of added energy is removed (i.e., the RF pulse is turned off), the spins will return to the lower energy state, emitting electromagnetic energy at the Larmor frequency. This is the signal measured in the NMR experiment. The return to equilibrium is characterized by two relaxation processes, T_1 and T_2.

2.2.2. Relaxation processes

Absorption of radiation at the Larmor frequency causes a change in the net magnetization of the excited spins. If the magnetization along the z direction is examined, the net magnetization is reversed towards -z as the energy from the radiofrequency (RF) pulse is absorbed. After the radiation ceases, the nuclei relax back toward the lower energy state, aligned with B_o. The decay of the net magnetization back toward equilibrium is called the spin lattice relaxation or longitudinal relaxation. This decay of the longitudinal magnetization is called simply T_1

relaxation as it is characterized by the exponential decay constant T_1, the longitudinal, or spin-lattice relaxation time.

Absorption of energy at the Larmor frequency also has an effect on the magnetization in x - y plane, perpendicular to B_o. Immediately after the RF pulse ceases, the precession of the nuclei in this plane is synchronized; that is, the phase coherence of the of the population of spins is established. This phase coherence is lost exponentially as the net magnetization in x - y plane goes to zero (i.e., a random orientation of spins). This transverse, or spin-spin relaxation is called T_2 relaxation. It is characterized by the exponential decay constant, T_2.

These two relaxation times, T_1 and T_2, are the properties that are intrinsic to the molecules measured in the experiment. In proton NMR, water is the main species being measured. In a solution of pure water devoid of any influencing factors (see Section 2.2.3), T_1 and T_2 are quite similar, approximately 3 seconds at 0.5 T. Several factors can alter the T_1 and T_2 of water protons. These are discussed below.

2.2.3. Factors that effect T_1 and T_2

In liquids, the main mechanism causing relaxation is interaction with local dipolar magnetic fields. These local fields are constantly fluctuating according to the random molecular motion of the water molecule. These random variations in molecular motions are characterized by a correlation time (τ_c), which sets a time scale to these random variations. A quantitative description of correlation times can be found elsewhere [Dwek,

1973; Abargam, 1961]. What is important for this discussion is an understanding that, at room temperature in a homogeneous magnetic field, the τ_C of interacting water protons is short and relaxation is generally inefficient process in water solutions.

The measurement of spin-spin relaxation (T_2 relaxation), however, is quite susceptible to inhomogeneity in the applied magnetic field. The decay of the magnetization in the x -y plane is accelerated by field inhomogeneities. The reduction in the FID due to field inhomogeneity precludes the measurement of the true T_2 using the FID. Therefore, Hahn proposed the spin echo method. However, diffusion of the spins (i.e., water diffusion, reduces the echo amplitude at long refocusing times. Carr and Purcell [1954] and Meiboom and Gill [1958] refined the spin echo pulse sequence to refocus and rephase the spins, eliminating diffusion effects. The combined sequence (called the CPMG sequence) ensures that a true T_2 is measured.

Two other factors that influence the relaxation times are the strength of the applied magnetic field and the temperature of the sample at the time of the measurement. In a solution, increasing the temperature or the field causes the relaxation times to increase (i.e., the relaxation rates decrease).

Because the local magnetic field (i.e., the proton chemical environment) exerts a strong influence on T_1 and T_2, molecules containing unpaired electrons can exert a dramatic effect on the relaxation process. An unpaired electron has a magnetic moment that is approximately three orders of magnitude larger than that of the nucleus, and the local field generated by the electron is

therefore much larger than that of the nucleus. The fluctuations of the large magnetic fields lead to a more efficient nuclear spin relaxation. In a dilute solution of paramagnetic ions, the strong field produced by the electron is coupled to the nuclear spin by dipole-dipole interactions. Other processes may also contribute to the relaxation. The mechanism of relaxation brought about by paramagnetic ions is dealt with in great detail in Chapter 9 of Dwek [1973], which contains a thorough explanation of the Solomon-Bloembergen equations [Solomon, 1955; Bloembergen, 1957] describing the process.

The effects on water protons relaxation rates brought about by paramagnetic ions in solution are not linear; rather, a linear correlation exists between the concentration of the paramagnetic ion and the reciprocal of the relaxation times ($1/T_1$, $1/T_2$). These reciprocal values are the relaxation rates R_1 and R_2.

A graph showing the linear relationship between the relaxation rate (R_1, R_2) of water protons versus the concentration of an added paramagnetic ion is shown in Figure 2.1 (Figures appear at the end of the text). Figure 2.1 is a specific example using the actual values of Mn^{2+} (for R_1 and R_2). The slope of these lines expressed as $(mM\ sec)^{-1}$ is the Molar Longitudinal Relaxation Enhancement (MRLE; T_1 relaxativity) and the Molar Transverse Relaxation Enhancement (MTRE; T_2 relaxivity).

One feature of relaxation enhancement by paramagnetic ions that is not shown in Figure 2.1 is the further enhancement of water proton relaxation that occurs when a paramagnetic ion is bound to a macromolecule (e.g., Mn^{2+} bound to a protein such as

albumin). This phenomena has been well described [Schleler, 1963; Mildvan and Cohn, 1970; Koenig, 1984a], and results from the decrease in rotational correlation time τ_R. Qualitatively, this means that the slow tumbling of Mn^{2+} bound to protein results in a longer time for the magnetic dipole of the free Mn^{2+} electron to interact with the dipole of the proton. This process results in an increase in the efficiency of relaxation.

2.3. NMR Imaging Background

The possibility that the phenomena of nuclear magnetic resonance could be used to produce an image was first suggested in 1973 [Lauterbur, 1973]. The rational behind this approach was the fact that specific tissues or regions in the body have unique local chemical environments, and that the water in these regions would have a range of relaxation times. The differences in water concentrations and relaxation times at the local NMR locations would lead to differences in signal intensities between the tissue types (e.g., tumor and healthy tissue). The key factor in transforming these signal intensity variations into an image was the realization that the application of a gradient in the magnetic field would allow the spins to be localized in space.

In order to understand how an NMR image (or Magnetic Resonance Image--MRI--as it has been renamed) is generated, a knowledge of three basic fundamentals of the system is needed. First, an understanding of the basic principles of NMR is required. This was presented in the previous Section (2.2). Second, information on how the spins are localized in space is needed. And

third, the pulse sequences that generate the images should be described and analyzed. These pulse sequences stimulate the trafnsmission and reception of the electromagnetic signals that are used to produce images of differing intensity and contrast. The description that follows is a summary derived from several sources [Budinger, 1986; Morris, 1986].

2.3.1. Spatial localization

Most currently employed clinical imaging systems use the two-dimensional Fourier transform method for generating an image. In this method, magnetic field and phase encoding gradients are used to localize spins. If all the protons in the sample are placed in a uniform magnetic field, these protons will precess at an identical Larmor frequency. On the other hand, if the protons are placed in a magnetic field gradient the nuclei will precess at slightly different frequencies according to their position in the gradient. The actual value at which the proton precess is directly related to their position in the magnetic field gradient. This gradient can be along any axis (x, y, or z with z being the direction of the main applied B_O). This relationship of spatial position to frequency is used to form a two-dimensional Fourier image. Performing a Fourier transform on the aggregate of the signals from all the nuclei in the gradient gives a distribution of the nuclei in the gradient.

In order to form an image of a selected "slice" of the sample, gradients are used in conbination with RF pulses in a pulse sequence. In chronological order, the application of gra-

dients is as follows. A magnetic field gradient is first applied in the z direction during the time of the initial RF excitation pulse. This is called the slice-select gradient. The incoming RF pulse is at a frequency that only excites nuclei at a certain position along the selected axis. In the time after the excitation pulse and before the echo, a phase encoding gradient, called the preparation gradient, is applied along the orthogonal axis. This gradient imparts a differing phase relationship to the spins in the selected slice. Finally, as the echo appears and as it is being received, a frequency encoding gradient is applied along the direction of the other axis orthogonal to the slice select gradient. This detection gradient (also call the readout gradient) imparts a different frequency to spins along the x axis. In summary, the first gradient in the z direction selects the slice to be examined, and then the x and y gradients give a unique phase and frequency to spins in the slice depending on their location in space. Several other pulses are applied as the signal is received (rephasing of the slice select gradient, dephasing in the read out, before normal read out for the echo and dephasing at the end). The signal that is received is converted to a two-dimensional distribution of spatial intensities, typically by using a two-dimensional fast Fourier transformation. The spatial intensities measured in this manner are then converted to a grey scale and this is the actual image.

2.3.2. The Spin-echo-sequence

The most common pulse sequence in use today for clinical

imaging is the standard spin-echo sequence. In this sequence the initial RF excitation pulse of "90^{o} pulse," a pulse that causes the net magnetization to be located in the transverse plane. After the 90^{o} pulse is turned off, the spins immediately begin to lose coherence (T_2 relaxation). In other words, if one were rotating at the Larmor frequency, the spins would appear to fan out. After a short delay, a 180^{o} pulse is then applied about an orthogonal axis. This "flips" the spins such that they begin to come together. This process produces an echo as the spins rephase. The echo time (TE) is the time at which the echo is observed (sampled). The repetition time (TR) is the time between successive 90^{o} pulses. Varying the TE and TR causes changes in the signal intensity seen on the resulting image. For standard imaging parameters TR and TE, the signal intensity in a spin echo image can be approximated by Equation (2.2) [Morris, 1986]

$$I = H\, f(\nu)\, [1 - e^{(-T_R/T_1)}]\, e^{(-T_E/T_2)} \qquad (2.2)$$

where H is the local hydrogen concentration, $f(\nu)$ is a function of the macroscopic motion of the water (e.g., arterial blood flow).

The equation is valid as long as a single echo sequence is used and TR > T2. If an image is acquired using small values for TR and TE, (i.e., smaller than tissue T_1 and T_2) the importance of T_2 is diminished and the image is said to be "T_1 weighted." On the other hand, a "T_2 weighted" image is obtained when longer values of TR and TE are used in the pulse sequence. It is impor-

tant to take these factors into consideration when evaluating changes in contrast.

One point that emerges from consideration of Equation (2.2) is that for a given TR and TE, a reduction of T_1 and T_2 may cause an increase in signal intensity up to a point, but any further reduction will cause a decrease in signal. If too much of a paramagnetic agent is added, then the signal is relaxed before the echo is sampled. In other words, all the nuclei will have relaxed in a time less than TE. Thus, in an in vivo experiment it is important to carefully calculate the dose of paramagnetic agent to be added.

2.4 Effects of Water Diffusion on Relaxation

The ability of a paramagnetic ion to increase the relaxation rate of water protons in a solution can be modulated by compartmentalization of the ion. This compartmentalization is an important consideration when the ion is encapsulated in a liposome. This factor is also important in vivo after the liposome encapsulated paramagnetic ion has been injected intravenously and localized in liver (or other tissue). It is necessary, therefore, to examine the mechanism whereby paramagnetic ions in one compartment may interact with water protons in adjacent compartments.

A paramagnetic agent in one compartment can relax water protons in another compartment if the water can exchange between the compartments on a time scale that is shorter than the intrinsic relaxation time in that compartment. For example, an encapsulated agent in the aqueous compartment of liposome can relax

extra-liposomal water protons if the exchange of water through the membrane is rapid enough. The mechanisms of relaxation in a two compartment system with exchange have been described extensively [Hazelwood, et al., 1974; Belton and Ratcliffe, 1985]. An understanding of the mechanism involved is necessary to characterize the relaxation behavior seen with different compositions of liposomes.

2.4.1. Measurement of the water exchange time

The measurement of relaxation behavior in a two compartment system has been used extensively as a method for measuring the exchange of water between two compartments in biological systems [Belton and Ratcliffe, 1985]. The rational underlying this approach is the realization that the measurement of the water exchange time (τ, also called the residence time) makes it possible to calculate the diffusional water permeability of the membrane (P_d) separating the two compartments.

Conlon and Outhred [1972] introduced this method, (later refined by Fabry and Eisenstadt [1975]), in the early 1970s to measure P_d of erythrocytes. The first step in Conlon and Outhred's method was to change the relaxation time of the plasma (i.e., the water outside the erythrocyte) by adding 25 mM Mn^{2+}. This reduced the T_2 time of the plasma water protons to a few milliseconds, while the intracellular water had a T_2 of approximately 140 ms. Because of water exchange (diffusion) through the red cell membrane, the proton spins within the red blood cell (i.e., the intracellular water) will be effectively relaxed by

the extracellular Mn^{2+} in the plasma. The relaxation rate of the intracellular water will therefore depend on the permeability of the erythrocyte membrane to water.

The Conlon and Outhred method can be used to measure the permeability of a liposome bilayer. Androsko and Forsen [1974] and Haran and Shporer [1976] applied this method in studies of liposome bilayer permeability.

The equation that describes the two component normalized relaxation curve (T_1 is used in this example, but T_2 measurement can also be used) in a two component system is [Belton and Ratcliffe, 1985]

$$h(t) = P'_i \exp(-t/T'_{1i}) + P'_o \exp(t/T'_{1o}) \qquad (2.3)$$

where P'_i and P'_o are the apparent water populations (P_i and P_o are actual water populations or volumes), and T_{1i}' and T_{1o}' are the corresponding apparent relaxation times measured in the experiment. The measured values are function of the times that would be measured with no water exchange across the membrane (T_{1i}, T_{1o}), and the residence time of water inside the liposomes (τ_i). Also, $P_i/\tau_i = P_o/\tau_o$ and by mass balance $P_i + P_o = 1$. When $\tau_{i,o} < T_{1i}$, T_{io}, a single exponential decay is seen and the system is said to be in the fast exchange region.

However, when $T_{1i} << T_{1o}$ and $\tau_i/T_{1i} > 1$, the apparent populations (P_i', P_o') are equal to the actual ones. Also, $T_{1i} \simeq T_{1i}'$. This set of conditions is referred to as intermediate exchange. If $P_o > P_i$, then a good approximation of $1/T'_{1o}$ (this

is the relaxation rate in the compartment outside of where the paramagnetic agent is; i.e., the water outside of the liposome) can be obtained by [Hazelwood, et al., 1974]:

$$1/T_{1o}' = \frac{P_o(\tau_i + T_{1i})}{T_{1o}(P_o\,\tau_i + T_{1i})} + \frac{P_i}{P_o\,\tau_i + T_{1i}} \qquad (2.4)$$

This shows that the apparent relaxation rate is a function of relative volumes (populations) of the two compartments, the residence time of the water inside the compartment containing the paramagnetic ion (e.g., τ inside of the liposome), and the relaxation rate of the water in both compartments.

If a high concentration of the paramagnetic ion is present in the compartment (e.g., placing a high concentration of Mn^{2+} inside liposomes) then $T_{1i} << \tau$ and the system will now be in what is called the "slow exchange" regime. In this Equation (2.4) reduces to

$$\Delta 1/T_{1o} = P_i/(P_o\,\tau_i) \qquad (2.5)$$

The paramagnetic contribution to exchange ($\Delta\ 1/T_1$) is thus equal to

$$\Delta\ 1/T_1 = 1/T_{1o}' - 1/T_{1o} \qquad (2.6)$$

Equation (2.5) indicates that once the slow exchange region is reached, the relaxation in the external compartment (e.g., the extra liposomal compartment) no longer depends on the relaxation rate or (i.e., the amount of paramagnetic agent) inside the lipo-

some. It depends only on the relative populations of the two compartments and the residence time of the water in compartment containing the paramagnetic agent.

This has important implications in vivo. Increasing the amount of a paramagnetic agent in the liposomes past a certain point will have no effect on the relaxation of the water external to the vesicle. It only depends on the water exchange time and the relative populations (volumes) of the two compartments. Also, if one is attempting to change contrast in an in vivo medical imaging situation, a small amount of contrast agent delivered into the compartment of interest (i.e., intracellular) is more effective than delivering a large quantity to a region near the compartment of interest. These implications have been more extensively outlined recently [Bacic, et al., 1987]. The results of these considerations formed the basis for the decision to examine several liposome formulations to determine if a liposome that was degraded rapidly would bring about more efficient contrast enhancement.

2.5. The Electron Spin Resonance Spectra of Manganese

The unpaired electrons of the manganese ion responsible for enhanced proton relaxation can be directly observed using electron spin resonance (ESR). The spectrum of the ion in solution is measured in the X-band (9.5 GHz). Electron spin resonance spectra have been used to study the interactions of Mn^{2+} with proteins [Reed and Cohn, 1970], enzymes [Reed and Cohn, 1972, 1973; Reed and Scrutton, 1974] mitochrondria [Bragadin, et al,

1983] and cells [Ash and Schramm, 1982; Getz, et al., 1979]. These studies have taken advantage of the fact that Mn^{2+} bound to proteins, such as enzymes, or to other cell constituents, has a different spectrum than the aqueous form [Mildvan and Cohn, 1970; Dwek, 1973; Getz, 1979]. At 9.6 GHz, free Mn^{2+} in solution has a sharp six line spectrum while bound Mn^{2+} is broadened away and gives an almost flat line (see Figure 4.8 for example).

The fact that the free Mn^{2+} spectrum is broadened beyond detection when the ion is tightly bound to a protein [Getz, 1979] or a liposome (see Section 4.6) allows one to quantitate the amount of Mn^{2+} inside of the liposomes that was rotationally free and visible in ESR (see Section 4.6). Once the liposome was degraded, the Mn^{2+} became bound to proteins or tissues and was therefore ESR "invisible." This characteristic was used as a way to monitor the state of the ion in <u>in vitro</u> and <u>in vivo</u> experiments.

CHAPTER 3

MATERIALS AND METHODS

3.1. Materials

All phospholipids used were obtained from Avanti Polar Lipids (Birmingham, AL) and certified to be greater that 98% pure. Thin layer chromatography of DPPC and DPPG in chloroform: methanol:water:(64:24:4) on silica gel yielded a single spot and all lipids were used without further purification. Cholesterol was obtained from Nu-Check Prep (Elysian, MN). All solvents and buffer ingredients were reagent grade or better. Special precautions were taken for the storage and handling of both types of ether (isopropyl and diethyl) used in this study. All ether was stored in dark amber bottles under N_2 gas to prevent peroxide formation. Before use, the ether was mixed with a 10% sodium bisulfite solution, shaken, and the top ether layer used for vesicle formation.

3.2. Methods of Liposome Preparation and Characterization

3.2.1. Liposome preparation

Large unilamellar liposomes (LUV) were prepared according to the reverse phase evaporation method of Szoka and Papahadjopolous [1978] as modified by Magin and Niesman [1984a] for temperature sensitive liposomes. To make temperature sensitive LUV, 135 μmoles of DPPC and 35 μmoles of DPPG were dissolved in 4 ml of chloroform and combined with 8 ml of isopropyl ether. This organic phase was then warmed to 50^{o}C, 9^{o}C above the phase

transition temperature (T_m) of the component phospholipids. The aqueous phase (100 mM $MnCl_2$, pH 6.4) was then warmed to 50°C and the aqueous and organic phases combined. Nitrogen was added to the flask and this two phase system sonicated in a bath sonicator (Lab Supply Company, Hicksville, NY) at 50°C for 5 minutes, until a homogeneous emulsion was formed. The emulsion was placed in a rotary evaporator flask and the organic solvents removed under reduced pressure. The reduction in pressure was achieved gradually, in order to minimize the vigorous foaming that can occur during rapid solvent removal. After the solvent was removed, when no more foaming was seen, the preparative procedure was complete. The volume of the liposome suspension was measured and readjusted to the initial aqueous phase volume of 4.0 ml using distilled water. The liposomes were cooled to room temperature and dialyzed (dialysis tubing M.W. Cutoff, 12,000 - 14,000)to remove the unencapsulated $MnCl_2$. The dialysis solution (Hepes buffered saline) was changed at least three times over 24 hours before liposomes were used for experiments. Vesicles made with dimyristoylphosphatidylcholine/dimyristoylphosphatidylserine/cholesterol were formed using this same procedure. (Cholesterol was added with the phospholipids at the beginning of the formation procedure.

For LUV made using phospholipids with a T_m below 30°C (i.e., those with unsaturated fatty acid chains), the formulation process used was similar to that used with DPPC/DPPG LUV, with a few minor changes. First, all preparations containing phospholipids with unsaturated fatty acid chains (e.g., PC, PG, or PS) were

formed at room temperature. Diethyl ether was used since it is not as explosive at room temperature as it is at 50°C. The use of diethyl ether makes the emulsion less likely to foam violently when removing the organic phase, and makes LUV preparation easier. Also, since the phospholipids containing unsaturated fatty acids are more soluble in diethyl ether, the addition of chloroform to the organic phase was unnecessary. In some cases when diethyl ether was used, the liposome emulsion would form a caked gel on the bottom of the flask during evaporation. This could be disrupted by simple vortex mixing, followed by continued solvent removal.

For some in vivo experiments, the liposomes were filtered to narrow their size distribution. This was done by filtering through a polycarbonate membrane filter (0.4 μm polycarbonate, Biorad, Los Angeles, CA) as previously described [Szoka, et al., 1980]. All liposomes containing cholesterol were filtered at room temperature. Liposomes made from DPPC/DPPG were filtered above T_m (at 45°C) by connecting a polycarbonate filter holder to two syringes with luer-lok fittings and filtering in a heated water bath.

3.2.2. Liposome characteristics

In order to determine the suitability of different liposome preparations for in vivo experiments, the ability of the vesicles to capture $MnCl_2$ and their stability in serum were measured using several techniques.

3.2.2.1. Radioisotope methods

Radioisotopes were used to assess the amount of ^{3}H-sucrose that could be entrapped within the liposomes. For these experiments, 0.5 μCi of ^{3}H-sucrose (Amersham, Arlington Heights, IL) was included in the aqueous phase. After the LUV were formed and had been dialyzed for 24 hours (three 1 liter buffer changes), triplicate 25 μl aliquots of the liposome suspension were taken and counted in a liquid scintillation counter (Beckman LS7500), along with triplicate 25 μl samples of the original aqueous phase. The amount of sucrose captured was calculated as follows:

$$\% \text{ capture} = \frac{^{3}\text{H sucrose DPM in LUV}/25\ \mu\text{l} \times (100)}{^{3}\text{H sucrose DPM in aqueous}/25\ \mu\text{l}}$$

Any dilution of the liposomes during dialysis or handling before the measurement of capture was taken into account.

Liposome stability in fetal bovine serum, which was used to predict LUV stability <u>in vivo</u>, was assessed using liposomes containing radioisotopes. Liposomes were made with ^{3}H-sucrose (as an aqueous phase marker) and with 0.5 μCi ^{14}C-DPPC (lipid bilayer marker). The vesicles were incubated at 37^{o}C in 50% fetal bovine serum (Gibco, Grand Island, NY) for various periods of time (0 - 2 hours). The samples were cooled on ice and centrifuged in a table top ultracentrifuge for 15 minutes at 100,000 x G to pellet the liposomes. The amount of ^{3}H-sucrose released from the vesicles into the supernatent was measured using a liquid scintillation counter.

The percent of label released was calculated as follows.

$$\% \text{ release} = \frac{^{3}\text{H Sucrose DPM supernatent/50 } \mu\text{l}}{^{3}\text{H Sucrose DPM/50 } \mu\text{l liposomes}} \text{ x (100)}$$

Inclusion of the ^{14}C-DPPC in the bilayer made it possible to confirm that there were no LUV remaining in the supernatant.

Radioisotopes were also used to measure the heat release properties of temperature-sensitive liposomes. A detailed explanation of the methodology can be found elsewhere [Magin and Niesman, 1984a]. Briefly, the procedure involved heating a sample of liposomes to 35, 37, 39, 40, 41 and 43^{o}C in a staircase manner. After 5 minutes at each temperature, a 100 μl aliquot was removed and spun in the ultracentrifuge. A 50 μl sample of the supernatent was counted in a liquid scintillation counter to determine the amount of radioactive sucrose released from the vesicles. The percent release was calculated as shown previously for stability experiments.

3.2.2.2. ESR methods

Radioisotope methods provide a simple and rapid method for characterization of the properties of several formulations of LUV. After this screening procedure was completed, ESR methods were used to directly measure the release of the actual paramagnetic ion (Mn^{2+}).

To measure the capture of $MnCl_2$, a 50 μl aliquot of the undiluted liposomes in a glass capillary was placed in a Varian E

109 spectrometer operating at 9.5 GHz. A six line spectrum characteristic of Mn^{2+} was recorded using a 2000 gauss scan range, 10 gauss modulation amplitude, and 20 mW of microwave power. The measurement was then repeated under the same conditions, with a manganese atomic absorption standard (18.2 mM, Johnson Matthey, Norwalk, CT) as the sample. Finally, a background scan at the same gain was taken to ensure a flat baseline was present (i.e., no cavity contamination). Data were collected using a Zenith Z-100 computer and stored for later analysis.

To determine the <u>in vivo</u> stability of different preparations containing Mn^{2+}, liposome samples in 50% fetal bovine serum were placed in the spectrometer and the temperature maintained at $37^{o}C$. The temperature control accessary was capable of temperature control to $\pm$ $1^{o}C$. Instability in serum was manifested by a reduction in peak height of the ESR signal. This reduction in peak height is due to the leakage of Mn^{2+} from the vesicles and the subsequent binding of the ion to protein in the serum. Mn^{2+} bound to large proteins in serum is virtually ESR invisible, due to its much slower tumbling rate and broadened signal (see Section 2.5). This methodology was shown to be valid by heating a sample of temperature sensitive liposome in 50% serum through T_m and then returning to $37^{o}C$ and recording another spectrum. The Mn^{2+} signal was nearly eliminated (the peak height was reduced by more than 90% of its original value). This same experiment was used to monitor the release of Mn^{2+} near T_m for different preparations of temperature sensitive LUV.

3.2.2.3. ^{31}P NMR methods

Although it is well documented that LUV produced by the REV method are predominately unilamellar [Szoka and Papahadjopolous, 1978], samples were measured by ^{31}P NMR to demonstrate that the LUV used in these studies were, in fact, unilamellar. Other investigators have previously used this same technique [Hope, et al., 1985]. A ^{31}P NMR spectrum of a 5 ml suspension of liposomes was obtained on a GN-300 high resolution NMR spectrometer operating at 121.5 MHz. After the addition of $MnCl_2$ to a final concentration of 3 mM, the liposomes were returned to the spectrometer and a second spectrum recorded under identical conditions. The Mn^{2+} added outside completely broadened the signal arising from the phospholipid head groups in the outer leaflet of the bilayer, and the size of the phosphorus peak was reduced. If the LUV were entirely unilamellar in nature, the reduction in the area under the curve should equal 50%. If multiple bilayers are present (MLV), the reduction in signal will be less than 50%, because the inner bilayers are shielded from the broadening agent. In the control experiment, temperature sensitive liposomes were heated through the phase transition and the signal was completed eliminated.

3.2.2.4. Phospholipid concentration

After liposome formation and dialysis to remove unencapsulated Mn^{2+}, lipid concentration was determined according to the method of Bartlett (1959). A set of six phosphorus standards and triplicate aliquots (25 or 50 μl) of liposomes were heated at

160°C for three hours with 0.5 ml of 10N H_2SO_4. An additional 0.5 ml of 30% H_2O_2 was added to each sample, followed by overnight incubation at 160°C. The following day, 4.6 ml of 0.22% ammonium molybdate was added to a sample and mixed vigorously. A 0.5 ml aliquot of Amidol reagent (2,4-diaminophenol dihydrochloride) was then added to each sample with rapid mixing. All the samples were then placed in a boiling H_2O bath for 10 minutes to develop the color. The phosphate concentration of the liposome samples was determined by comparing their absorbance at 830 nm with that of the standards.

3.3. In Vitro Techniques

3.3.1. Tissue isolation

In order to measure the clearance of free and liposome encapsulated Mn^{2+}, it was necessary to collect blood from mice. Mice were anesthetized with chloral hydrate (52.5 mg/ml, 0.1 ml per 10 g body weight) and injected in the tail vein with LUV or free $MnCl_2$. At appropriate times (0 - 0.2 hours) after injection, with the mice still anesthetized, a 0.5-0.8 ml sample of blood was obtained by brachial laceration. The 1.0 ml syringe, into which the sample was drawn, was preloaded with 5 μl of sodium heparin. The blood sample was placed in a 1.5 ml centrifuge tube containing an additional 15 μl of heparin. The tube was capped and the blood and heparin thoroughly mixed to prevent clotting.

Liver samples for ESR or NMR measurements were taken from the same animals from which the blood samples were removed. Imme-

diately after the blood sample was obtained, the animal was sacrificed by cervical dislocation, and a midsagittal, subxiphoid incision was made, exposing the peritoneal cavity. The liver was quickly exteriorized and dissected away at its base. The organ was then blotted with a piece of tissue paper and weighed. It was placed in a glass vial and kept on ice. All NMR and ESR measurements were made within six hours of excision. Measurements during this period varied less than 5%.

3.3.2. NMR proton relaxation measurements

All relaxation measurements were made using an IBM Multispec PC-20 pulsed NMR spectrometer operating at 0.47T (20 MHz proton frequency). It is equipped with plug in ROM chips that allow the measurement of T_1 using an inversion recovery sequence and the measurement of T_2 using the Carr-Purcell-Meiboom-Gill (CPMG) sequence. In order to ensure that accurate results were obtained when using the PC-20, several premeasurement checks were required.

First, the fine adjustment of the magnetic field was made while visualizing the free induction decay (FID) on an oscilloscope following a 90^{o} pulse. The field was adjusted (shimmed) until the observed FID was in resonance and the length of the decay maximized. The oscilloscope was then used to set the optimum pulse width to obtain true 90^{o} and 180^{o} pulses. Finally, the probe was tuned in order to obtain maximum sensitivity. This was especially important when liver samples were measured. Their irregular shape in the NMR tube could cause the FID to be out of

phase, and so the probe tuning was always checked. Some of the relaxation measurements were made using a variable temperature NMR probe. The temperature in this probe was controlled by flowing N_2 gas through a dewar surrounding the NMR tube. Temperature variation from the top to the bottom of the sample in the tube was found to be $\leq 0.1^{o}C$. The variable temperature probe was able to control the temperature of the sample within a range of $\pm 0.1^{o}C$. When the variable temperature probe was not used, all measurements were made after the sample had equilibrated at $37^{o}C$, the equilibrium temperature of the sample probe of the Multispec PC-20. A thermocouple probe was used to measure the temperature of the sample before and after each measurement.

3.3.2.1. Free and LUV encapsulated Mn^{2+}

Relaxation measurements of solutions of $MnCl_2$ and of suspensions of LUV with and without encapsulated Mn^{2+} were made using a 650 - 700 μl sample. The pH of $MnCl_2$ solutions was 6.3 to 6.5. This was not adjusted to pH 7.4, in order to prevent the possibility of Mn^{2+} precipitation, which is seen at pH 7.8 and above. All LUV were made and diluted in Hepes buffered saline, which was adjusted to pH 7.4 in order to be suitable for later <u>in vivo</u> experiments.

3.3.2.2. Blood samples

Heparinized blood samples were measured in a manner similar to that used for liposomes. Most measurements were made at $37^{o}C$, except for the measurement of blood samples containing LUV made

from DPPC/DPPG. These measurements were made at 34-35°C, so that no leakage of Mn^{2+} would occur (LUV made from DPPC/DPPG begin to leak a small percentage of their contents as they near T_m).

The volume of some of the blood samples was quite small (100 - 200 μl). These samples were measured after adjusting the height of the sample in the probe to get the maximum signal from the receiver coil, as visualized on the oscilloscope.

3.3.2.3. Liver

T_1 and T_2 measurements on liver samples were made using procedures similar to those used for liposomes and blood. The irregular shape of the liver meant that the probe tuning needed to be checked after the insertion of each liver sample. For mouse liver measurements, the entire liver was used. For rat liver measurements, the front left lobe (approximately 1.5 g) was dissected away from the liver and used as a representative sample.

3.3.3. ESR Measurements

Samples of LUV and heparinized blood (50 μl) were placed in a quartz ESR sample tube and measured in the spectrometer using a time constant of 64 ms and a 4 minute scan time. For blood samples, measurements were made shortly after isolation and then repeated at approximately 3 hours after the first measurement to ensure that no degradation of the sample occurred during the time of the experiment.

Liver samples were sliced with a homemade sample holder to a size of approximately 5 mm^2 by 1 mm thick. Samples were taken

from the frontal lobe of the mouse liver. The tissue was weighed and then placed in an ESR quartz flat cell for measurement in the spectrometer. Samples weighed between 15-20 mg and were centered in the cavity to obtain maximum signal. Samples were kept on ice until the time of measurement. Measurement of a sample was done as soon as possible after excision, and some samples were repeated up to 4 hours later to determine if any deterioration in the sample could be observed.

3.3.4. Atomic absorption spectroscopy

Atomic absorption spectroscopy was used to determine the amount of Mn^{2+} present in liposomes and digested liver samples. To assay the level of Mn^{2+} in liposome samples, a wet ashing procedure was used [Goresuch, 1974]. For this procedure, 2 ml of 4:1 mixture of concentrated nitric and perchloric acid was added to the liposome sample (100 μl). The sample was then warmed on a hot plate at 85^{o}C until most of the liquid had evaporated and the solution was colorless. The sample ($\leq$ 1 ml) was carefully poured into a 5 ml volumetric flask. The beaker in which the digestion had taken place was then carefully rinsed with three washes of 1 ml of deionized, distilled water. The volumetric flask was then filled to the 5 ml mark.

For liver digestion, a dry ashing procedure was performed [Goresch, 1974]. The livers were weighed into tared 5 ml acid washed Pyrex beakers and then placed in a drying oven overnight at 105^{o}C. After drying, the samples were placed in a muffle furnace at 550^{o}C for 12 hours. This first ashing was not suffi-

cient for complete tissue digestion. After the samples had cooled, 20 μl of ash-aid (10% KSO_4 in concentrated HNO_3) was added to each beaker along with 500 μl of concentrated HNO_3. The concentrated nitric acid was slowly evaporated on a hot plate in a fume hood. When dry, the samples were placed again in the muffle furnace for 12 hours at 550^{o}C. This cycle of adding acid and ash-aid followed by 12 hours in the furnace was repeated one additional time, after which the tissues were found to be completely digested. The beakers were allowed to cool to room temperature. Then 50 μl of concentrated HNO_3 and 1.0 ml of water were added and the samples warmed on a hot plate. The contents were then transferred to a 5 ml volumetric flask for later analysis.

A Jarrell-Ash model 450 AA spectrometer was used for all measurements. Duplicate liver samples and duplicate or triplicate samples of LUV were measured. The amount of Mn^{2+} measured in LUV samples is given in units of millimoles per liter (mM), with the concentration reported representing the value that would be seen if the liposomal contents were distributed throughout the solution. The concentration of Mn^{2+} in liver was calculated as the percentage of injected dose per gram of liver tissue.

3.3.5. Phosphorus NMR measurements

Phosphorus NMR was also performed on excised mouse liver. Excised livers were kept on ice and then warmed to room temperature and placed in a 12 mm probe. After field adjustment, 4096 accumulations were made for a total acquisition time of 20 min-

utes. The control spectrum was taken and compared to the spectrum an animal given DPPC/DPPG liposomes containing $MnCl_2$. The liver containing liposomes was heated to 45°C for 10 minutes and then an additional measurement was made. Finally, the original control liver was measured again and the first and last spectra compared to ensure that no changes in inorganic phosphate level had occurred.

3.4. Tumor Model

The tumor model chosen for this study is a recently described mammary adenocarcinoma specific to Fisher 344 rats [Saini et al., 1987]. It has several characteristics that make it useful for liver imaging. First, it is an encapsulated tumor that grows slowly in the liver, allowing one to monitor its progress every few days. It does not metastasize, allowing a longer period for experimentation before the animal becomes gravely ill. Also, it remains in the liver parenchyma until it attains a diameter of approximately 1.5 cm or larger.

Tumor passage was carried out in young (90-110g) female Fisher 344 rats. The tumor was allowed to grow subcutaneously in the flank of the rat until it had attained a size of 1 cm in diameter. After the tumor had attained this size, the animal was sacrificed while under Metafane anesthesia. The tumor was quickly excised and placed in ice cold tissue culture media (Eagles minimum essential media). The tumor was then sliced into small 1 mm^3 pieces. The pieces were loaded into a 16 gauge

trochar and the tumor fragment implanted subcutaneously in the flank of a lightly anesthetized female rat.

For liver implantation, the tumor was excised and placed on ice as described above. Retired breeder Fisher 344 rats were placed under deep anesthesia using ketamine/acepromazine (10mg/100g body weight). The abdomen was shaved and rinsed with isopropyl alcohol. A small midsagittal incision of approximately 2 cm in length was made directly below the sternum and a lobe of the liver exteriorized. An 18 gauge trochar loaded with a small (1 mm^3) tumor fragment was then inserted into the liver parenchyma. The trochar was carefully withdrawn and the liver compressed until bleeding ceased. The wall of the peritoneum was then closed using 2.0 silk and the skin sutured with 5.0 silk to close the wound. The animals were kept warmed and monitored for 3 hours. Following recovery they were returned to their cages and given food and water.

3.5. Imaging Experiments

All imaging experiments were performed at St. Francis Medical Center in Peoria, IL. The system used was a 0.5T, Siemens whole body imaging system. Dr. Steven Wright of the MRI center assisted in the study by designing and fabricating the surface coils that were used to obtain the images on the small laboratory animals.

As was explained in Chapter 2, the appearance of the image in an NMR imaging experiment is dependent on the pulse sequences used to obtain that image. In these studies, four categories of

images were used: (1) very fast imaging sequences, which used short TR and TE values, and field gradient echoes; (2) spin echo sequences with short TR and TE values (e.g., TR=100 ms, TE=15ms; often referred to as "T_1 weighted sequences"); (3) spin echo sequences with intermediate TR and TE values (e.g., TR=600 ms, TE=35 ms); and (4) spin echo sequences with relatively long TE and TR values (sometimes referred to as "T_2 weighted sequences" TR=1000 ms, TE=105 ms).

In some images, several phantoms consisting of solutions of $MnCl_2$ at various concentrations were positioned next to the animals . These solutions were used as reference points for comparing intensity differences in different images. This makes it possible to compare changes in intensity in different images taken on different days or at different times.

In some cases, subtraction images are shown to compare the changes in intensity before and after the injection of a contrast agent. To obtain subtraction images without moving the animal, a 25 gauge catheter was implanted in the tail vein of the anesthetized rat. The catheter was connected to a syringe filled with 0.9% saline. The rat was then placed into the magnet and a precontrast image was taken. The saline filled syringe was then exchanged for one containing the agent to be injected. The injection was given and the second image recorded. If dynamic imaging was performed, a volunteer (MRN) was positioned in the magnet with the animals and the injection given between images.

CHAPTER 4

RESULTS

4.1. Liposome Characteristics

In previous work with LUV composed of DPPC and DPPG, the liposomes were found to be stable and easily formed with a high encapsulation efficiency [Magin and Niesman, 1984a; 1984b]. Because of these properties, this phospholipid composition was chosen initially to encapsulate $MnCl_2$. Since, divalent cations such an Mn^{2+}, and others like Ca^{2+} and Ni^{2+}, have been shown to be detrimental to liposome stability, causing liposome aggregation and fusion [Chauhan, 1986; Bentz, 1983], the first step in this study was to demonstrate that $MnCl_2$ could be encapsulated at a relatively high concentration (e.g., 50 - 100 mM). In additon, it was necessary show that LUV containing a high concentration of the compound were stable during storage and when injected into the bloodstream.

Several other liposome formulations were tested during the course of these experiments. These included the following compositions: (1) dipalmitoylphosphatidylcholine (DPPG) and dipalmitoyphophatidylglycerol (DPPG), 4:1 molar ratio; (2) egg phosphatidylcholine (PC) and egg phosphatidylglycerol (PG), 4:1 molar ratio; (3) PC/PG liposomes plus cholesterol (CHOL), in a 4:1:5 molar ratio, (4) PC, phosphatidylserine (PS) and cholesterol in a 3:1:3 molar ratio; (5) dimyristoylphosphatidylcholine (DMPG), dimyristoylphophatidylglycerol (DMPG) and cholesterol, 4.5:1:5:4

molar ratio, (6) DMPC, dimyristoylphosphatidyserine (DMPS) and cholesterol, 4.5:1.5:4 molar ratio.

Our original composition (DPPC:DPPG) was tested most extensively since its temperature sensitive property made it possible to make measurements before and after release of liposome contents. Additional liposomes were made using phospholipids containing unsaturated fatty acids (PC, PS, PG) or saturated fatty acids have phase transition temperatures at or below 37°C (DMPC, DMPG, DMPS). Further, phospholipids with the phosphatidylserine headgroup (DMPS, PS) were tested. These changes in phospholipid composition were in order to determine what effect the changes had on *in vitro* characteristics and the effectiveness of encapsulated $MnCl_2$ *in vivo* as a contrast agent.

The encapsulation efficiency of liposomes made with $MnCl_2$ was investigated using a radiolabel (^3H sucrose) and by measuring the amount of entrapped $MnCl_2$ using ESR spectroscopy and atomic absorption spectroscopy. Radiolabeled sucrose was added to the aqueous phase at tracer levels because the methodology used to measure the amount entrapped and released during storage was quite simple. The encapsulated sucrose behaves like other water soluble markers used in previous studies, and is a good measure of liposome integrity. Table 4.1 compares the results for encapsulation efficiency as determined by different methods. The peak height measurement in ESR only gives the amount of free Mn^{2+}, while the double integral measures free and bound Mn^{2+} (i.e., some Mn^{2+} is bound to the negatively charged DPPG). Double inte-

gral measurements were used for dose calculation for liposome injections.

In order to ensure that the ESR spectrometer could measure quantitatively the amount of Mn^{2+} in a sample a calibration curve was constructed using six different concentrations of a $MnCl_2$ atomic absorption standard. The samples were placed in 50 μl glass capillary tube for ESR measurements. The standard curve was linear throughout the range of concentrations measured (0.025 -3.25 mM) and is shown in Figure 4.1. Whenever ESR measurement of Mn^{2+} concentrations in liposomes were made, an atomic absorption standard was included as a reference.

The stability of LUV was measured by incubating the liposomes with 50% serum and monitoring the ESR peak height. A reduction in peak height occurs when the liposomes breakdown or leak, the released Mn^{2+} binds to protein or lipid in the solution, and the signal is broadened beyond detection (see Section 2.5; also Figure 4.5). The values for encapsulation efficiency and stability in fetal bovine serum for LUV containing $MnCl_2$ are given in Table 4.2.

The release of the liposome contents as they are heated through T_m was monitored in one experiment in which ^3H sucrose was incorporated in the aqueous phase as a tracer. The midpoint of release of the radiolabel was identical to that obtained in previous studies (40^oC). Also the maximum amount of release in serum at 40^oC after 5 minutes of heating was greater than 90%, in good agreement with previous results [Magin and Niesman, 1984a].

Thus, for all the parameters measured, the characteristics of temperature-sensitive liposomes containing high concentrations of $MnCl_2$ were found to be functionally equivalent to those that contain other markers. The encapsulation efficiency and release at T_m were nearly identical.

4.2. NMR Relaxation Measurements

In order to explain the relaxation behaviors seen *in vivo* after liposomes are injected, it is important to have a complete understanding of the relaxation process in the liposome system *in vitro*. It was necessary, therefore, to investigate the contributions made by each component of the LUV/$MnCl_2$ system to the relaxation process. The factors examined were: (1) the lipid bilayer phospholipids, (2) the aquaion in solution, (3) the Mn^{2+} bound to phospholipids, and (4) water exchange through the phospholipid bilayer, whereby Mn^{2+} inside the liposomes can relax the H_2O outside the liposomes.

4.2.1. Relaxation effects of phospholipids

Previous NMR experiments examining water exchange in phospholipid vesicles [Haran and Schporer, 1976; Andrasko and Forsen, 1973] did not mention any measurement of the contribution of the phospholipids to the relaxation process. In order to determine if the phospholipid content of the liposome has any influence on protein relaxation, measurements of the T_1 of pure buffer (T_{1b}) and liposome suspensions (T_{1s}) in the identical buffer solution were made. The phospholipid concentration was 30

mg/ml. The molar longitudinal relaxation enhancement was then calculated as follows

$$\text{MLRE} = \frac{1/T_{1s} - 1/T_{1b}}{\text{LIPID CONCENTRATION (mM)}} \qquad (4.1)$$

with the resultant value expressed in units of sec^{-1} mM^{-1}. The value obtained at 20 MHz for a suspension of DPPC/DPPG LUV at 37°C and pH 7.4 is 0.001 sec^{-1} mM^{-1}. Clearly the lipids have a negligible effect on T_1.

4.2.2. Relaxation effects of $MnCl_2$ in aqueous solution

Manganese has been known for some time to be an effective relaxation enhancing agent for water protons [Eisinger, et al., 1962; Dwek, 1973]. In a more recent paper [Kang, et al., 1984], the values at 37°C for MLRE (T_1 enhancement) and molar transverse relaxation enhancement (MTRE, T_2 enhancement) were measured using the same instrument (Multispec PC 20) and frequency (20 MHz) used in this study. No estimate for the error of the measurement was given in that paper, but a comparison of these values with the values in this study shows close agreement. For the MLRE, Kang et al. [1984] reported a value of 7.52 (sec^{-1} mM^{-1}) compared to a value of 7.8 ± 0.3 sec^{-1} mM^{-1} measured in this study (5 concentrations measured). The MTRE value of 41.6 compares closely to the value of 43.5 ± 1.0 found in this study. Thus, there is close agreement between these two sets of data performed with the same instrument at the same temperature and field strength.

4.2.3. Relaxation effects of bound $MnCl_2$

Manganese, when bound to macromolecules, becomes a very effective relaxation enhancing agent. This was shown previously for solutions containing Mn^{2+} bound to DNA [Eisinger, et al., 1962] and to proteins [Mildvan and Cohn, 1963; Ruben and Cohn, 1970; Navon, 1970]. A detailed study of the effects of Mn^{2+} binding to macromolecules in solution and to sites in tissue has been made by Koenig and associates [Koenig and Brown, 1984a; 1984b; 1985a; Koenig, et al., 1985]. Figure 4.2 adapted from Bacic et al. [1987] shows the relaxivity of free and liposome encapsulated Mn^{2+} over a range of field strengths. A peak in the relaxivity values of the liposome associated Mn^{2+} is due to the Mn^{2+} that is bound to the outer surface of the vesicle bilayer. This is similar to a peak reported for other negatively charged phospholipid vesicles [Koenig and Braun, 1985].

A more detailed study of Mn^{2+} bound to vesicles was performed at 20 MHz using Multispec PC-20. LUV made from DPPC and DPPG were tested at a phospholipid concentration of 25 mg/ml to determine their ability to enhance relaxation when Mn^{2+} was bound to the bilayer surface. Aliquots were added to achieve a range of concentrations from 0.01 to 3.2 mM $MnCl_2$. Measurements of the longitudinal relaxation decay over time were made and from this data the molar relaxivity (MLRE) was calculated. The values for MLRE were obtained using the theory outlined in Section 2.4.1, with the exception that Mn^{2+} was outside (not inside as presented there). The corrected value for T_{1o} was calculated and the value divided by the concentration of Mn^{2+} added. Figure 4.3 shows a

comparison of the values for the MLRE versus concentration of Mn^{2+}. The behavior in solution is flat. Conversely, the values for Mn^{2+} added to phospholipid vesicles decrease as the manganese concentration increases.

Two mechanisms contribute to this behavior. Free and bound Mn^{2+} both contribute to the overall enhancement. As more and more Mn^{2+} is added to the solution, the ratio of bound to free Mn^{2+} decreases, causing a decrease in the overall relaxivity. Secondly, as the number of bound Mn^{2+} ions increases, the probability decreases that a water proton that comes into contact with the bound Mn^{2+} will not have been previously relaxed. In other words, as the Mn^{2+} concentration goes up, many of the paramagnetic ions will interact with water protons that have already relaxed. Therefore, for these water protons, no effect on relaxation results from the additional manganese.

This type of behavior illustrates the complexity that may occur in vivo when biological samples contain many compartments that may bind, concentrate or exclude Mn^{2+}. What is apparent from these in vitro results is that when Mn^{2+} binds to the vesicle, its relaxation efficiently is greatly enhanced. An awareness of the magnitude of this effect is important for interpretation of the in vivo results of this study.

4.2.4. Measurement of the water permeability of the liposome bilayer

Belton and Ratcliffe [1985] give a thorough review of NMR measurements of water diffusion between compartments. This is an

important consideration in this research because the contribution of liposome encapsulated Mn^{2+} to increased relaxation rates in liver tissue will be different than the contribution due to released Mn^{2+} bound in tissues. Measurement of the bilayer permeability was accomplished using the method Conlon and Outhred [1972]. One significant change in the methodology was included. In experiments where the water permeability of the erythrocytes [Conlon and Outhred, 1972] and liposomes [Andrasko and Forsen, 1974; Haran and Shporer, 1976; Lipschitz-Farber and Degani, 1980] was measured, a high concentrations (30 mM) of Mn^{2+} was added to the buffer to reduce the T_1 in the external solution (fast relaxing compartment). However, because high concentrations of Mn^{2+} may alter the bilayer structure and thereby its intrinsic water permeability characteristics, a low concentration of Mn^{2+} (1.6 mM) was used for DPPC/DPPG vesicles. This approach was shown to give better results by Pirkle, et al., [1979] in the measurement of erythrocyte permeability. In my experiment with DPPC/DPPG liposomes, it was possible to use a low concentration of added Mn^{2+} because the water permeability of this bilayer was low, meaning less Mn^{2+} was required to distinguish the two components (i.e., the τ_i is long). Also, the LUV used have a larger diameter than the SUV previously measured, making a further contribution to the increased τ_i. Furthermore, Mn^{2+} bound to DPPG enhanced the relaxation so that less Mn^{2+} had to be added to distinguish the two components. However, it should be noted that the entire method is invalid if Mn^{2+} crosses the bilayer during the time of measurement. Confirmation of the fact that $MnCl_2$ did

not cross the bilayer was obtained by measuring the magnetization decay immediately after addition of $MnCl_2$ and again 24 hours later. The magnetization curves were identical. In contrast, the intracellular slow relaxing component was reduced by 50% when liposomes where incubated for 24 hours with Gd-DPTA.

Manganese was not used for the measurement of the residence time of PC/PG and PC/PS/CHOL liposomes (see Section 4.4.3). These liposomes contain unsaturated phospholipids (with T_m of < 30^oC, the measurement temperature). Liposomes containing phospholipids with unsaturated fatty acid side chain are more permeable to water above the phase transition and therefore a high concentration of Mn^{2+} would have been necessary to measure water exchange. Pirkle, et al. [1979] have shown that high Mn^{2+} concentrations (5 mM and higher) may lead to erroneous results. It also was feared that Mn^{2+} might cross the membrane of PC/PG liposomes lacking cholesterol. Therefore, it was necessary to employ a different relaxation probe.

The probe that was chosen, dextran-magnetite, is a 5 - 20 nm core of magnetite coated with dextran giving an overall particle size of approximately 30 - 40 nm. It has been shown to be quite effective at enhancing relaxation rates (R_2 [Ogushi, 1978; R_1 [Bacic, et al., 1984]). It was used in a study that measured the residence time of erythrocytes using the Conlon and Outhred method [Ashley and Goldstein, 1980]. It does not bind to the lipid bilayer and it has no effect on the osmolarity of the solution at the concentration needed to perform the measurements. The results obtabined by Ashley and Goldstein showed that the resi-

dence time measured when dextran-magnetite was used was equal to the value obtained when a low concentration of Mn^{2+} was used.

The residence times for liposomes of different phospholipid compositions are given in Table 4.3. Also given in the table are values for the diffusional water permeability (Pd) calculated as $Pd = r/3\tau$ where r is the vesicle radius and τ is the residence time [Haran and Shporer, 1976]. The average radius of DPPC/DPPG LUVs measured previously was 100 nm [Magin, et al., 1984a]. This value was used in calculations for both types of vesicles. Since no channels are present in the artificial membranes, diffusional water permeability is approximately equal to the osmotic water flux through the membrane (Pf) [Deamer and Bramhall, 1986]. Therefore, values of Pf obtained by Carruthers and Melchoir [1983] can be used for comparison. These were the only measurements in the literature of liposome water permeability that did not seem to have a flaw in experimental design (e.g., Haran and Shporer [1976] assume unilamellar vesicles and show a micrograph containing multilamellar vesicles). The data obtained by the two methods are in good agreement. Calculation of these values makes it possible to determine whether the water permeability of the liposome is a critical factor controlling contrast changes in vivo.

4.3. Evaluation of Manganese Toxicity in Mice

Data in the literature suggests that "Manganese is the least toxic of all trace metals" [Zlotkin, 1985] and on the other hand that manganese is "quite toxic" [Venugopal and Lucky, 1978]. Some

data exists on the toxic levels, but much of the data expresses toxicity in less than useful measures, such as LD_{100} or minimum lethal dose (MLD). Therefore, the acute toxicity of $MnCl_2$ given intravenously to mice was evaluated.

Although manganese is a very effective chemical for increasing the relaxation rates of water protons, it is a divalent metal ion and therefore is significantly toxic when injected into animals [Venugopal and Luckey, 1978]. Normally one would find the values in the literature for the toxic level (LD_{50}) of the compound when injected intravenously, and then compare this to the dose needed to elicit the desired response (e.g., the dose needed to double the relaxation rate). Unfortunately, the data in the literature [i.e., Venugopal and Luckey, 1978] expresses toxicity as the lethal dose to kill 100% of the animals (LD_{100}) or the minimum lethal dose (MLD). As pointed out by Goldstein, et al. [1974], neither of these two measures of toxicity is very useful. Therefore, the acute toxicity of $MnCl_2$ was evaluated by measuring the dose necessary to cause death to 50% of the animals (LD_{50}) after intravenous injection. The toxicity of lipid vesicles alone has been evaluated previously and reviewed [Mayhew and Papahadjopolous, 1983}. Although long term administration of liposomes may induce some low grade toxicity, the acute toxicity of liposomes injected at the concentrations injected here (i.e., as high as 30 mg/ml) has not been seen; therefore, the toxicity of empty liposomes was not evaluated.

Work by others [Wolf and Baum, 1983; Mendonca-Dias, et al., 1984] suggested that the acute toxic effects of intravenous $MnCl_2$

are due to disruption in the cardiac cycle. Related to this is the fact that it was noted in the course of this study that the rate of injection appeared to have an impact on mouse survival after injection. Therefore, the injections were given slowly, averaging about 1.75 minutes to administer (range 1.5 - 2.0 minutes). The volume injected was kept below 10% of the total blood volume of the mouse, the solution was made to be isotonic (280 -300 mOsm range), and the solution pH kept between 6.5 and 7.0. The injection volume was 0.05 ml/10 g body weight.

The results of the toxicity experiment are listed in Table 4.4. As can be seen, the number of deaths increases sharply with a small increase in the dose. At 400 μmole/kg, deaths after the injection were quite rapid, with all animal deaths occurring within 4 minutes after the injection was completed. In fact, of the 20 deaths recorded in this study 18 occurred within 10 minutes after the injection. The other deaths (2) occurred between 1 and 2 hours after injection. After 1 week, all of the surviving animals appeared normal with no apparent signs of ill health.

Probit analysis was used to determine the LD_{50} for intravenously injected $MnCl_2$. [Goldstein, et al., 1974; Litchfield and Wilcoxen, 1949]. The graph showing the results of the probit analysis is shown in Figure 4.4. The LD_{50} calculated from the data is 272 μmole/kg with the 95% confidence limits ranging from 227 - 326 μmole/kg. This is in close agreement with an LD_{50} of 0.22 mm/kg reported by Wolf, et al. [1985].

After determining the toxicity of intravenously injected free $MnCl_2$, the toxicity of liposomes containing Mn^{2+} was

examined. Because liposomes can only encapsulate a certain amount of $MnCl_2$, 135 μmole kg^{-1} was the highest dose that could be given (in DPPC/DPPG liposomes). Analysis of the dose response curve (Figure 4.4) leads to the prediction that approximately 1.5% of the animals given this dose in free form are likely to die. As is shown, none of the animals given an injection of liposome encapsulated Mn^{2+} died. In order to determine that liposomes did not increase the toxicity of free Mn^{2+}, liposomes were heated, releasing the $MnCl_2$, and this suspension of liposomes and free Mn^{2+} was injected. No deaths resulted in this group. Since the PC/PS/CHOL vesicle encapsulated less than half of the amount entrapped with DPPC/DPPG liposomes, toxicity experiment with these vesicles were not done.

It was noted, however, that animals receiving 135 μmoles/kg $MnCl_2$ in liposomes did not exhibit the gasping and wheezing behavior seen in mice before death at high doses and present to some extent in mice given $MnCl_2$ in free form at lower doses (e.g., as low as 50 μmoles/kg).

4.4. Animal Experiments

Several sets of experiments were carried out to determine how liposome encapsulated $MnCl_2$ would be processed by the liver after intravenous injection. Particular attention was given to liposomes made from DPPC and DPPG. In many experiments, the ability to heat these liposomes, release their contents, and then make another measurement after release of the internal contents proved invaluable. Outlined below are the results of NMR, EPR,

and atomic absorption spectroscopy experiments performed on tissue samples from male B2D6F$_1$ mice.

4.4.1. Effect of free $MnCl_2$ injection

It was necessary to measure the effect of intravenously injected $MnCl_2$ on liver relaxation rates. Single doses were given at 2.5, 5, 10, and 25 μmoles/kg. A large reduction in T_1 was expected, as has been previously described [Mendonca-Dias, 1983; Koenig, et al., 1984]. Figure 4.5 shows the graph of the longitudinal relaxation rate (R_1;T_1^{-1}) versus the injected dose of free $MnCl_2$. The graph is linear in the range of doses given (0 to 25 μmole/kg). The data shows how effective $MnCl_2$ is at enhancing relaxation rates at 20 MHz. A dose of 20 μmole/kg, more than 10 times less than the LD_{50}, increases the R_1 of mouse liver by a factor of more than five (5.6).

Careful examination of the relaxation decay shows single exponential behavior at the low doses and at the highest dose the behavior is nonexponential.

4.4.2. Effect of liposome encapsulated $MnCl_2$ injection

Previous work in which magnetic resonance images of mouse liver were obtained after injection of liposome encapsulated $MnCl_2$ [Magin, et al., 1986b] had suggested that in the first hour after injection, $MnCl_2$ was not as effective at reducing relaxation times as was free $MnCl_2$. Therefore, liposomes containing $MnCl_2$ (25 μmole/kg) were injected intravenously into mice and the livers excised at various times after injection. In this preli-

minary experiment, single mice were sacrificed at each time point and the T_1 measured at 35°C. The results are displayed in Table 4.5. The results show that over the course of 2 hours, the liposomes break down gradually. However, heating of the livers to 45°C for 10 minutes and remeasuring the T_1 at 35°C shows that a majority of the Mn^{2+} present in the liver is not effective at reducing T_1. It can be released upon heating and become effective at reducing relaxation times.

The same data are shown in Figure 4.6 as a bar graph of liver and blood R_1 values before and after tissue heating. The data are presented to show the large differences in relaxation before and after heating. $MnCl_2$ is present in both blood and liver, but in the encapsulated form, the paramagnetic ion does not influence a large number of water protons.

These initial experiments suggested that the breakdown of DPPC/DPPG liposomes in the Kupffer cells was a somewhat slow process, taking several hours or more to complete. Since humans whose intake of manganese is greater than total body stores rapidly eliminate it from the liver (halflife of elimination equals 1.5 days; [Mahoney and Small, 1968]), it was thought that the manganese might possibly be excreted in the bile as it was released from the vesicles. It seemed appropriate to ascertain whether another liposome composition could be found that might be degraded more quickly, giving rise to a higher peak manganese concentration.

In order to determine whether a more rapid break down of liposomes in Kupffer cells was the cause of more rapid increase

in relaxation rates, it is necessary to monitor several factors. One should ideally be able to monitor the clearance, uptake, and breakdown of the liposome in vivo. In the experiments that are described below, atomic absorption spectroscopy was used to quantify liver uptake of Mn^{2+}, and ESR spectroscopy was used to measure clearance of Mn^{2+} from the blood stream and to provide a measure of liposome integrity in the liver. Before these extensive experiments were initiated, several possible liposome compositions were screened in order to find the best possible candidate to test and to compare with liposomes made from DPPC/DPPG.

4.4.3. Breakdown of liposomes with varying lipid compositions

Since it was apparent that liposomes composed of DPPC/DPPG were not going to be effective at inducing large reductions in T_1 and T_2 within 2 hours (unless the liver was heated), liposomes with different lipid compositions were produced and evaluated to determine if, in fact, the lipid composition had an effect on the time needed to degrade the vesicle. It has been shown that liposomes containing phosphatidylserine (PS) are taken up more rapidly by Kupffer cells [Spanjer, et al., 1986]. In addition, hydrolysis of phospholipids by phospholipase A is at a maximum near and above T_m [Vandenbranden, et al., 1984], suggesting that lipid with unsaturated fatty acid would be degraded more quickly.

Table 4.2 shows the encapsulation efficiency and stability of several liposome preparations that were screened for possible use as quickly degrading compositions. The PC/PG liposomes proved too unstable for further testing and liposomes made from

PC/PG/CHOL did not have a high enough encapsulation efficiency to be useful. The other four combinations were tested in mice. Each was diluted to an equal Mn^{2+} concentration to be injected intravenously via the tail vein.

The mice were each given an i.v. injection of liposomes diluted to 5.0 mM total Mn^{2+}. (0.05 ml injection per 10 g body weight; final dose 25 μmoles/kg.) Three mice were sacrificed at each time point (1 and 2 hours). The results of this experiment are shown in Table 4.6.

The data in the table clearly show that DPPC/DPPG LUV are the least efficient at reducing relaxation times. They apparently released Mn^{2+} more slowly than any other composition. Liposomes composed of PC/PS/CHOL are apparently degraded the most rapidly. The T_1 and T_2 times were nearly as low as those seen when the DPPC/DPPG liposomes were heated and release their contents.

4.4.4. Liposome clearance

The results shown in Section 4.4.3 indicated that liposomes composed of PS/PC/CHOL brought about an increase in relaxation rates much faster than did DPPC/DPPG liposomes. To determine whether this difference was influenced by rate of clearance of each liposome composition from the blood, the rate of clearance of PS/PC/CHOL liposomes was compared with the clearance of DPPC/DPPG liposomes. The results for PC/PS/CHOL liposomes are the means of three animals at each time point. The results for DPPC/DPPG clearance are compiled with each point representing 6

animals. The data points are plotted with error bars representing the standard error of the mean. Both liposome suspensions were filtered through 0.4 μm polycarbonate filters [Szoka and Papapahadjopoulos, 1980] to reduce the heterogenity of the size distributions and to allow the clearance comparison to be made using liposomes of approximately the same size. The two compositions of liposome have different encapsulation efficiencies. Therefore, if the dose of Mn^{2+} injected was to be the same, then the concentration of phospholipid injected would not be identical. For the clearance experiments, phospholipid dose was kept as constant as possible. Liposomes formed using DPPC/DPPG were injected at a phospholipid concentration of 7.2 mg ml^{-1} and PC/PS/CHOL liposomes were injected at 14 mg ml^{-1}. The mice receiving injections of DPPC/DPPG liposomes were given 0.1 ml per 10 g weight daily and the PC/PS/CHOL liposomes were given in a volume of 0.06 ml per 10 g body weight. Therefore, the total phospholipid dose for DPPC/DPPG was 100 μmole total lipids and for PC/PS/CHOL was 112 μmoles total lipids or nearly the same dose. The amount of $MnCl_2$ in the blood representing 100% was calculated assuming a blood volume of 8% of total body weight [Hwang, 1987].

The clearance curves for both liposome types are shown in Figure 4.7. As can be seen from the data, more than 90% of both vesicle types are removed from the circulation 2 hours after the injection. The clearance of PC/PS/CHOL vesicles appears almost first order while the DPPC/DPPG liposome have a slower clearing component. Possible reasons for the differences are outlined in Section 5.2.1. The clearance of free $MnCl_2$ was reported pre-

viously in this strain of mice [Magin, et al., 1986b] and in dogs [Atkins, et al., 1979]. In all species, 95% or more of free $MnCl_2$ is cleared from the circulation in one minute. The mouse data was obtained with dose levels nearly identical to the present study. The clearance of Mn^{2+} from the blood is quite rapid, and so the clearance of free Mn^{2+} versus time is not shown.

4.4.5. Liver uptake of liposome encapsulated $MnCl_2$

Atomic absorption spectroscopy was used to measure the total uptake of Mn^{2+} into liver tissue. Duplicate samples of each liver from the clearance experiments were analyzed for manganese content. The amount of manganese present in these livers at each time point is reported as percentage of dose per gram of tissue.

The results are given in Table 4.7. They show that at the earlier time points, where the two clearance curves are similar, the uptake in the liver is similar for both types of liposomes. However, at 2 hours, where the clearance of PC/PS/CHOL is essentially complete, the liver uptake of Mn^{2+} is greater than that seen in animals injected with DPPC/DPPG vesicles.

4.4.6. The state of Mn^{2+} in the blood and liver as determined by ESR

Although there are quantitative differences in the uptake of Mn^{2+} into the liver, the differences in amount are not sufficient to account for the differences in relaxation times seen after injection of the two types of liposomes. In order to investigate

the state of Mn^{2+} in the liver (i.e., free versus bound), ESR spectroscopy was employed to examine blood and liver samples.

As was explained in Section 2.5, the ESR spectrum of Mn^{2+} is extremely dependent upon its environment. In order to verify that this technique was applicable in vivo, a sample of blood was taken 30 minutes after injection of DPPC/DPPG liposomes containing Mn^{2+}. A spectrum was recorded, the sample was heated, and the spectrum recorded again. Figure 4.8 shows the two spectra. The spectrum measured after heating is reduced by nearly 70% when compared to that before heating. Thus, free Mn^{2+} must be present in the blood, probably sequestered in the liposomes, where it is rotationally free and gives a strong signal. When released and bound to proteins in the plasma, the signal is reduced. The signal is not entirely eliminated, and this is most likely due to the saturation of high affinity binding sites in the blood. A titration experiment showed that the blood was saturated (i.e., free Mn^{2+} signal appeared in the ESR measurement) when Mn^{2+} was added to a final concentration of 1 mM.

This method was used to determine the state of Mn^{2+} in the liver. DPPC/DPPG LUV were injected at a dose of 26 μmole kg^{-1} and the mouse was sacrificed 30 minutes after liposome injection. Figure 4.9 shows 4 spectra taken after the liver was excised. Spectrum A was recorded immediately after liver excision. The liver was heated to 42^{o}C for 10 minutes and then Spectra B was recorded. The peak height was reduced by 60%. After 40 minutes, Spectra C was recorded. The second peak now measures only 20% of its original height, probably because of released Mn^{2+} diffusing

away from its site of release and binding to more distant sites in the liver. The figure also shows an injection of free Mn^{2+} at the same dose for comparison.

This experiment provided evidence that the state of Mn^{2+} in the liver could be monitored using the ESR spectra. Therefore, experiments were performed using both DPPC/DPPG liposomes and PC/PS/CHOL liposomes. ESR spectra were taken from livers excised at various times after injection. The signal height (2nd peak, peak-to-peak height) was then measured for livers from three different animals at each time point. Background spectra were taken at ten times higher gain to ensure a flat baseline.

In order to make a meaningful comparison, the results of the two experiments were normalized to the same gain setting. This number was then divided by the amount of Mn^{2+} present in the tissue at the time of excision as determined by atomic absorption spectroscopy. The number arrived at then is the signal height (free Mn) per μmole of Mn present in the liver. This value then represents a measure of the breakdown of the liposomes in the liver.

The results of these experiments are shown in Table 4.8. As can be seen in the table, the peak height per μmole of Mn^{2+} is much higher with DPPC/DPPG liposomes at every time point measured. Thus, the breakdown and release of Mn^{2+} must be proceeding more rapidly in PS/PS/CHOL liposomes.

4.4.7. Phosphorus NMR of excised liver

Phosphorus NMR of excised liver tissue was done after the

injection of DPPC/DPPG liposomes in order to confirm that Mn^{2+} was localized in hepatocytes after release from Kupffer cells. Because hepatocytes contribute nearly 80% of the volume of the liver, [Blouin, et al., 1977] almost 100% of the inorganic phosphorus signal (P_i) originates from the hepatocytes. Further, Mn^{2+} is a very good broadening agent for P_i (P_i is negatively charged), such that a low concentration Mn^{2+} in the same compartment will totally broaden the P_i signal beyond detection.

In Figure 4.10, the signal from P_i in the control liver is fairly large, superimposed on a broad sugar phosphate peak. Once the liver is heated and the Mn^{2+} released from the liposomes, the P_i peak is eliminated, strongly suggesting that Mn^{2+} is in the hepatocytes. Schramm and Brandt [1986] have shown that Mn^{2+} is carried into hepatocytes by facilitated diffusion. Therefore, it is not surprising that Mn^{2+} that escapes the Kupffer cell is then found to diffuse into the cytoplasm of the hepatocyte. However, since the liver here was excised and not living, it was not possible to eliminate the alternate explanation that the breakdown of the plasma membrane allowed Mn^{2+} to leak into the hepatocytes.

4.4.8. Measurement of water premeability of hepatocytes

In the process of completing work on a related manuscript, Dr. Goran Bacic has recently measured the water permeability of mouse hepatocytes [Bacic, et al., manuscript in preparation]. The isolation of hepatocytes was accomplished according to the procedure of Gravela, et al., [1977] and resulted in cells that were > 90% hepatocytes and > 95% viable as measured by trypan

blue exclusion. A suspension of 1 x 10^7 cells was mixed with dextran magnetite (DM) to a final concentration of 5 mg DM/ml. The T_1 measurements were made at 37^o and 0.5 T using the PC-20. Measurements were made in 5 minutes or less so no cell death or settling occurred. Analysis of the two component relaxation curve gave a T'_{1i} = 61 ms. Since the sample is now in slow exchange condition, $1/\tau_i = 1/T'_i - 1/T_{1i}$ where T_{1i} is the T_1 in the cell with no relaxation agent (340 ms). Therefore, the residence time of water inside the hepatocyte, τ_i = 74 ms. Using the y-intercept of the relaxation curve to obtain the total internal volume and knowing the number of cells present (counted in a light microscope), the volume of an individual mouse hepatocyte was calculated as 11.3 x 10^{-9} ml. With this volume, the radius of the hepatocyte is calculated as $V = 2\pi r^3$ and r = 12.2 μm, which is in agreement with observations of these cells under the light microscope. Therefore, if one wishes to calculate a diffusional permeability (Pd) of water through the membrane of these cells, the formula used is $Pd = V/A\tau_1$ and a Pd = 6 x 10^{-3} cm/s results. This is two times greater than the value measured for erythrocytes, but is close to epithehlial cells [Finkelstein, 1984]. This calculation assumes spherical geometry, a shape hepatocytes are known to assume in suspension after isolation from liver tissue.

4.5. Tumor Imaging

The hypothesis underlying this research was the idea that normal liver has a large complement of Kupffer cells that effi-

ciently remove liposomes from the circulation. Because of this, it was thought that liposomes would not penetrate tumors to any extent before being removed from the circulation. If this [Poste, 1983; Weinstein, 1987] proved to be the case, then encapsulation of Mn^{2+} in LUV should increase the contrast difference between normal and diseased tumor.

The first experiment performed was to characterize the response of the tumor to free Mn^{2+}. Tumors in two sites were imaged. In one image (not shown), a flank tumor used for passage of the tumor cell line was imaged before and after the injection of $MnCl_2$ (25 μmole/kg). Before the injection, the tumor mass was visible on the animals left side. After injection there was considerable brightening of the tumor in the image suggested that the tumor took up $MnCl_2$, or $MnCl_2$ was bound to the surface of some fraction of the tumor cells.

This same response was seen when images were taken of a tumor implanted in the liver. The control images of tumor are shown in Figures 4.11 and 4.12. After injection of free Mn^{2+}, the tumor, which can be visualized in a T_1 weighted image (Figure 4.13, TR = 100 ms TE = 100 ms), is no longer distinguishable from normal liver tissue after the injection of $MnCl_2$ (Figure 4.13). Both liver and tumor had short relaxation times and appeared bright with this pulse sequence.

Figure 4.12 also shows the R3230AC tumor in the liver. This image was taken before injection of PC/PS/CHOL liposomes (35 μmole/kg. After injection one can see the definite improvement

enhancement was apparent 15 minutes after injection and peaked after 30 minutes. It was constant for the next 90 minutes.

Relaxation measurements were made on excised livers and tumors from rats. The data are shown in Table 4.9. Also shown are the results of measurements made after injections of PC/PS/CHOL. The dose for free and encapsulated Mn^{2+} is the same (35 μmole/kg). The table shows that the liposomes had a greater effect on the liver than they did on the tumor. This was most apparent in T_1.

CHAPTER 5

DISCUSSION

The discussion of the results of these experiments is divided into four major sections. The first section examines the characteristics of the various liposome compositions tested during the course of the thesis research. The importance of understanding the properties of each preparation and how these characteristics influence in vitro behavior is emphasized. The second section discusses the in vivo experimental data for the two compositions most thoroughly studied; DPPC/DPPG and PC/PS/CHOL liposomes. In the third section, the results are explained in terms of a model of uptake and breakdown that takes into account important features of liver anatomy. The fourth section discusses results of imaging experiments in an animal (rat). The advantages and disadvantages of liposome encapsulated $MnCl_2$ as a liver specific contrast agent will be summarized in Chapter Six.

5.1. Liposome Characteristics

Divalent cations, such as Ca^{2+}, Mg^{2+}, and Mn^{2+}, are known to have potentially detrimental effects on liposome structure and stability. For example, 1 - 10 mM concentrations of Ca^{2+} have been shown to cause lipid vesicle fusion [Bentz, 1983] and gross changes in ultrasonic absorption properties and differential scanning calorimetry characteristics [Ma, et al., 1987]. Calcium also shifts the temperature at which temperature sensitive LUV release their contents by as much as 1.0^{o}C [H. Chan and R. L.

Magin, unpublished]. Therefore, it was necessary to make liposomes from several different phospholipids and determine if a high concentration of $MnCl_2$ could be encapsulated in vesicles that would remain stable for an extended period. Manganese was encapsulated at 100 mM because this concentration is approximately isotonic when compared to blood (300 mOsm). Measurement of the osmolarity of the solution gave a valve of 275 mOsm, close to the desired value.

The data in Table 4.1 shows that DPPC/DPPG liposomes encapsulate over 20% of the manganese originally present in the aqueous phase. This is slightly lower that the 30% capture routinely achieved when DPPC/DPPG liposomes were made with encapsulated cytosine arabinoside [Magin and Niesman, 1984a; 1984b]. However, the cytosine arabinoside vesicles are made in low ionic strength buffer which increases the encapsulation efficiency; the 20% value is in good agreement with previous data obtained by others using a high ionic strength aqueous phase [Szoka and Papahadjopoulos, 1978]. The release of the vesicle contents after heating was identical to previous results [Magin and Niesman, 1984a], and this property of the liposome proved useful for examining relaxation times and taking ESR spectra after the Mn^{2+} was released from the vesicles.

Since liposomes were successfully made using DPPC/DPPG, other phospholipid compositions were formulated and their encapsulation efficiency and stability evaluated. The data, shown in Table 4.2, indicated that vesicles containing cholesterol were as stable as DPPC/DPPG vesicles. It appeared that the liposomes

containing saturated phospholipid capture more than the vesicles containing unsaturated phospholipid, but the sample size here was too small to make a general conclusion. The PC/PC vesicles were not used for *in vivo* testing due to their instability; they were used in *in vitro* tests of membrane permeability in order to compare results obtained using Dextran-Magnetite with previous studies (see Table 4.3).

It was extremely important to show that the vesicles were stable in serum, which simulates liposome stability in the blood. Previous work [e.g., Bertinchamps, et al., 1966; Papavasiliou, et al., 1966; Mendonca-Dias, et al., 1984] has shown that free manganese goes to the liver after injection and that blood clearance is quite rapid [Cotzias, et al., 1960; Mendonca-Dias, 1984; Magin, et al., 1986b). If the liposomes were unstable in the blood and broke down, releasing their contents into the blood to be transferred to the liver to some extent, no valid conclusions could be reached. The stability in serum (Table 4.2) implies that the vesicles are stable in blood and the clearance data (see Figure 4.7), which shows a much slower blood clearance for liposome encapsulated Mn^{2+} than the clearance of free Mn^{2+} previously published [Mendonca-Dias, et al., 1983; Magin et al., 1986b] strongly suggests that no breakdown occurred.

Liposome encapsulated manganese may exert an effect on the water protons outside the vesicle if water molecules can diffuse through the membrane and be relaxed by the entrapped paramagnetic ion. The magnitude of this effect can be predicted if the water permeability of the vesicle bilayer is known (see [Belton and

Radcliffe, 1985], for a complete discussion of relaxation in two compartment systems). Since it was thought that this permeability might limit the interaction of Mn^{2+} with the water protons in the liver, the permeability of several formulations was measured. The data (Table 4.3) agrees with the more recent data in the literature [Carruthers and Melchoir, 1983; Deamer and Bramhall, 1986]. There is some disagreement with earlier studies that used high manganese concentrations [Andrasko and Forsen, 1974] and measured liposomes after passing them through the phase transition [Lipshitz-Farber and Degani, 1980]. However, both of these studies used SUV, which are more likely to be unstable with Mn^{2+} added to the solution.

The data indicate that the water permeability of the LUV liposomes made for this project does not differ significantly from the values measured by others. The permeability values are useful for determining later the amount of interaction that can occur between encapsulated Mn^{2+} extra-liposomal water. By using the simple equation for diffusion (Section 5.3) one can calculate roughly how far water can diffuse to be relaxed and compare this to the water exchange time.

Figures 4.2 and 4.3 emphasizes the importance of another factor, the increased relaxivity of bound Mn^{2+}. The NMRD curve in Figure 4.2 shows a peak at 20 MHz for liposomes containing Mn^{2+}. This corresponds to the water relaxed by Mn^{2+} bound to the outer membrane surface of the liposome bilayers. The Mn^{2+} inside the liposome is at a high concentration (100 mM) and the water in the liposome has s $T_1 < 1$ ms and is "invisible" because of the long

dead time of the machine (> 50 ms). Figure 4.3 shows data specifically at 20 MHz.

In Figure 4.3, when liposomes were present in the solution, nearly all the Mn^{2+} was bound at low concentrations. As more Mn^{2+} is added, the liposomal binding sites are becoming saturated and the relaxivity decreases as more Mn^{2+} is added. The behavior of a solution of Mn^{2+} without liposomes ("free") is shown for comparison. These results suggest that in vivo, the higher the percentage of Mn^{2+} present in the tissue that becomes bound to protein, the more efficient the relaxation process will be.

Thus the experiments characterizing liposome behavior indicate that the vesicles are stable with entrapped Mn^{2+} and can be used to study liposomal contrast agent delivery in vivo. The data also indicates the important role binding of Mn^{2+} plays in enhancing relaxation rates.

5.2. In Vitro and In Vivo Experiments.

Work by Koenig and Brown [1985] with rabbit liver and Mendonca-Dias, et al. [1984] with dog liver showed that Mn^{2+} localized in the liver after intravenous injection reduced T_1 in the tissue significantly. The dose response curve shown in Figure 4.5 was done with individual animals to confirm that the doses used in rabbits and dogs were acceptable for mice. The results show that a dose of 25 μmole/kg increases the relaxation rate by a factor of six. To achieve this dose in mice using an injected volume of 0.15 ml, a solution of 5 mM $MnCl_2$ is needed. Since it was possible to entrap Mn^{2+} at this concentration in several

different liposome formulations, (Table 4.2) each type was injected into mice and the time course of the change in relaxation times followed. Table 4.5 shows the relaxation times after one and two hours after an injection of an equal dose of Mn^{2+} using the four compositions. Unheated DPPC/DPPG liposomes were slower at changing relaxation times than any other composition. Liposomes formed from PC/PS/CHOL brought about the most rapid reduction in T_1 and T_2. These two preparations were selected for more careful study.

5.2.1. Liposome clearance

The clearance of the liposomes from the blood as measured by ESR is shown in Figure 4.7. Initially, the DPPC/DPPG vesicles cleared somewhat faster then the PC/PS/CHOL LUV. The PC/PS/CHOL liposomes continue to clear at the same rate while the DPPC/DPPG liposomes seem to have a slower clearing second component. The liver uptake, as measured by atomic absorption spectroscopy, does not totally parallel this behavior. Liver uptake is greater at every time point for PC/PS/CHOL liposomes. This result may be explained by uptake of liposomes in other organs that were not assayed, especially the spleen, which in some cases may trap a large amount of liposomes [Magin, et al., 1986a; Weinstein, 1987]. Alternatively, the PC/PS/CHOL liposomes may be more efficiently removed from the circulation by Kupffer cells. Spanjer, et al. [1986], (Figure 5.2) have shown results that support this hypothesis. The atomic absorption data on liver Mn^{2+} levels is consistent with the ESR data that shows the uptake being com-

pleted after 60 minutes with PC/PS/CHOL vesicles. It also shows the liver uptake of Mn^{2+} from DPPC/DPPG vesicles plateaued after 90 minutes, which corresponds to a flat portion of the clearance curve.

The clearance experiments measured the removal of the liposomes from the blood, but they do not provide any information on the breakdown of the vesicles in vivo. Hwang [1987] has shown the value of measuring liposome breakdown (i.e., the state of liposome) in vivo using gamma-emitting radioisotopes and perturbed angular correlation spectroscopy (PAC). However, only a few instruments capable of this measurement exist. To obtain this type of information, ESR was used to monitor Mn^{2+} release in excised livers. It had been shown previously that the Mn^{2+} spectra is very sensitive to state of ion, depending on whether it was bound to a macromolecule or free in solution (see Section 2.6). Figures 4.8 and 4.9 show the spectra from blood and liver respectively. The liver data showed that it was possible to monitor the breakdown of the vesicle in vitro after liver excision.

More extensive experiments to quantify this breakdown were performed. Table 4.8 shows the data quantifying the breakdown of vesicles. The ESR signal height in arbitrary units was divided by the amount of Mn^{2+} present in the tissue. The larger the peak height, the less Mn^{2+} had been released. At every time point, PC/PS/CHOL liposomes show more breakdown. However, the errors are large. This is most likely a result of the small sample size that could be accommodated in the ESR spectrometer. This small

sample size may lead to errors if the liposomes are not uniformly distributed in the liver. Each sample took approximately 10 minutes to measure and so to do measurement of samples from 15 - 20 animals took considerable time. Only one 15 - 20 mg sample out of each 1.0 - 1.4 gm liver was measured. Still, at the last three times measured, the values were significantly different at the $p < 0.05$ level, indicating that PC/PS/CHOL liposomes released their contents more rapidly.

If manganese was being released from the liposomes, then it would be useful to know the location of the ion after release. Was the ion entering hepatocytes? Schramm and Brandt [1986] have given evidence for facilitated diffusion as the mechanism of Mn^{2+} uptake by hepatocytes. This implies that any Mn^{2+} that left the Kupffer cells due to exocytosis would be taken into hepatocytes very efficiently. To determine if Mn^{2+} was located intracellularly in hepatocytes, ^{31}P NMR was performed on excised liver after injection of DPPC/DPPG liposomes. These liposomes were injected and the ^{31}P NMR inorganic phosphate peak (Pi) was measured. Since hepatocytes contain almost 80% of the volume of the liver and Kupffer cells contain only 3% of the volume, the Pi peak measured arises almost exclusively from hepatocytes. If DPPC/DPPG liposomes were injected into mice and the animal sacrificed after 90 minutes, the peak was reduced. However, if the liver was heated, the contents of the vesicle were entirely released, eliminating the peak. The spectra could be interpreted to suggest that free Mn^{2+} released from Kupffer cells does enter hepatocytes. As has been shown previously, a small amount of

Mn^{2+} if the compartment of interest (in the hepatocyte) will be much more effective at increasing relaxation rates that a large quantity outside of the compartment. The ^{31}P data, along with the ESR and NMR data, strongly suggest that Mn^{2+} is most effective when released from Kupffer cells, and that following release, some of the Mn^{2+} is taken into hepatacytes. However, since these measurements were made in excised livers, it is difficult to be absolutely positive that these results are not due to the breakdown seen in dying tissue.

5.3. Model for Liposome Uptake

Liposomes deliver Mn^{2+} effectively to liver tissue, but the kinetics of uptake is quite different from free Mn^{2+}. Free Mn^{2+} is taken into hepatocytes very efficiently [Schwam and Brandt, 1986]. The bulk of the data suggest that liposomes and their contents are sequestered by Kupffer cells and that until the Mn^{2+} escapes from the vesicle and the cell, relaxation enhancement is insignificant. The bulk of evidence supporting this explanation is outlined below.

The data on water permeability of liposomes in a suspension might lead one to conclude that the liposome permeability to water is a major factor in limiting the relaxation effects of encapsulated $MnCl_2$. One could reason that the Mn^{2+} released from liposomes but still remaining within the Kupffer cells, would be an effective relaxation agent. The first important consideration is to recall that the binding of Mn^{2+} in tissue is an important factor in the effectiveness of Mn^{2+} <u>in vivo</u>. The data shown in

Section 4.2.3 clearly demonstrates the large increase in relaxation rates seen when Mn^{2+} is bound to liposomes in vitro. Others have clearly shown this striking effect in vivo as well [Lauterbur, et al., 1978; Mendonca-Dias, et al., 1984; Koenig, 1985]. Furthermore, the ESR data in Figure 4.9 clearly shows a difference in binding of Mn^{2+} in liver before and after heating of the DPPC/DPPG vesicles. The relaxation times corresponding to spectra A and spectra B in the figure B are the times shown in Figure 4.5 for 30 minutes. Before release T_1 is 228 ms and after release it is 109.

From this data, one could postulate that DPPC/DPPG vesicles containing $MnCl_2$ are ineffective until heated because encapsulation prevents binding of Mn^{2+} to sites in the tissue. This hypothesis does not exclude the low water permeability of the membrane from contributing to the lack of effectiveness. The data generated for this project support this hypothesis. However, two other sets of experimental results, one performed in a related project using dextran magnetite, give evidence that another factor is even more important.

First of all, for Mn^{2+} to exert the greatest influence on relaxation rates in tissue, it must be evenly distributed throughout the tissue. This reduces the distance that water protons must diffuse to be relaxed by Mn^{2+}. If one examines the anatomy of the liver at the cellular level, it becomes obvious that this is not the case for Kupffer cells [Wisse and Deleeuw, 1984; Kessel and Hardon 1979]. These cells, which are responsible for the large liver uptake of liposomes [Weinstein, 1984;

1987], occupy only 2% of the volume of the liver [Blouin, et al., 1977]. Kupffer cells line the fenestrated liver capillaries (sinusoids), and are frequently located in regions where the sinusoids branch [Kessel and Hardon, 1979]. The distribution of liposomes taken up by Kupffer cells is not uniform. The liposomes are thereby concentrated (i.e., compartmentalized) into a small volume of the liver.

The effect of this compartmentalization on particles taken into Kupffer cells has been seen in results presented by Holtz and Klaveness [1986]. In that study, starch microspheres with covalently bound gadolinum (Gd) were injected into rats. The livers were excised at various times after injection and relaxation measurements were made on the excised tissue. The authors found very little increase in relaxation rates. This occurred even though the starch microspheres were known to be localized in the liver in Kupffer cells, despite the fact that no liposome membrane was involved that could limit permeability or water access to the paramagnetic material, and despite the fact that the Gd was already bound to a slowly tumbling macromolecular complex and had a quite high value for relaxtivity. However, when the livers were homogenized and the homogenate remeasured, the T_1 was greatly reduced.

In related experiments in which I was involved [Bacic, et al., 1987c], dextran-magnetite was injected intravenously in rats to evaluate its potential as a possible liver specific contrast agent. It is a particle slightly smaller in size than the liposome (2 - 20 nm) [Moulday, et al., 1978], but large enough to be

removed from the circulation by Kupffer cells. When injected into rats, it caused a large change in contrast in the liver. When the relaxation times of dextran-magnetite are measured in cell free buffered saline solution, the particle causes a large decrease in T_1 and T_2 at 20 MHz (MLRE = 22 sec^{-1} mM Fe^{-1}, MTRE = 1770 sec^{-1} mM Fe^{-1}). However, when the relaxation rates of the livers from rats given intravenous injections of dextran-magnetite were measured, no change was seen in R_1, while a large change in R_2 was seen. To explain this behavior one must understand the mechanism whereby dextran-magnetite reduces T_2.

The magnetite particle has the property termed superparamagnetism. When placed in a strong magnetic field, magnetite becomes magnetic and its magnetic field disturbs the local field homogeneity for quite a distance around the particle. This local field inhomegeneity produces a large increase in R_2. Because of this field effect, intracellular dextran-magnetite can cause decreased T_2 of the water outside the cell without exchange of water across the membrane. However, the effect on R_1 from the particle does not extend outward for a great distance. For dextran magnetite to exert its influence on T_1 the particle must be in the same compartment (i.e., in the Kupffer cell) to be relaxed.

When the results of the liposome encapsulated Mn^{2+}, Gd-microsphere and dextran magnetite experiments are considered together, the evidence suggests that a contrast agent ingested by Kupffer cells must be released from these cells to increase relaxation rates. Whenever any of these molecules are compart-

mentalized in the Kupffer cell, there is no T_1 effect seen. Only the magnetite particle, whose magnetic field (T_2 effect) may extend to micron distances for a 20 nm particle [Saini, 1987] exerts any effect while isolated in the Kupffer cells. Once released from the Kupffer cell, both Gd-microspheres and Mn^{2+} show a large effect on relaxation rates. Thus, it appears that the sequestration of contrast agent in the small volume of the liver comprised by Kupffer cells requires water to diffuse large distances to be relaxed. The data summarized above suggest that the time required to diffuse these distances is longer than the intrinsic relaxation time of the liver tissue protons.

A consideration of the water permeability of hepatocytes and of liver anatomy supports the hypothesis that compartmentalization into Kupffer cells is responsible for the results seen in the experiments summarized above. From the experiments measuring the permeability of mouse hepatocytes (Section 4.4.8), the volume of these cells was measured using NMR and found to be 11.3×10^{-9} ml. Assuming the cells to be spherical in solution then $V = 2\pi r^3$, where V is equal to the cell volume and r is the radius. Substitution for V results in $r = 12.2$ μm. Therefore, the average diameter of these cells is 25 μm. Rat hepatocytes have been shown to be 18 -20 μm in diameter [Wisse and Deleew, 1984]. To calculate water diffusion in the simplest case of one dimensional diffusion, the distance diffused in time (t) is given by the formula

$$t = d^2/D_W$$

where d = distance and D_W is diffusion coefficient of water. The value for D_W in rat liver has been measured to be 0.7 x $10^{-5}cm^2/S$ at 37^oC [Cooper, et al., 1974]. The time needed to diffuse the distance equal to the diameter of the average hepatocyte is approximately 500 ms, nearly two times as long as the intrinsic relaxation time. Furthermore, this assumes no barriers to diffusion exist (i.e., membranes). When the restrictions due to the hepatocyte membrane and Kupffer cell membrane are considered, it is not surprising that no T_1 effect can be measured when a paramagnetic agent is sequestered in a Kupffer cell.

In the case of the liposomes, the problems associated with sequestering of Mn^{2+} in the Kupffer cells can be overcomes by using a liposome that quickly releases Mn^{2+} after phagocytosis. The results show that liposomes made from PC/PS/CHOL appear to be degraded more rapidly than any other composition studied. Several possible explanations exist for this behavior.

Previous studies indicated that changing from phospholipids with saturated fatty acid side chains to those containing unsaturated fatty acids would allow for faster degradation in the Kupffer cell [Dijkstta, et al., 1985]. It has also been noted that rat phospholipase A processes phospholipids in the fluid state more quickly than those in the gel state [Vandenbranden, et al., 1984]. At normal body temperature, phospholipids with unsaturated fatty acids would be above T_m and be degraded more quickly. Also, a recently published report has shown that an anticancer agent encapsulated in liposomes made from PC/PS/CHOL (i.e., has unsaturated fatty acids) exerts an antitumor effect almost imme-

diately. Vesicles that were made containing only saturated lipids made from disearlyphosphatidylcholine (DSPC), DPPG, and cholesterol exhibited a delayed antitumor effect of three days [Storm, et al., 1987]. These authors used in vivo experiments to show that the processing rate of the PC/PS/CHOL liposomes was much greater than the DSPC/DPPG/CHOL liposomes in the liver and spleen, the two organs responsible for a majority of liposome uptake.

While it is not possible to determine which, if any, of the mechanisms listed above are responsible for the increased rate of processing of PC/PS/CHOL liposomes, the fact that similar results were obtaining independently by the investigators using similar liposomes points out the importance of the bilayer composition in determining the time course of liposome degradation.

5.4 In Vivo Experiments in Rats with Liver Tumors

The experimental determination of the toxic level of Mn^{2+} suggested that injection of liposomes at doses (25 - 40 μmole Mn^{2+}/kg) that reduce T_1 and T_2 substantially in the liver would not result in deaths to the animals. Therefore, experiments were undertaken to determine if differential uptake of liposomes by Kupffer cells would selectively increase liver relaxation rates in an animal tumor model. It was postulated that differential uptake of LUV by the Kupffer cells would increase relaxation rates in the liver without affecting the tumor.

The magnetic resonance images obtained from the rats confirm that the uptake of liposomes is much greater in healthy liver

than in tumor. Figures 4.11 and 4.12 show the coronal and axial images respectively, of a female Fisher 344 rat with an implanted liver tumor. Using a spin echo sequence with a short TE (100 ms) and short TR (20 msec), the tumor is visibly darker than the liver in these images, as would be predicted from the relaxation data. When $MnCl_2$ (25 μmole/kg) is injected intravenously, the liver and tumor both exhibit an increase in intensity (Figure 4.13) using the same imaging parameters as the control images. The image of the tumor is no longer discernable after the injection of free Mn^{2+}. However, after the injection of 40 μmole/kg of Mn^{2+} encapsulated in PC/PS/CHOL liposomes, the liver is seen to brighten, while the tumor remains dark.

The contrast differential is greatly increased after injection of liposomes containing Mn^{2+}. The data in Table 4.9 show that the relaxation rates for tumor are increased but that the increase in the R_1 for healthy liver is double the change in the tumor tissue. These results indicate that Mn^{2+} encapsulated in PC/PS/CHOL liposomes has the ability to improve the contrast difference between tumor and healthy tissue in the liver using MRI.

Since Mn^{2+} must be released from the liposome and Kupffer cell in order to relax the bulk of the liver water, it might be expected that some of the Mn^{2+} leaving the Kupffer cell would end up in the tumor. The relaxation data (Table 4.9) and the image shown in Figure 4.14 strongly suggest that this is not the case. Efficient uptake of Mn^{2+} by hepatocytes in the liver is probably the reason that there is little tumor uptake. After intravenous injection of an $MnCl_2$ solution the uptake into the liver is

nearly instantaneous [Mendonca-Dias, 1983]. Schramm and Brandt [1986] have proposed that the mechanism for Mn^{2+} uptake is facilitated diffusion by a membrane protein or carrier.

If one carefully considers liver anatomy, the fact that the Kupffer cells are in close proximity to the hepatocytes implies that any Mn^{2+} released from the Kupffer cells will be taken into the hepatocytes. The tumor does not have many Kupffer cells or fixed macrophages in its blood vessels [Weinstein, 1987]. Therefore, liposomes are not likely to accumulate and release their contents in the tumor.

CHAPTER 6

CONCLUSION

This thesis project was begun in 1985 in an attempt to take advantage of two conclusions that were reached after approximately a decade of intensive research examining the drug delivery potential of liposomes. The vast majority of accumulated data suggested that liposomes do not become localized in solid tumors. Instead, most of the liposome dose is found in the liver and spleen after intravenous injection, and the uptake by the liver can be especially pronounced with liposomes of certain sizes and phospholipid composition. This combination of factors formed the basis for the hypothesis that was tested in the project. Namely, would the uptake of a liposome encapsulated MRI contrast agent by healthy liver and the lack of uptake of liposome by solid tumors lead to an improvement in the contrast differential between the two types of tissue?

To test this hypothesis, it was necessary to determine if stable liposomes could be made using relatively high concentrations of $MnCl_2$. This was successfully accomplished using vesicles of several phospholipid compositions. In addition, the amount of encapsulated Mn^{2+} was equivalent to the dose required to bring about an increase in relaxation rates if it was injected in free form. However, initial experiments with liposome encapsulated Mn^{2+} is DPPC/DPPG liposomes showed little change in liver relaxation rates during the first two hours after injection unless the liposomes were heated to release their contents. In order to

explain this specific behavior and to obtain a better understanding of liposomal processing in general, extensive tests were performed using two different liposome compositions (DPPC/DPPG and PC/PS/CHOL). These two compositions were chosen because they brought about the slowest and the most rapid changes (respectively) in liver relaxation rates after intravenous injection.

The results of the comparison of the two types of vesicles led to several conclusions. First, the clearance of the two types of liposomes was not statistically different at the lipid dose employed. Second, even though the clearance was not different, the amount of Mn^{2+} released from the PC/PS/CHOL vesicles was significantly higher at 1.0, 1.5, and 2.0 hours after injection. Relaxation studies supported this conclusion, since the relaxation times of livers taken from the animals given PC/PS/CHOL were always lower than livers from animals given an equivalent dose of Mn^{2+} in DPPC/DPPG liposomes. Third, neither type of vesicle encapsulated enough Mn^{2+} so as to be acutely toxic.

These data, when considered in conjunction with other published reports in the literature [Holtz and Klaveners, 1986] lead to an important generalization that applies to any particulate agent intended for use as liver contrast agent in MRI imaging. This is, the contrast agent entrapped in Kupffer cells will be ineffective until it is released. The only exception to this generalization is the T_2 effect of dextran magnetite (or similar particles) which can be exerted over a large (> 20 μm in some cases) distance. This T_2 effect can still be exhibited even with the particle sequestered in Kupffer cells.

The in vivo relaxation data and images obtained from rats with liver tumors were encouraging. The liver tissue relaxation rates measured after liver excision were increased to much greater extent than the tumor tissue. The T_1 weighted images obtained after injection of PC/PS/CHOL show the somewhat dramatic effect of the liver brightening, outlining the dark tumor. More experimentation is needed to determine if the small increase in tumor relaxation rates can be reduced or eliminated.

Liposome encapsulated Mn^{2+} appears to be an MRI contrast agent with potential clinical uses. To be effective as a liver specific agent suitable for tumor detection, it has been stated [Ferrucci, 1987] that a compound (i.e., liposome encapsulated Mn^{2+}) should possess the following four characteristics: (1) uptake by normal liver, (2) exclusion by cancerous tissue, (3) magnetic activity sufficient to alter relaxation times of normal tissue without affecting adjacent tumor, and (4) low toxicity (high margin of safety at effective dose). Liposome encapsulated $MnCl_2$ seems to fulfill all of these requirements, although more toxicity data would be needed to prove its margin of safety.

Liposomes compare favorably when compared to other potential liver specific contrast agents. For example, Gd-DTPA, the first clinically useful contrast agent, is currently being tested as a potential liver contrast agent. This method combines pluses sequences with short TR and TE values with the use of an intravenous injection of the contrast agent to image the liver. This combination of fast imaging techniques and intravenous Gd-DTPA has shown mixed results, with some researchers seeing improvement

in the ability to diagnose liver metastases [Hamm, et al., Saini, 1986], and others finding no improvement or even a reduction in the ability to visualize disease conditions [Runge, 1986]. Its success is dependent on rapid imaging of the bolus of contrast agent flowing through the liver. After 5 to 10 minutes, the tumor is actually obscured rather than highlighted [Ferrucci, 1986].

Hepatobiliary contrast agents [Lauffer, 1987] offer potential highlighting of liver structure. These agents are iron chelates to EHPG, (N-N'-ethylenebis(2-hydroxyphenlycine)ethylinediamine. They may be potentially useful since they pass quickly from the blood into the bile. This may allow for highlighting normal liver tissue, and more importantly, for future studies of liver metabolism.

The most directly comparable liver contrast agents are magnetic particles like the dextran magnetite used in this study for water permeability measurements. Several reports of this type of particle have been published [Farrucci, 1986; Saini 1987]. These particles are similar in size to liposomes, [Moulday, 1978] and are localized in Kupffer cells. They exert a strong T_1 and T_2 effect in solution, but little T_1 effect while in Kupffer cells [Bacic, et al., 1987c]. A recent publication using a similar particle shows improved tumor detection [Saini, et al., 1987]. The particle appears to be quite nontoxic, since it is effective at very low doses. The only potential drawback to the magnetite particles lies in the determination of what size lesions will be detectable. Because of the strong field effect, it is possible that small lesions may be lost due to the blurring of the mag-

netic field. However, the fact that the particles are compartmentalized into Kupffer cells (as liposomes are initially) suggests that this may not be a significant problem and these particles may be very effective.

The potential disadvantages to liposome encapsulated Mn^{2+} are related to its potential toxicity and to the potential for Mn^{2+} to be released from liposomes and localized into the tumor instead of in Kupffer cells and hepatocytes. The toxicity problem is one that needs more experimentation to reach a definite determination.

Future work with Mn^{2+} is liposomes is being planned to determine the extensiveness of the tumor uptake of Mn^{2+}. Is the uptake just in the peripheral areas of the tumor? Is a portion of the Mn^{2+} that is released from the Kupffer cell taken up in the tumor before it is transferred to the hepatocytes? Is it possible that a more slowly degraded liposome (e.g., DPPC/DPPG) might transfer less Mn^{2+} to the tumor? How long does it take for injected Mn^{2+} to clear from the liver? These are some of the questions remaining to be answered.

It has been shown that liposomes containing Mn^{2+} can deliver this potential contrast agent to liver tissue and cause it to be largely excluded from tumor tissue, confirming the main hypothesis of the research. Future studies will determine if the technique will allow the diagnosis of small liver metastases. Improvement in the diagnosis of these small lesions may allow for early surgical intervention and potential cures of these life threatening tumors.

Table 2.1*

Characteristics of Liposomes Made with DPPC/DPPG[1]

	SUV	MLV	LUV
Size Range (nm)	20 - 50	100 - 2000	70 - 800
Encapsulation Efficiency (%)	0.5 - 2.0	5 - 14	10 - 65
Entrapped Volume (μl/mg lipid)	0.1 - 0.6	5 - 7	7 - 12

*Adapted from Magin and Weinstein, 1984
DPPC = Dipalmitoylphosphatidylcholine
DPPG = Dipalmitoylphosphatidylglycerol
SUV = Small unilamellar vesicles
MLV = Multilamellar vesicles
LUV = Large unilamellar vesicles

[1] Each preparation made with a 4:1 mole percent mixture of the DPPC/DPPG

Table 4.1. Encapsulation Efficiency of DPPC/DPPG LUV*.

Measurement Technique	Encapsulation Efficiency
^{3}H Sucrose	22.5
Atomic Absorption Spectroscopy	22.3 ± 2.6
Electron Spin Resonance	
a) Peak Height	18.4 ± 1.4
b) Double Integral	24.1 ± 0.8

* Atomic absorption and ESR measurements were made on the same same of liposomes. The values are the mean of two measurements ± S.D. The ^{3}H sucrose measurement was made on an independent sample.

Table 4.2. Encapsulation Efficiency and Stability of Different Liposome Preparations Measured by ESR.

Composition (mole ratio)	Encapsulation Efficiency[1] %	Release of Contents after 2.0 Hours in 50% Calf Serum[2]
DPPC:DPPG (4:1)	21.1	< 5%
DMPC:DMPS:CHOL (4.5:1.5:4)	11.3	N.D.
DMPC:DMPG:CHOL (4.5:1.5:4)	13.0	< 5%
PC:PS:CHOL (3:1:3)	7.2	< 5%
PC:PG:CHOL (4:1:5)	1.9	N.D.
PC:PG (4:1)	N.D.	95%

[1] Original aqueous phase is 100 mM $MnCl_2$, so % encapsulation is equal to $MnCl_2$ concentration measured by ESR spectroscopy.

[2] As measured by decrease in ESR signal height of $MnCl_2$ spectrum.

N.D. Not done.

Table 4.3. Residence Times and Water Permeability of Liposome with Different Phospholipid Compositions.

Lipid Composition	τ(ms)	Pd	Pf*
DPPC/DPPG[a]	625	5.3×10^{-6}	4.7×10^{-6}
PC/PS/CHOL/αTocoperol[1,b]	135	2.5×10^{-5}	N.D.
Egg PC[b]	24	1.4×10^{-4}	2.1×10^{-4}

* [Carruthers and Melchoir, 1983].

1 Five mole % α-tocopherol included to prevent lipid oxidation.

a Measured using Mn^{2+} as relaxation probe.

b Measured using dextran magnetite as relaxation probe.

Table 4.4. Result of $MnCl_2$ Toxicity Experiment

Dose $MnCl_2$ (μmole kg^{-1})	Death/Total	% Response
400	6/6	100
355	8/10	80
300	5/8	62.5
200	1/6	16.7
135 in DPPC/DPPG LUV[1]	0/6	0
135 in LUV, heated before injection[2]	0/6	0

1 Mice injected with liposomes were not included in calculations of the LD_{50}.

2 LUV heated to 45°C for 10 minutes, cooled to room temperature, then injected.

Table 4.5. Mouse Liver T_1 30 Minutes after Intravenous Injection of Liposome Encapsulated $MnCl_2$ (25 μmole/kg^{-1}).

Time After Injection (min)	T_1 (ms)	
	Before Heat	After Heat
15	285	135
30	228	109
60	178	96
120	177	89
Control (No $MnCl_2$)	375	370

Table 4.6. Liver Relaxation Times After Injection of $MnCl_2$ in Liposomes (25 μmole kg^{-1}).

Composition	T_1(ms)		T_2(ms)	
	1 Hour*	2 Hours	1 Hour	2 Hours
Control	348 ± 19	N/A	43.8 ± 1.9	N/A
DPPC/DPPG (No Heat)	248 ± 19	177 ± 19	39.2 ± 0.6	36.8 ± 1.3
DPPC/DPPG (Heated[1])	162 ± 5	89 ± 13	31.4 ± 5	26.0 ± 3.5
DMPC/DMPG/CHOL	231 ± 19	154 ± 5	37.6 ± 2.6	31.3 ± 0.9
DMPC/DMPS/CHOL	187 ± 4	143 ± 2	32.7 ± 1.2	34.1 ± 1.5
PC/PS/CHOL	119 ± 4	92 ± 5	29.3 ± 0.5	25.6 ± 1.0

Each data point is mean ± S.D. of three animals.

* Time after injection.

[1] Liver was measured once, heated in water bath at 45°C for 10 minutes, cooled to 35°C and remeasured.

Table 4.7. Liver Uptake of Mn as Determined by Atomic Absorption Spectroscopy*

Minutes After Injection	DPPC/DPPG LUV[1]		PC/PS/CHOL LUV[2]	
	μmole/g	% dose/g	μmole/g	% dose/g
15	0.32 ± 0.07	12.8 ± 2.7	0.24 ± 0.06	20.6 ± 5.1
30	0.37 ± 0.07	14.8 ± 3.1	0.24 ± 0.01	20.9 ± 1.0
60	0.48 ± 0.06	19.3 ± 2.2	0.40 ± 0.04	34.3 ± 3.7
90	0.57 ± 0.07	23.2 ± 3.1	0.38 ± 0.01	32.9 ± 0.9
120	0.58 ± 0.05	23.7 ± 4.6	0.37 ± 0.03	31.8 ± 2.2

* Mean ± standard deviation for 3 animals at each time period.

[1] 2.46 μmole/kg injected dose of $MnCl_2$.

[2] 1.15 μmole/kg injected dose of $MnCl_2$.

Table 4.8. Comparison of ESR Signal Height/μmole Mn in Liver Versus Time*.

	PC/PS/CHOL	DPPC/DPPG
15 min	15.7 ± 4.8	28.2 ± 9.2[b]
30 min	17.0 ± 3.7	32.6 ± 13.2[b]
60 min	10.5 ± 2.0	36.3 ± 18.2[a]
90 min	7.4 ± 5.2	25.9 ± 10.4[a]
120 min	11.4 ± 4.0	37.3 ± 19.2[a]

* N = 3 at each time point.

[a] The means of the two measurements are significantly different at 0.05 level, using students t-test.

[b] The means of the two measurement are significantly different at the 0.10 level, using students t-test.

Table 4.9. Relaxation Times of Liver from Fisher 344 Rats with Liver Implants of R3230 AC Mammary Adenocarcinoma.

	T_1		T_2	
	Liver	Tumor	Liver	Tumor
Control	339.0 ± 9.6	768.0 ± 72	50.5 ± 2.1	101.0 ± 7.0
After Injection of Free Mn^{2+}	35.9 ± 2.1	109.8 ± 34.2	17.8 ± 0.8	40.9 ± 11.9
After Injection of PC/PS/CHOL LUV Containing Mn^{2+}	78.5 ± 6.1	377.0 ± 76	25.5 ± 1.6	68.3 ± 6.3
Ratio:				
$\frac{\text{PS/PC/CHOL } T_{1,2}}{\text{Control } T_{1,2}}$	0.23	0.49	0.50	0.68
$\frac{\text{Free } Mn^{2+} T_{1,2}}{\text{Control } T_{1,2}}$	0.11	0.14	0.35	0.40

Values for T_1 and T_2 represent the mean of three animals ± the standard deviation of the sample.

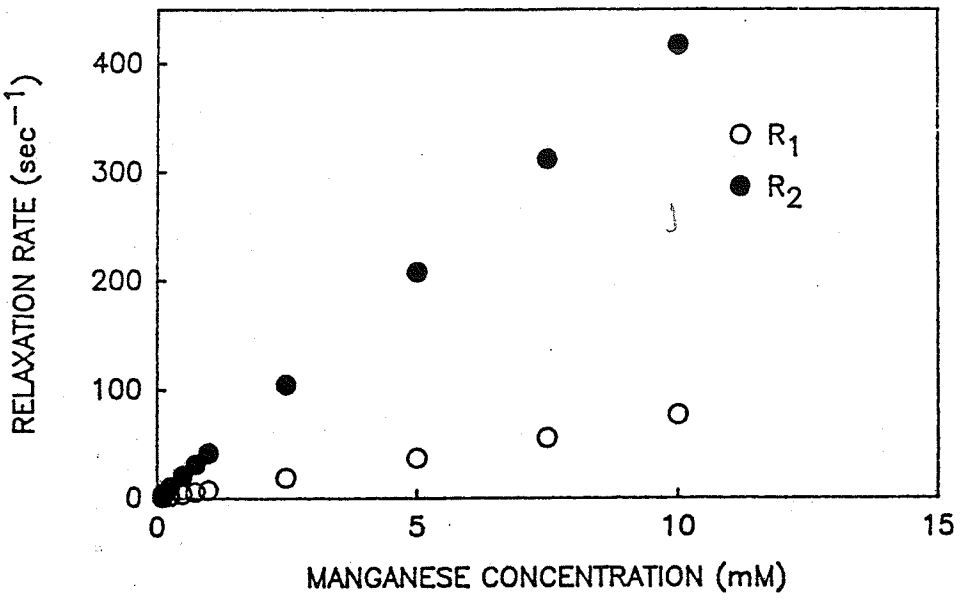

Figure 2.1. Graph of longitudinal (R_1) and transverse (R_2) relaxation rates versus concentration of paramagnetic ion (Mn^{2+}).

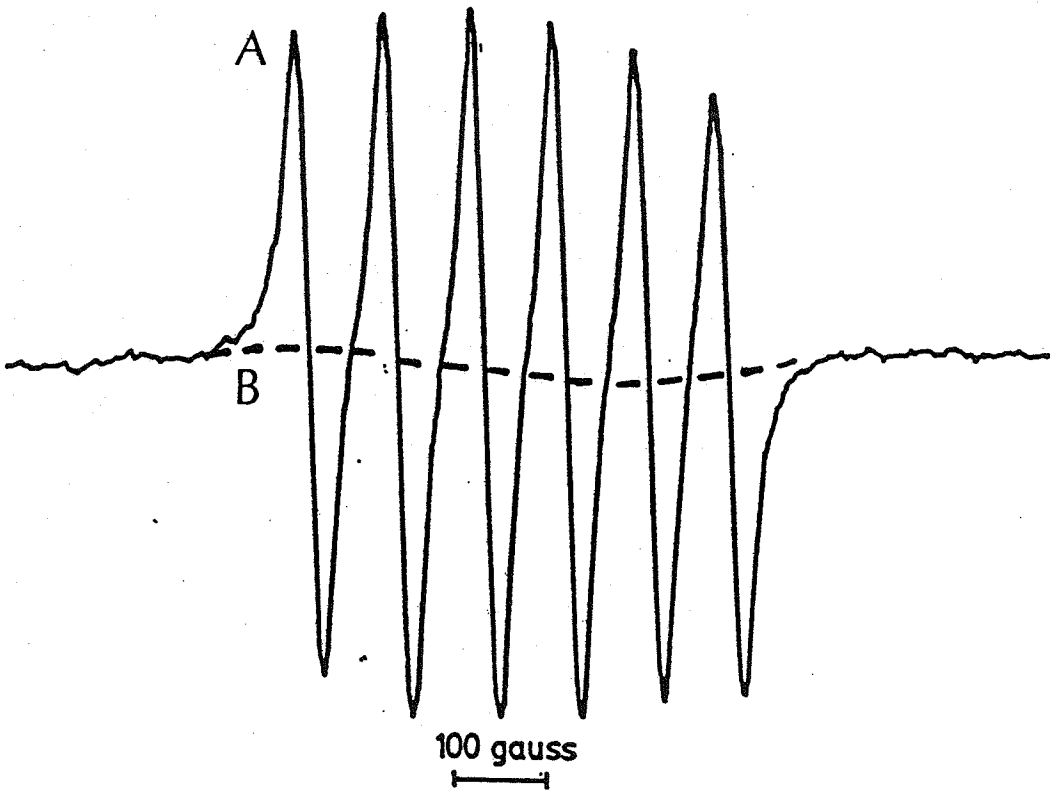

Figure 2.2. Schematic diagram showing the spectra obtained when measuring Mn^{2+} free in solution (A) or bound to a large macromolecule (B).

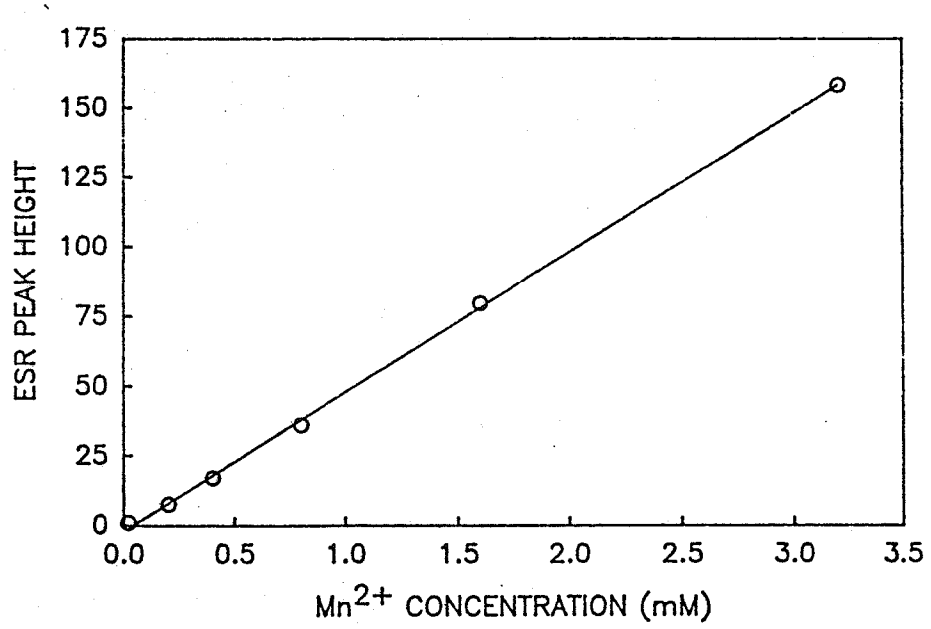

Figure 4.1. ESR calibration curve showing the linear relationship between peak height and concentration of Mn^{2+} in solution. r = 0.999

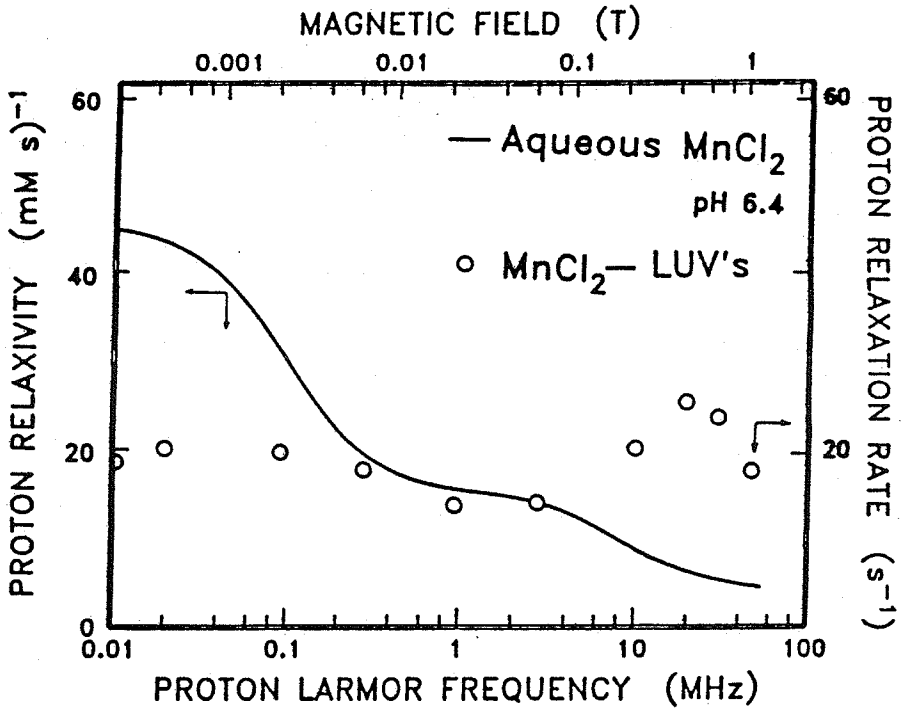

Figure 4.2. Nuclear Magnetic Resonance Dispersion (NMRD) curve for an aqueous solution of $MnCl_2$ and a solution of liposomes containing 100 mM $MnCl_2$. The peak in the liposome curve near 20 MHz results from $MnCl_2$ bound to the outer leaflet of the liposome bilayer.

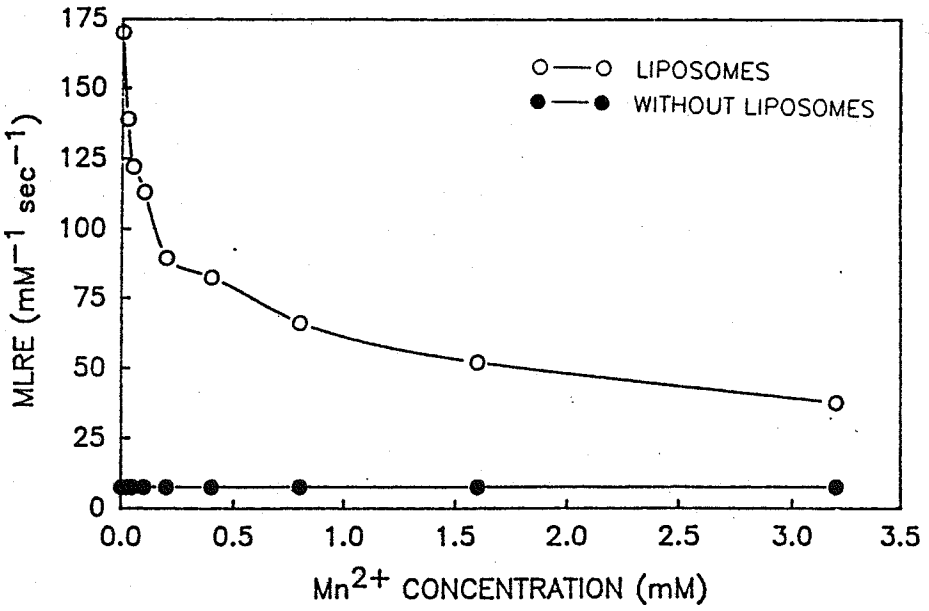

Figure 4.3. MLRE vs. concentration of Mn^{2+} in solution containing liposomes (o—o) and in an aqueous solution without liposomes (•——•). The binding of Mn^{2+} to the liposomes has a dramatic effect on the values for relaxation enhancement.

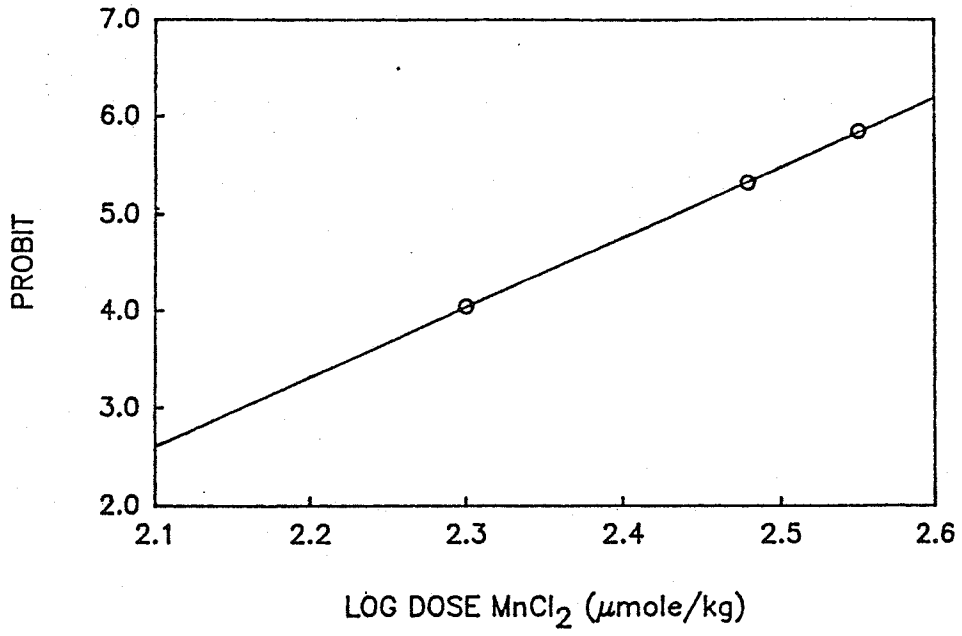

Figure 4.4. The results of the probit analysis of intravenous $MnCl_2$ toxicity in male B6D2F_1 mice. The LD_{50} from the analysis of this graph is 272 μmole Kg^{-1}.

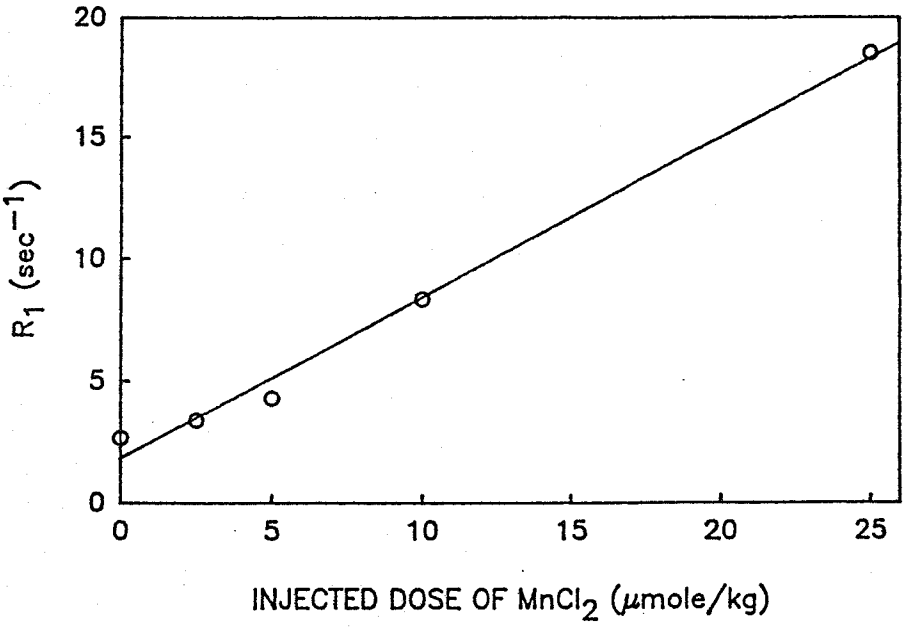

Figure 4.5. The R_1 versus the injected dose of $MnCl_2$. Individual animals were sacrificed for the measurement of each dose. r = 0.996

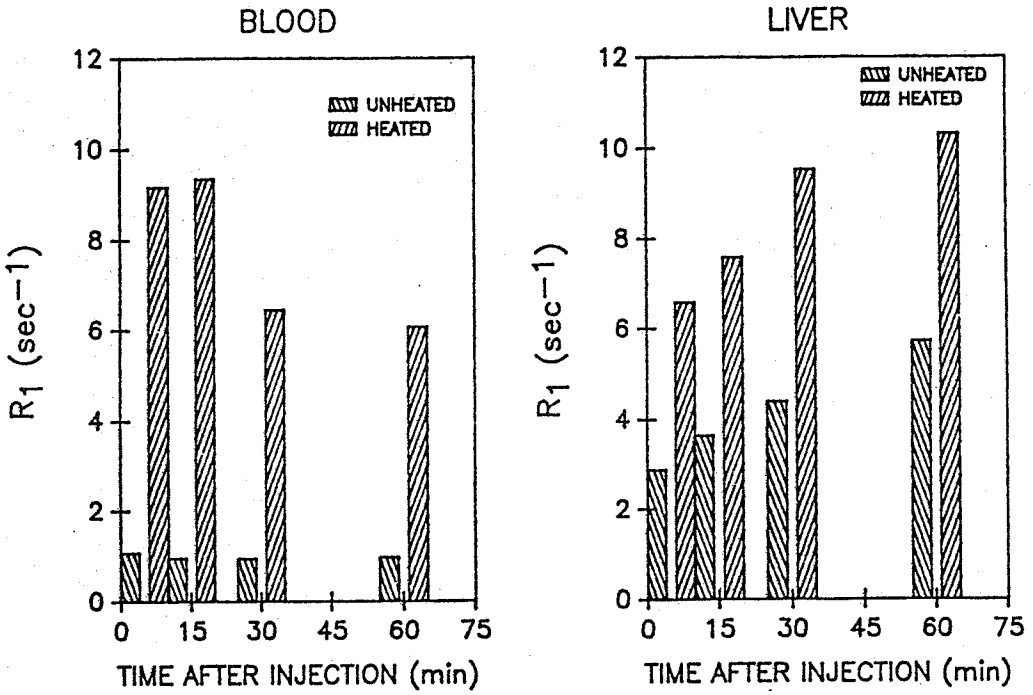

Figure 4.6. The R_1 of blood and liver after the injection of $MnCl_2$ encapsulated in liposomes. The value of R_1 was measured immediately after liver excision and again after heating the tissue to 42°C for 10 minutes.

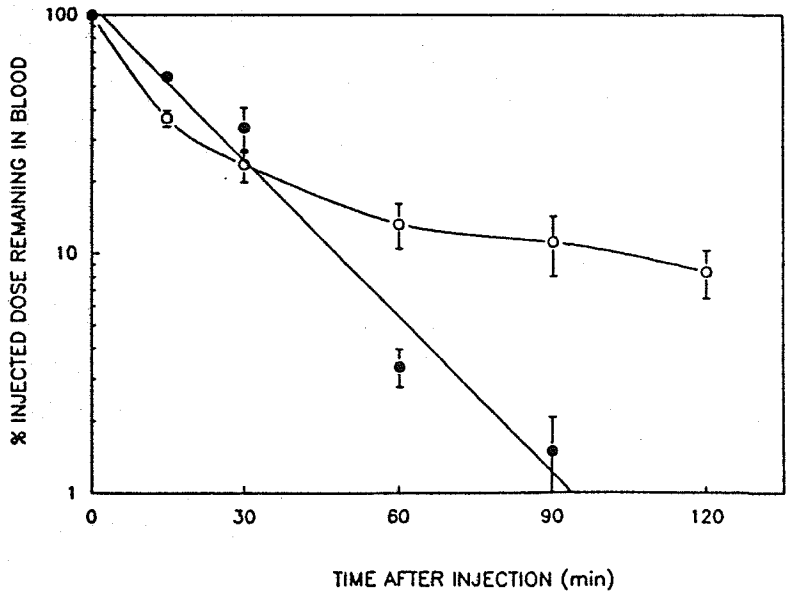

Figure 4.7. The blood clearance of DPPC/DPPG and PC/PS/CHOL liposomes . The values plotted for each time point are mean of six (DPPC/DPPG) or three (PS/PC/CHOL) animals. The error bars represent ± the standard error of the mean.

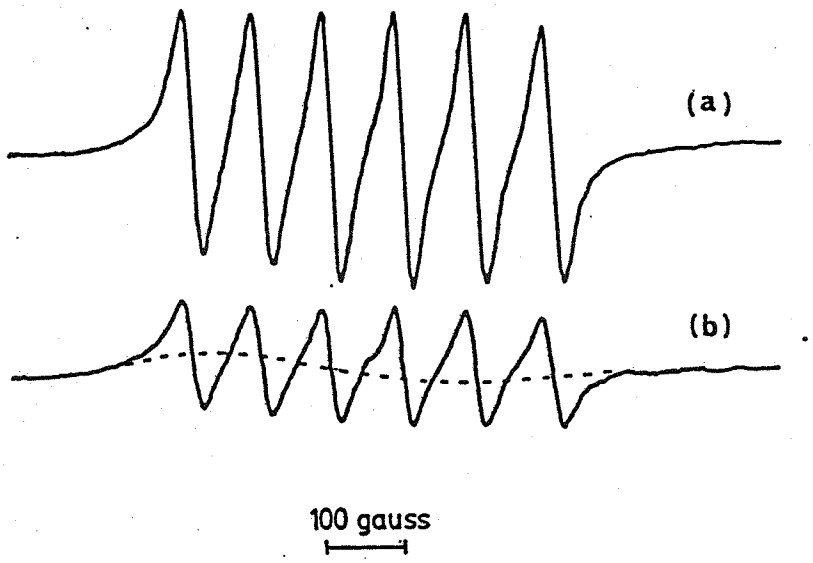

Figure 4.8. ESR spectra of blood taken from a mouse 30 minutes after injection of $MnCl_2$ in DPPC/DPPG liposomes. Spectrum A was taken immediately after the sample was taken. Spectrum B is from the same sample as A after heating to 42°C for 10 minutes. The dotted line in B represents the signal that would be seen if the Mn^{2+} was fully bound.

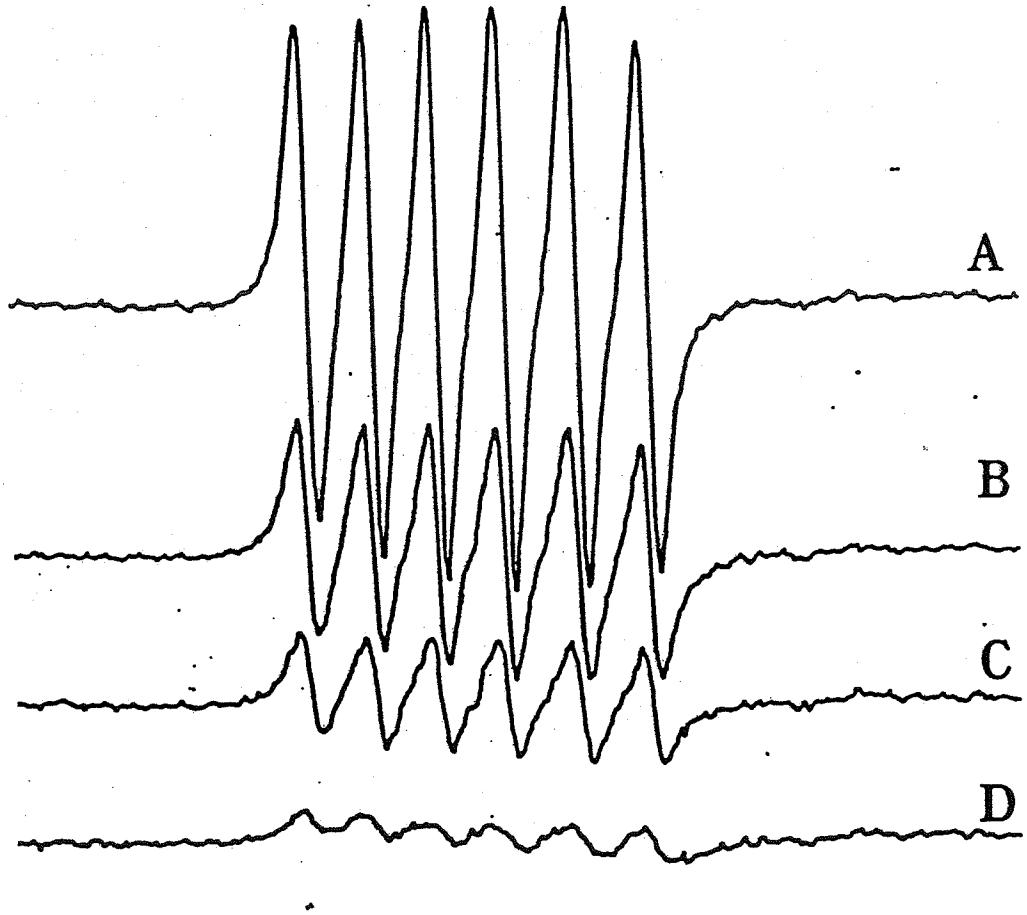

Figure 4.9. ESR spectra of liver tissue from mice 30 minutes after injection with DPPC/DPPG liposomes containing $MnCl_2$ (A-C) or free $MnCl_2$ (D). Spectrum A was taken immediately after liver excision. Spectrum B was taken after heating the liver to 42°C for 10 minutes. Spectrum C was taken 40 minutes after Spectrum B. Spectrum D was taken from a sample of liver excised from a mouse receiving an identical amount of $MnCl_2$ as A, but in free rather than encapsulated form.

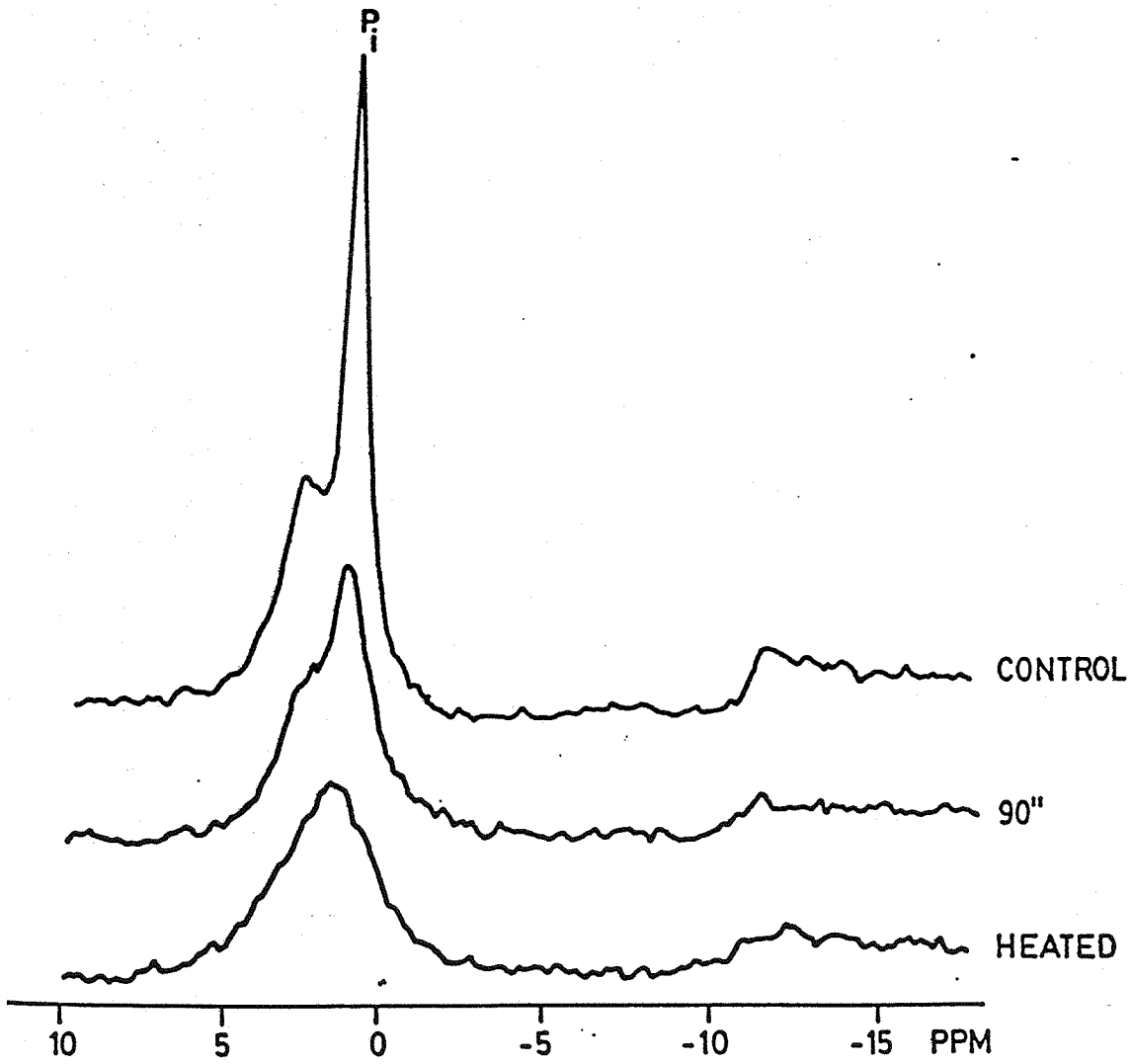

Figure 4.10. ^{31}PNMR of mouse livers. The control spectrum shows a large inorganic phosphate peak (P_i) superimposed on a broad sugar phosphate peak. The middle spectrum shows liver excised 90 minutes after injection of DPPC/DPPG liposomes. The bottom sample is the 90 minute sample after heating (42^{o}C, 10 minutes).

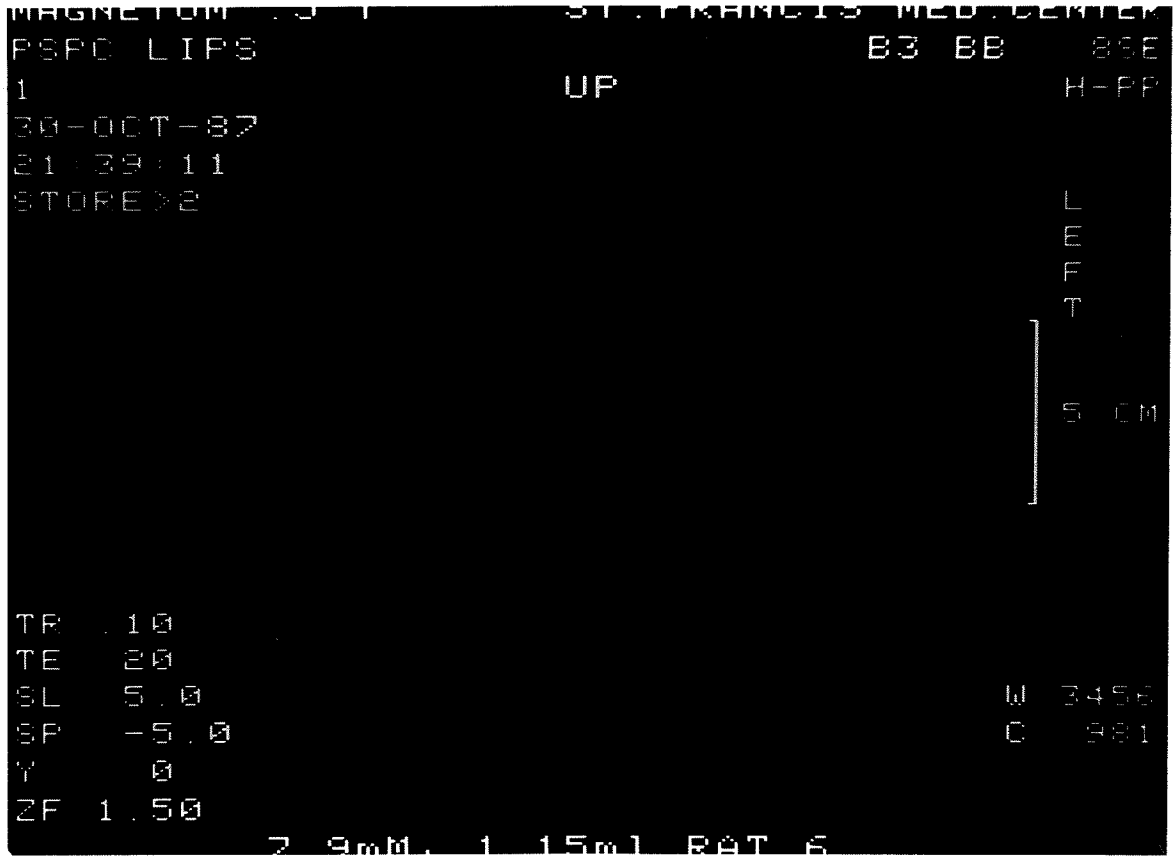

Figure 4.11. A coronal MRI image of a tumor in the liver of a Fisher 344 rat.

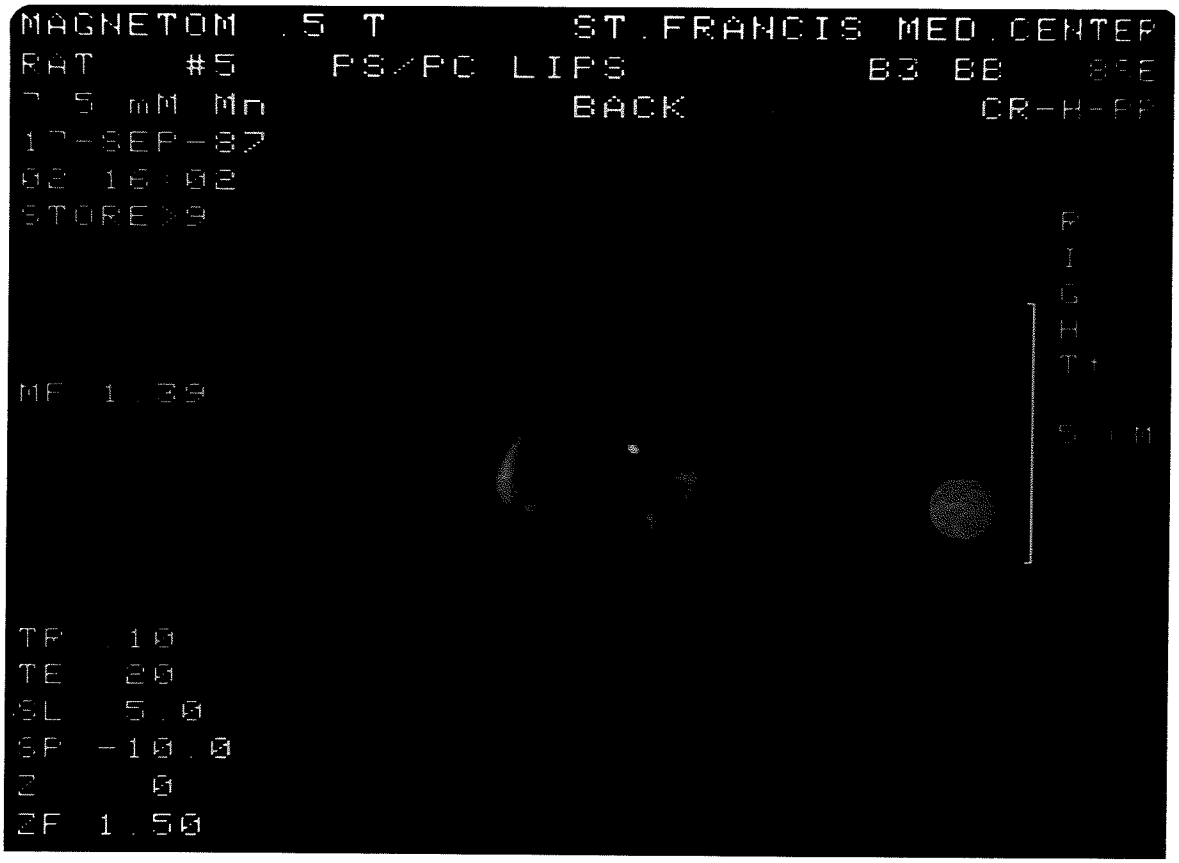

Figure 4.12. Control image of a tumor implanted in rat liver. Compare to Figure 4.12 and Figure 4.14.

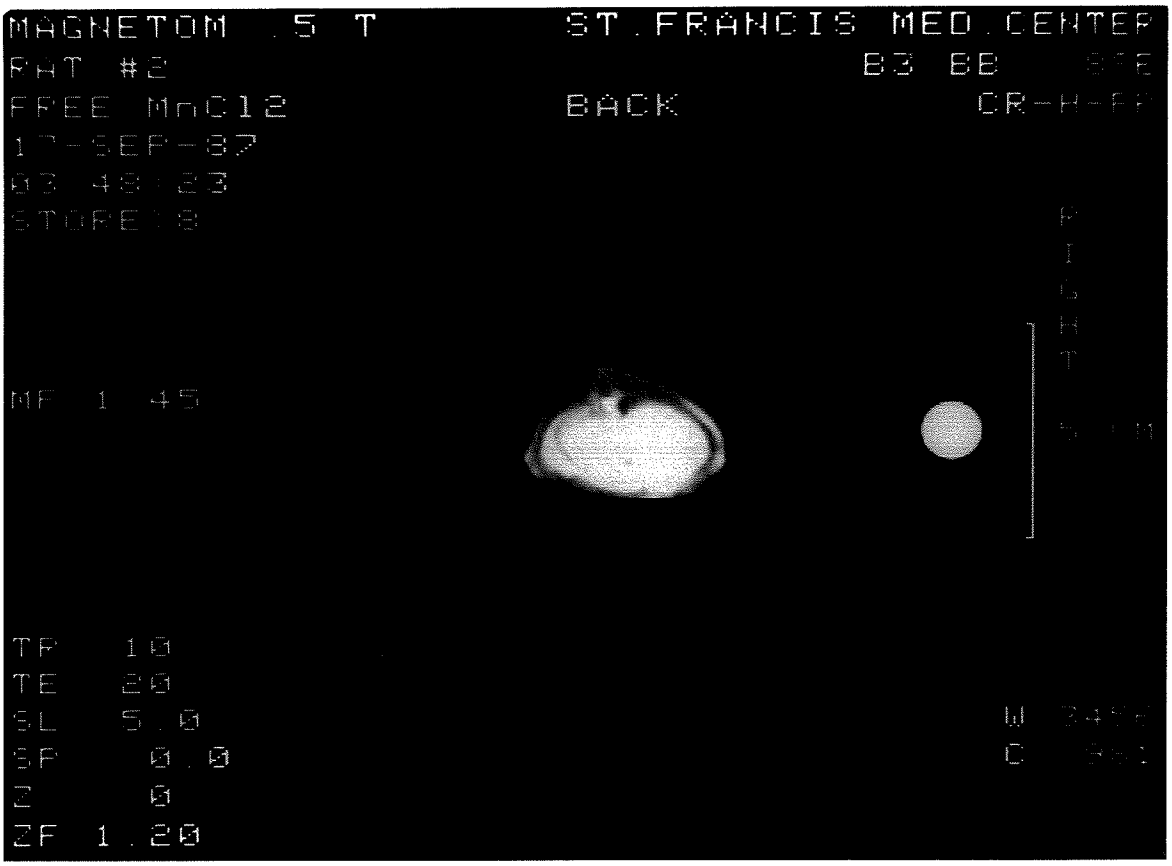

Figure 4.13. An axial image of a tumor implanted in the liver of a fisher 344 rat. This image was taken after injection of free Mn^{2+} (25 μmole/kg). The signal intensity increases in both the tumor and liver compared to the control (Figure 4.12).

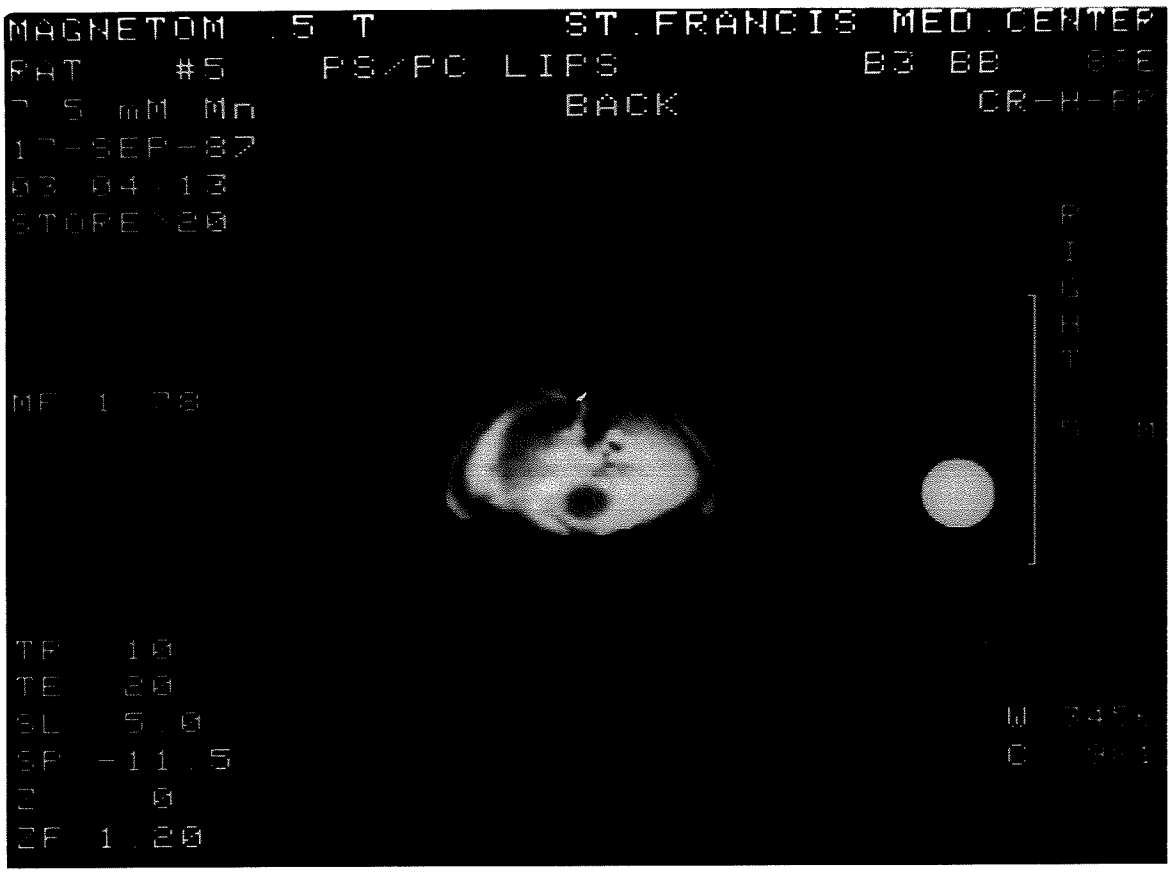

Figure 4.14. Image of liver tumor after injection of PC/PS/CHOL liposomes containing $MnCl_2$ (40 μmole Kg^{-1}). Compare to Figures 4.12 and 4.13.

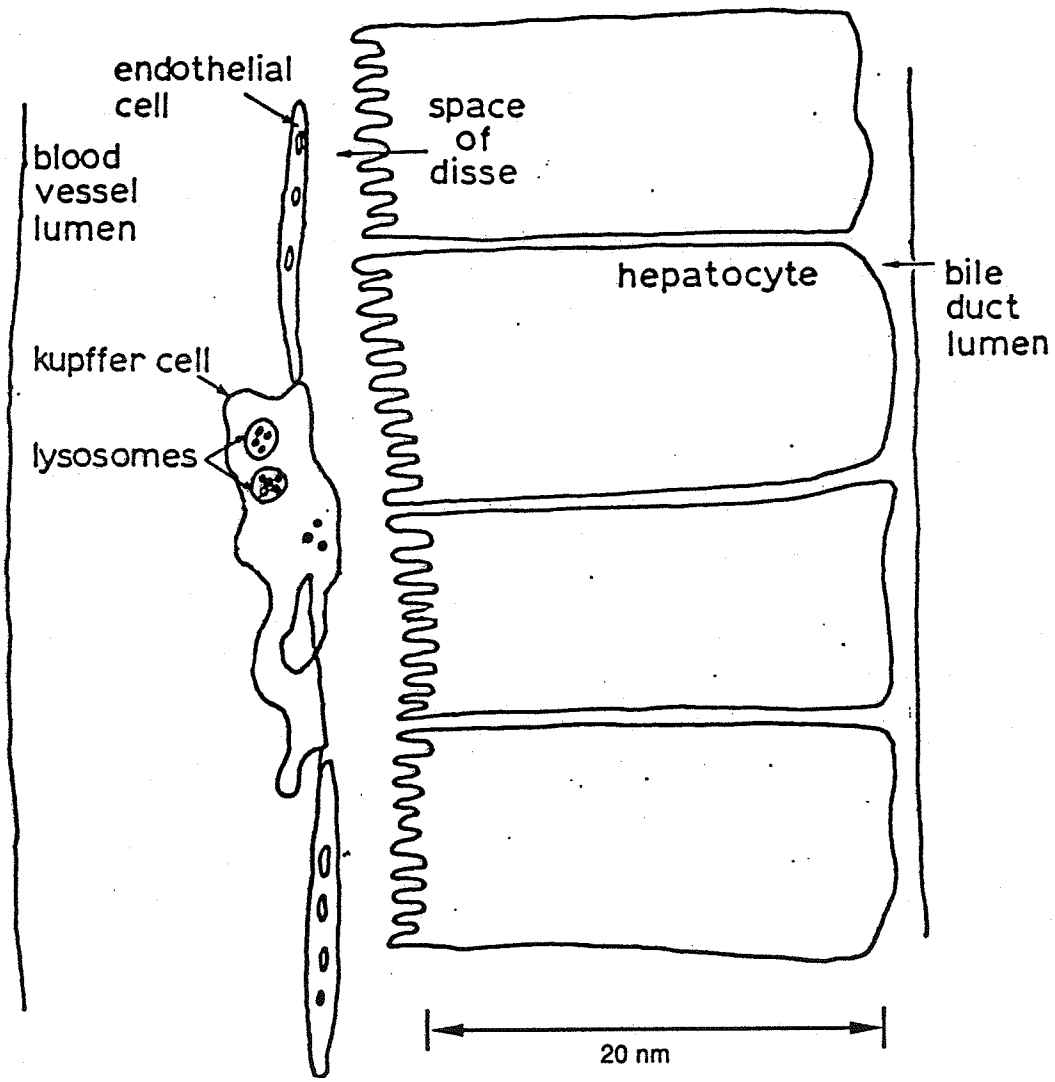

Figure 5.1. Schematic diagram of a liver sinusoid. Shown are the main cell types and structural organization of the sinusoid.

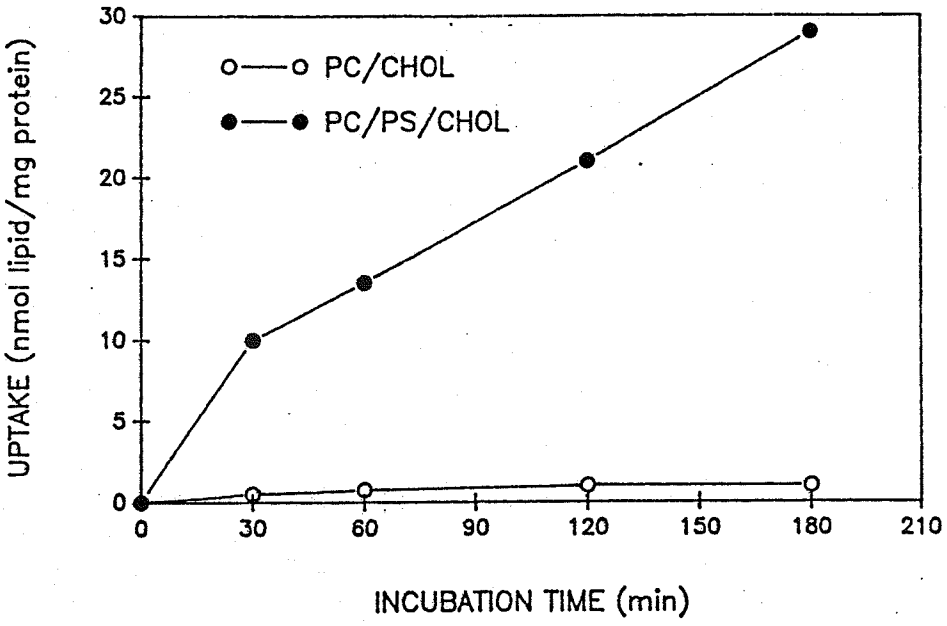

Figure 5.2. Uptake of PC/PS/CHOL and PC liposomes by Kupffer cells in vitro. Differences in uptake between the two types are striking (redrawn from Spanjer, et al., 1986).

REFERENCES

Abra, R.M., and C.A. Hunt (1981). Liposome disposition in vivo III: dose and vesicle size effects. Bioch. Biophys. Acta 666, 493-503.

Alving, C.R., and C.M. Swartz, Jr. (1984). Preparation of liposomes for use as drug carriers in the treatment of leshmaniasis, in Liposome Technology, Vol. III. G. Gregoriadis, (Ed.) CRC Press, Boca Raton, FL. 55-68.

Andrasko, J., and S. Forsen (1974). NMR study of rapid water diffusion across lipid bilayers in dipalmitoyl lecithin vesicles. Biochem. Biophys. Res. Comm. 60, 813-819.

Ash, D.E. and V.L. Schramm (1982). Determination of free and bound manganese(II) in hepatocytes from fed and fasted rats. J. Biol. Chem. 257, 9261-9264.

Ashley, D.L. and J.H. Goldstein (1980). The application of dextran-magnetite as a relaxation agent in the measurement of erythrocyte water exchange using pulsed nuclear resonance spectroscopy. Biochem. Biophys. Res. Comm. 97, 114-120.

Atkins, H.L., P. Som, R.G. Fairchild, J. Hui, E. Schachner, A. Goldmand, and T. Ku (1979). Myocardial positron tomography with manganese-52m. Radiology 133, 769-774.

Bacic, G. and S. Ratkovic (1984). Water exchange in plant tissue studied by proton NMR in the presence of paramagnetic centers. Biophys. J. 45, 767-776.

Bacic, G., S. Ratkovic (1987a). NMR studies of radial exchange and distribution of water in maize roots: The relevance of modelling of exchange kinetics. J. Exp. Botany 38, 1284-1297.

Bacic, G., M. R. Niesman, H. F. Bennett, R. L. Magin, and H. M. Swartz (1987b). Modulation of water proton relaxation rates by liposomes containing paramagnetic materials. Magnetic Resonance in Medicine, in press.

Bacic, G., M.R. Niesman, R.L. Magin, S.M. Wright, and H.M. Swartz (1987c). The use of dextran magnetite for liver contrast enhancement, Abstract, Sicth Annual Meeting of Society for Magnetic Resonance in Medicine, p. 328.

Bartlett, G.R. (1959). Phospholipid determination for column chromatography. J. Biol. Chem. 466-468.

Belton, P.S. and R.G. Ratcliffe (1985). NMR and compartmentation in biological tissues. Prog. NMR Spectroscopy 17, 241-279.

Bertinchamps,A.J., S.T. Miller, and G.C. Cotzias (1966). Interdependence of the routes excreting manganese. Am. J. Physiol. 211, 217-224.

Bloch, F. (1946). Nuclear induction. Phys. Rev. 70, 460-474.

Bloembergen, N. (1957). Proton relaxation times in paramagnetic solutions. J.Chem.Phys. 27, 572-573.

Blouin, R. P., Bolender, and E. R. Weibel (1977). Distribution of organelles and membranes between hepatocytes and nonhepatocytes in the rate liver parenchyma. J. Cell. Biol. 72, 441-455.

Borg D. and G.C. Cotzias (1958). Manganese metabolism in man: rapid exchange of ^{54}Mn. J. Clin. Invest. 37, 1269-1278.

Bragadin, T.P. and G.F. Azzone (1983). Nature of the electron spin resonance signal during aerobic uptake of Mn+2 in mitochondria from rat liver. Biochem. 134, 385-390.

Brasch, R.C. (1983). Work in progress: methods of contrast enhancement for NMR imaging and potential applications. Radiololgy 147, 781-788.

Brasch, R.C., D. London, G. Wembley, T. Tozer, D. Nitecki, R. Williams, J. Doemeny, L. Tuck, and D. Lallemand (1983). Work in progress: nuclear magnetic resonance study of paramagnetic contrast agent for enhancement of renal structures in experimental animals. Radiology 147, 773-779.

Budinger, T.F. and P.C. Lauterbur (1984). Nuclear magnetic resonance technology for medicals studies. Science 226, 288-298.

Budinger, T.F. and A.R. Margulis (1986). Medical magnetic resonance imaging and spectroscopy. Society of Magnetic Resonance in Medicine, Berkeley.

Caride, V.J. (1985). Liposomes as carriers of imaging agents. Crit. Rev. Ther. Drug Carrier Syst. 1, 121-153.

Caride, V.J., W. Taylor, J.A. Cramer, and A. Gottschalk (1976). Evaluation of liposomes-entrapped radioactive tracers as scanning agents. Part I: Organ distribution of liposomes ^{99m}Tc-DTPA in mice. J. Nucl. Med. 17, 1067-1072.

Caride, V.J., H.D. Sostman, J. Twickler, S. Orphanoudakis, and C.C. Jaffer (1982) Brominated radioopaque liposomes: Contrast agents for computed tomography of liver and spleen. A preliminary report. Invest. Radiol. 17, 381-385.

Caride, V.J. and H.D. Sostman (1984). Methodological considerations for the use of liposomes in diagnostic imaging, in Liposome Technology, Vol 2, G. Gregoriadis (Ed.). CRC Press, Boca Raton, FL.

Caride, V.J., H. D. Sostman, R.J. Winchell, and J.C. Gore (1984). Relaxation enhancement using liposomes containing paramagnetic species. Magn. Res. Imag. 2, 107-112.

Carr, D.H., J. Brown, G.M. Bydder, H. Weinmann, V. Speck, D. Thomas. and F. Young (1984). Intravenously chelated gadolinium as a contrast agent in NMR imaging of cerebral tumors. Lancet 484-486.

Carr, H.V. and E.H. Purcell (1954). Effects of diffusion on free precession in nuclear magnetic resonance experiments. Phys Rev. 94, 630-638.

Carruthers, A. and D.L. Melchior (1983). Studies of the relationship bewteen bilayer water permeability and bilayer physical state. Biochem. 22, 5797-5807.

Chauhan, A., V.P.S. Chauchan, and H. Brockeroff (1986). Effect of cholesterol on Ca^{2+}induced aggregation of liposomes and calcium diphosphatidate. Biochemistry 25, 1569-1573.

Conlon, T., and T. Outhred (1972). Water diffusion permeability of erythrocytes using a nuclear magnetic resonance technique. Biochim. Biophys. Acta 288, 354-361.

Conner, J. and L. Huang (1986). pH sensiitive immunoliposomes as efficient and target specific carrier for antitumor drugs. Cancer. Res. 46, 3431-3435.

Cooper R. L., D. B. Chang, A. C. Young, J. Martin, and B. Ancker-Johnson (1974). Restricted diffusion in biological systems. Biophysical Journal 14, 161-177.

Cotzias, G.C., D. Borg, and A. Bertinchamps (1960). Clinical-experiences with manganese, in Metal Binding in Medicine. M. Seven and L. Johnson, (Eds.) Lippincott, Philadelphia, PA, p. 50.

Cotzias, G.C., and P.S. Papavasiliou (1962). State of binding of natural manganese. Nature 195, 823-824.

Danchin, A. and M. Gueron (1979). Proton magnetic relaxtion study of manganese transfer-RNA complex. J. Chem. Phys. 53, 3599-3609.

Deamer, D.W. and J. Bramhall (1986). Permeability of lipid bilayers to water and ionic solutions. Chemistry and Physics of Lipids. 40, 167-188.

Dijkstra, J., M. Van Galen, C. Hulstaert, D. Kalicharan., F. Roerdink and G. Scherphof (1984). Interactions of liposomes with Kupffer cells in vitro. Exper. Cell Res. 150, 161-176.

Dijkstra, J., M. Van Galen, and G. Scherphof (1985). Influence of liposome charge on the association of liposomes with liposomes in vitro: effect of divalent cations and competition with latex particles. Bioch. Biophys. Acta. 813, 287-297.

Dijkstra, J., M. Van Galen, D. Regts, and G. Scherphof (1985). Uptake and processing of liposomal phospholipids by Kupffer cells in vitro. Eur. J. Biochem. 148 391-397.

Eisinger, J., R.G. Shulman, and B.M. Szymanski (1962). Transition metal binding in DNA solutions. J. Chem. Phys. 36, 1721-1729.

Fabry, M.H., S.H. Koenig, and W.E. Schillinger (1970). Nuclear magnetic relaxation dispersion in protein solutions. IV-Proton relaxation at the active site of carbonic anhydrase. J. Biol. Chem. 245, 4256-4262.

Fabry, M.E. and M. Eisenstadt (1975). Water exchange between red cells and plasma. Biophys. J. 15, 1101-1110.

Ferrucci, J.T. (1986). MR Imaging of the liver. AJR 147, 1103-116.

Fettiplace, R. and D. A. Haydon (1980). Water permeability of lipid membranes. Physiol. Rev. 60, 510-550.

Fidler I. and W.E. Fogler (1982). Activation of tumoricidial properties in macrophages by lymphokines encapsulated in liposomes. Lymphokine Res. 1, 73-77.

Finklestein, A. (1984). Water movement through membrane channels. Curr. Topics Trans. 21, 295-308.

Fornasiero, D., J.C. Bellen, R.J. Baker, and B.E. Chatterton (1978). Paramagnetic complexes of manganese (II), iron (III) and gadolinium (III) as contrast agents for magnetic resonance imaging: the influence of stability constants on the biodistribution of radioactive aminopolycarboxylate complexes. Invest. Radiol. 22, 322-327.

Getz, D., J.F. Gibson, R.N. Sheppard, K.J. Micklem, and C.A. Pasternak (1979). Manganese as a calcium probe: Electron paramagnetic resonance and nuclear magnetic resonance spectroscopy of intact cells. J. Memb. Biol. 50, 311-329.

Goresuch, T.T. (1970). The Destruction of Organic Matter, Peragom Press (Oxford), pp. 116-117.

Gravela, E., G. Poli, E. Albano, and M.V. Dianzani (1977). Studies on fatty liver with isolated hepatocytes. Exp. Mol. Path. 27, 339-352.

Gregoriadis, G., J. Senior, and A. Trouet (Eds.) 1982. Targeting of Drugs. Plenum Press, New York.

Gregoriadis, G. (Ed.) (1984) Liposomes Technology. Vol. 1-3. CRC Press, Boca Raton, FL.

Grossman, R.J., P.M. Joseph, G. Wolf, D. Biery, J. McGrath, H.L. Kunkel, J.E. Fishman, R.A. Zimmerman, H.L. Goldberg, and L.T. Bilanink (1985). Experimetal intracranial septic infarction: magnetic resonance enhancement. Radiology 155, 649-653.

Hamm, T. Romer, K.J. Wolf, R. Felix, H.J. Weinmann (1986). Contrast Enhancement and Dynamic Studies with Gd-DTPA in MRI Focal Liver Lesions. Abstract, Society of Magnetic Resonance in Medicine, p. 23.

Haran, N. and M. Shporer (1976). Study of water permeability through phospholipid vesicle membranes by ^{17}O NMR. Biochim. Biophys. Acta 426, 638-646.

Hazelwood, C.H., P.C. Chang, B.L. Nichols, and D.E. Woesner (1974). Nuclear magnetic resonance transverse relaxation times of water protons in skeletal muscle. Biophys. J. 14, 583-606.

Heath, T.D., J.A. Robertson, J.R. Piper, and D. Papahadjopoluios (1983). Antibody-targeted liposomes: increase specific toxicity of methotrexate-γ-asparatate. Proc. Natl. Acad. Sci. USA 80, 1377-1381.

Herbst, M.D. and Goldstein, J.H. (1984). Monitoring red blood cell aggregation with nuclear magnetic resonance. Biochim. Biophys. Acta 805, 123-126.

Holtz, E. and H. Klaveners (1986). Abstract Fifth Annual Meeting SMRM, p. 1467.

Hope, M.J., M.B. Bally, G. Webb, and P.R. Cullis (1985). Production of large unilamellar vesicles by a rapid extrusion procedure: Characterization of size, trapped volume and ability to maintain a membrane potential. Biochim. Biophys. Acta 812, 55-65.

Hwang, K.J. (1987). Liposome pharmacokinetics in Liposomes from Biophysics to Therapeutic Applications, M.J. Ostro (ed.) Marcel Dekker, New York, p. 109-156.

Hyde, J.S., H.M. Swartz, and W.E. Anthdine (1979). The spin-probe spin label method, in Spin Labeling II., L.J. Berliner (Ed.) Academic Press, New York. Chapter 2.

Jonas, A. (1980). A review of plasma apolipoprotein A-1 interactions with phosphatidylcholines. Exp. Lung Res. 6, 255-270.

Kang, Y.S., J. Gore, and I.M. Armitage (1984). Studies of factors affecting the design of NMR contrast agents: manganese in blood as model system. Mag. Res. Med. 1, 396-409.

Kessel, R. G. and R. H. Hardon (1979). Tissues and Organs: A Text Atlas of Scanning Electron Microscopy. W. H. Freeman, San Francisco, p. 187-196.

Kirby, C., J. Clarke, and G. Gregoriadis (1980). Effect of cholesterol content of small unilamellar liposomes on their stability in vivo and in vitro. Biochem. J. 156, 591-598.

Knight, C.G. (Ed.). 1981. Liposomes, from Physical Structure to Therapeutic Application. Elsevier/North-Holland, New York.

Koening, S.H., and R. Brown Jr. (1984a). Determinants of proton relaxation in tissue, Mag. Res. Med. 1, 437-449.

Koening, S. H. and R. Brown Jr. (1984b). Relaxation of solvent protons by paramagnetic ions and its dependence on magnetic field and chemical environment: implications for NMR imaging. Mag. Res. Med. 1, 478-495.

Koening, S. H., and R. Brown Jr. (1985). The importance of the motion of water for magnetic resonamce imaging. Invest. Radiology 20, 297-305.

Koening, S.H, R. Brown, E. Goldstein, K. Burnett, and G. Wolf (1985). Magnetic field dependence of proton relaxation rates in tissue with added Mn2+: rabbit liver and kidney. Mag. Res. Med. 2, 159-168.

Kressel, H.Y. (1987). MRI of the upper abdomen. Abstract, Sixth Annual Meeting of Society for Magnetic Resonance in Medicine, p. 83.

Lauffer, R.B. (1987). Paramagretic metal complexes as water proton relaxation agents for NMR imaging. Theory and design. Chem. Rev. 87, 901-927.

Lauterbur, P.C., M.H. Mendonca-Dias, and A.M. Rudin (1978). Augmentation of tissue water proton spin lattice relaxation rates by in vivo addition of paramagnetic ions. Frontiers of Biological Energetics Vol 1, 752-759.

Lauterbur, P.C. (1973). Image formation by induced local interactions: Examples employing nuclear magnetic resonance. Nature 242, 190-191.

Leach, R.M. and M.S. Lilburn (1978). Manganese metabolism and its function. Wld. Rev. Nutr. Diet. 32, 123-134.

Lipschitz-Farber, C. and H. Degani (1980). Kinetics of water diffusion across phospholipid membranes. ^{1}H and ^{17}O-NMR relaxation studies. Biochim. Biophys. Acta 600, 291-300.

Litchfield, J.T. and F. Wilcoxen, F. (1949). A simplified method of evaluation dose-effect experiments. J. Pharmocol. Exp. Therap. 96, 99-117.

Ma, L.D., R.L. Magin, and F. Dunn (1987). Effects of divalent cations on the ultrasonic absorption coefficient of negatively charged liposomes (LUV) near their phase transition. Biochim. Biophys. Acta 902, 183-192.

Magin, R.L., M.R. Niesman, J.K. Hunter, and G.A. Bark (1986a). Effect of vesicle size on the clearance, distribution and tumor uptake of temperature sensitive liposomes. Cancer Drug Delivery 3, 223-237.

Magin, R.L., S.M. Wright, M. R. Niesman, H.C. Chan, and H. M. Swartz (1986b). Liposome delivery of NMR contrast agents for improved tissue imaging, Mag. Res. Med. 3, 440-442.

Magin, R.L. and M.R. Niesman (1984a). Temperature dependent drug release from large unilamellar vesicles, Cancer Drug Delivery 1, 109-117.

Magin, R.L. and M. R. Niesman (1984b). Temperature dependent permeability of large unilamellar liposomes. Chem. Phys. Lipids 34, 245-256.

Magin R.L. and J. Weinstein (1984). The design and characterization of temperature-sensitive liposomes, in Liposome Tecnology., G. Gregoriadis, (Ed.) CRC Press, Boca Raton, FL, p. 137-155.

Mahoney, J.P., G. Sargent, and W.J. Small (1969). Mn determination in serum by atomic absorption spectroscopy. Clin. Chem. 15, 312-322.

Mahoney, J.P. and W.J. Small (1968). Studies on manganese(II) biological 1/2 life of ^{54}Mn in man. J. Clin. Invest. 47, 643-653.

Mansfield, P. and A.A. Maudsley (1983). Medical imaging by NMR. Br. J. Radiol. 50, 188-194.

Mayhew, E. and D. Papahadjopoulos (1983). Therapeutic applications of liposomes, in Liposomes, M.J. Ostro (Ed.) Marcel Dekker, New York, NY, pp. 289-341.

Maynard, L.S. and G.C. Cotzias (1955). The partition of manganese among organs and intracellular organelles of the rat. J. Biol. Chem. 214, 489-495.

Meiboom, S. and D. Gill (1958). Modified spin-echo method for meausuring nuclear relaxation times. Rev. Sci. Instrum. 29, 688-691.

Mendonca-Dias, M.H., E. Gaggelli, and P.C. Lauterbur (1983). Paramagnetic contrast agents in nuclear magnetic resonance medical imaging. Seminars in Nucl. Med. 4, 364-376.

Mildvan, A. S. and M. Cohn (1963). Magnetic resonance studies of the interaction of the manganous ion with bovine serum ablium. Biochemistry 2, 910-919.

Mildvan, A. S. and M. Cohn (1970). Aspects of enzyme mechanisms studied by nuclear spin relaxation induced by paramagnetic probes. Advances Enzymology 33, 1-70.

Moriariu, V., G. Benga (1977). Evaluation of a nuclear magnetic technique for the study of water exchange through erthrocyte membranes in normal and pathological subjects. Biochim. Biophys. Acta 469, 301-310.

Morris, P. G. (1986). NMR Imaging in Medicine and Biology. Oxford University Press, New York.

Moulday, R. S. and D. Mackenzie (1982). Immunospecific ferromagnetic iron-dextran reagents for the labeling and separation of cells. Immun. Meth. 52, 353-367.

Navon, G. (1970). Proton relaxation times and hydration numbers of manganese ions bound to enzymes. Chem. Phys. Lett. 7, 390-394.

Niccolai, N., E. Tiezzi, and G. Valensin (1982). Manganese(II) as a paramagnetic relaxation probe in the study of biomechanisms and biomolecules. Chem. Rev. 82, 359-384.

Nolden, P.W., and T. Ackermann (1975). A proton-relaxation enhancement study of the interaction of manganous ions with phospholipids in aqueous dispersions. Biophys. Chem. 3, 183-191.

Ohgushi, M., K. Nagayama, and A. Wada (1978). Dextran-magnetite: A new relaxation reagent and its application to T_2 measurements in gel systems. J. Magnetic Resonance 29, 599-601.

Ohtomo, K., Y. Itai, and M. Iio (1986). Magnetic resonance imaging of the liver, in Magnetic Resonance Annual, H. Kressel (Ed.) Raun Press, New York, NY, pp. 197-213.

Olson, F., C.A. Hunt, F.C. Szoka, W.J. Vail, and D. Papahadjopoulos (1979). Preparation of liposomes of defined size distribution by extrusion through polycarbonate membranes. Biochim. Biophys. Acta 557, 9-23.

Ostro, M.J. (Ed.). 1984. Liposomes. Marcel Dekker, New York.

Papavasiliou, P.S., S.T. Miller, and G.C. Cotzias (1966a). Essential trace metals in man: manganese. A study in homeostatsis. J. Chron. Dis. 19, 545-571.

Papavasiliou, P.S., S.T. Miller, and G.C. Cotzias (1966b). Role of liver in regulating distribution and excretion of manganese. Am. J. Physiol. 211, 211-216.

Pirkle, J.L., D.L. Ashley, and J.H. Goldstein (1979). Pulse nuclear magnetic resonance measurements of water exchange across the erthocyte membrane employing a low Mn concentration. Biophys. J. 25, 389-406.

Proffitt, R.T., L.E. Williams, C.A. Presant, G.W. Tin, J.A. Uliana, R.C. Gamble, and J.D. Baldeschwieler (1983). Tumor-imaging potential of liposomes loaded with In-111-NTA: Biodistribution of mice. J. Nucl. Med. 24, 45-51.

Poste, G., C. Bucana, A, Raz, P. Bugelski, R. Kirsh, and I. Fidler (1982). Analysis of the fate systemically administered liposomes and implications for their use in drug deliviery. Cancer Res. 42, 1412-1422.

Purcell, E.U., H.C. Torrey, and R.V. Pound (1946). Resonance absorption by nuclear magnetic moments in a solid. Phys. Rev. 69, 37-38.

Reed, G.H. and M. Cohn (1970). Electron paramagnetic resonance spectra of manganese(II)-protein complexes. Manganese(II)-concanavalin A. J. Biol. Chem. 245, 662-667.

Reing, J.W., A.J. Dwyer, J.A. Frank, D.L. Miller, G.W. Adams, A.E. Chang, and I.L. Doppman (1987). Comparison of liver metastesis detection at 0.5T and 1.5T. Abstract, Sixth Annual Meetin of Society for Magnetic Resonance in Medicine, p. 88.

Roerdink, F. J. Dykstra, G. Hartman, B. Bolscher, and G. Scherphof (1981). The involovement of parenchymal Kupffer and endothelial liver cells in the hepatic uptake of intravenously injected liposomes. Effects of lanthanum gadolinium salts. Biochim Biophys. Acta 667, 79-89.

Runge, V. M., J. Clanton, W. Herzer, S. Gibbs. A. Price, C. Partain, and A. James, Jr. (1984). Intravascular contrast agents suitable for magnetic resonance imaging. Radiology 153, 171-176.

Runge, V. M., S.M. Wolpert, A.C. Price, M. Laucella, D. Johnson (1986). Abstract, Sixth Annual Meeting of Society of Magnetic Resonance in Medicine, p. 1529.

Ryan, P.J., M.A. Davis, and D.L. Melchior (1983). The preparation and characterization of liposomes containing x-ray contrast agents. Biochim. Biophys. Acta 756, 106-110.

Saini, S., D.D. Stark, J. Wittenberg, T.J. Brady, and J.T. Ferrucci (1986). Dynamic gadolinium-DTPA imaging of liver cancer: animal investigation. AJR 147, 357-362.

Saini, S., D.D. Stark, P.F. Hahn, J. Wittenberg, T. J. Brady, and J.T. Ferrucci (1987). Gd-DOTA: Ferrite particles: A superparamagnetic MR contrast agent for the RES. Radiology 162, 211-216.

Scherphof, G. F. Roerdink M. Waite, and J. Parks (1978). Disintegration of phosphatidylcholine liposomes in plasma as a result of interactions with high density lipoproteins. Biochim. Biophys. Acta 542, 296-307.

Scheuhammer, A.M. and M.G. Cherian (1985). Binding of manganese in human and rat plasma. Biochim. Biophys. Acta 840, 163-169.

Schramm, V.L. and M. Brandt (1986). The manganese(II) economy of rat heptocytes. Fed. Proc. 45, 2817-2820.

Sherlock, S. and R. Dick (1986). The impace of radiology on hepatology. AJR 147, 1117-1122.

Slichter, C.P. (1980). Principles if Magnetic Resonance, 2nd Ed. Springer Verlay, New York.

Small, W.C. and J.H. Goldstein (1981). The effect of changing extracellular osmolality on water transport in the human red bolld cell as measured by the cell water residence time and the activation energy of water transport. Biochim. Biophys. Acta 640, 430-438.

Solomon, I. (1955). Relaxation procession system of two spins. Phys. Rev. 99, 559-565.

Spanjer, H., M. van Galen, F.H. Roerdink, J. Regts, and G.L. Scherphof (1986). Intrahepatic distribution of small unilamellar liposomes as a function of liposomal composition. Biochim. Biophys. Acta 863, 224-230.

Stastny, D, R.S. Vogel, and M.F. Picciano (1984). Manganese intake and serum manganese concentration of human milk-fed and formula-fed infants. Amer. J. Clin. Nutr. 39, 872-878.

Storm, G. F.H. Roerdink, P.A. Steerenberg, W.H. deJong, and D.J.A. Crommelin (1987). Influence of lipid composition on the antitumor activity exerted by poxosubicin-containing liposomes in a rat solid tumor model. Cancer Res. 47, 3366-3372.

Strause, L., J. Hegenauser, D. Burstein, and P. Saltman (1985). The oral assimilation of radiomanganese by the mouse. Biol. Trace Element Res. 7, 75-81.

Szoka, F. and D. Papahadjopoulos (1980). Comparative properties and methods of preparation of lipid vesicles (liposomes). Ann. Rev. Biophys. Bioeng. 9, 465-506.

Szoka, F., F. Olson, T. Heath, W. Vail, E. Mayhew, and D. Papahadjopoulos (1980). Preparation of unilamellar liposomes of intermediate size (0.1-0.2u) by a combination of reverse

phase evaporation and extrusion through polycarbonate membranes. Biochim. Biophys. Acta 601, 559-571.

Tacker, J.R. and R.U. Anderson (1982). Delivery of antitumor drug to bladder concer by use of phase transition liposomes and hyperthermia. J. Urol. 127, 1211-1214.

Tom B.H. and H. R. Six (1980). Liposomes and Immunobiology. Elsevier/North Holland, New York.

Underwood, E.J. (1977). Trace Element in Human and Animal Nutrition, Academic Press, New York, NY.

Vandenbranden, M., G. De Gand, R. Brasseur, F. Defrise-Quertain and J. Ruysschaert (1984). Hydrolysis of phosphatidylcholine liposomes by lhysosomal phospholipase A is maximal at the phase transition temperature of the lipid substrate. Bioscience Reports 5, 477-482.

Van Steenwinkel, R., F. Campagnari, and M. Merlini (1981). Interaction of Mn^{+2} with DNA as studies by proton-relaxation enhancement of solvent water. Biopolymers 20, 915-923.

Venugopal, B. and T.D. Luckey (1978). Metal Toxicity in Mammals. Vol 2. Plenum Press, New York.

Venugopal, B. and T.D. Luckey. Metal Toxicity in Mammals vol.2. Chemical toxicity of metals, and metalloids. Plenum Press, New York. Chapter 7.

Weinstein, J.N. (1984). Liposomes as drug carriers in cancer chemotherapy. Pharmacol. Ther. 24, 207-233

Weinstein, J.N., S. Yoshikami. P. Hnekart. R. Blumenthal, and W. A. Hugins (1977). Liposome cell interaction: transfer and intracellular release of a trapped fluorescent marker. Science 195, 489-492.

Weinstein, J.N. (1984). Liposomes as drug carriers in cancer therapy. Cancer Treat. Rep. 68, 127-135.

Williams, L.E., R.T. Proffitt, and L. Lovisatti (1984). Possible application of phospholipid vesicles (liposomes) in diagnostic radiology. J. Nucl. Med. Allied Sci. 29, 35-45.

Wisse, E. and A. M. DeLeeuw (1984). Structural elements determining transport and exchange processes in the liver. In Microspheres and Drug Therapy, S. Davis, L. Illum, J. McVie, and E. Tomlinson (Eds.). Elsevier (New York), pp. 1-24.

Wittenburg, J., D.D. Stark, P.F. Hahn, S. Saini, and J.T. Ferrucci (1987). Pulse sequence criteria for identifying and characterizing hepatic tumors. Abstract, Sixth Annual Meeting of Society of Magnetic Resonance in Medicine, p. 91.

Wolf, G.L. and Baum, L. (1983). Cardiovascular toxicity and tissue proton T_1 response to manganese injection in the dog and rabbit. Am. J. Roentenol. 141, 193.

Wolf, G., K. Burnett, E.J. Goldstein, and P. M. Joseph (1985). Contrast agents for magnetic resonance imaging, in Magnetic Resonance Annual., H. Kressel,(Ed.) Raven Press, New York, p. 231.

Yatvin, M.B. J.N. Weinstein, W.H. Dennis, and R. Blumenthal (1978). Design of liposomes for enhanced local release of drugs by hyperthermia. Science 202, 1290-1293.

Zlotkin, S.H. and B.E. Buchanan (1986). Manganese intakes in intravenously fed infants. Biol. Trace Element Res. 9: 271-280.

VITA

Michael Niesman was born on November 26, 1958 in Decatur, Illinois. He attended Millikin University in Decatur, Illinois, where he was a James Millikin Scholar. He received his Bachelor of Arts degree summa cum laude from Millikin in 1980. He attended the University of Illinois at Urbana-Champaign from 1980 to 1988. While at the University he received a Master of Science degree in Biology (1982) and was the recipient of a National Institute of Health predoctoral traineeship in Radiation Oncology. He graduated with the Ph.D. degree in Biology in 1988.